Koninklijke Sterrenwacht van België
Observatoire royal de Belgique
Royal Observatory of Belgium

Jaarverslag 2013
Rapport Annuel 2013
Annual Report 2013

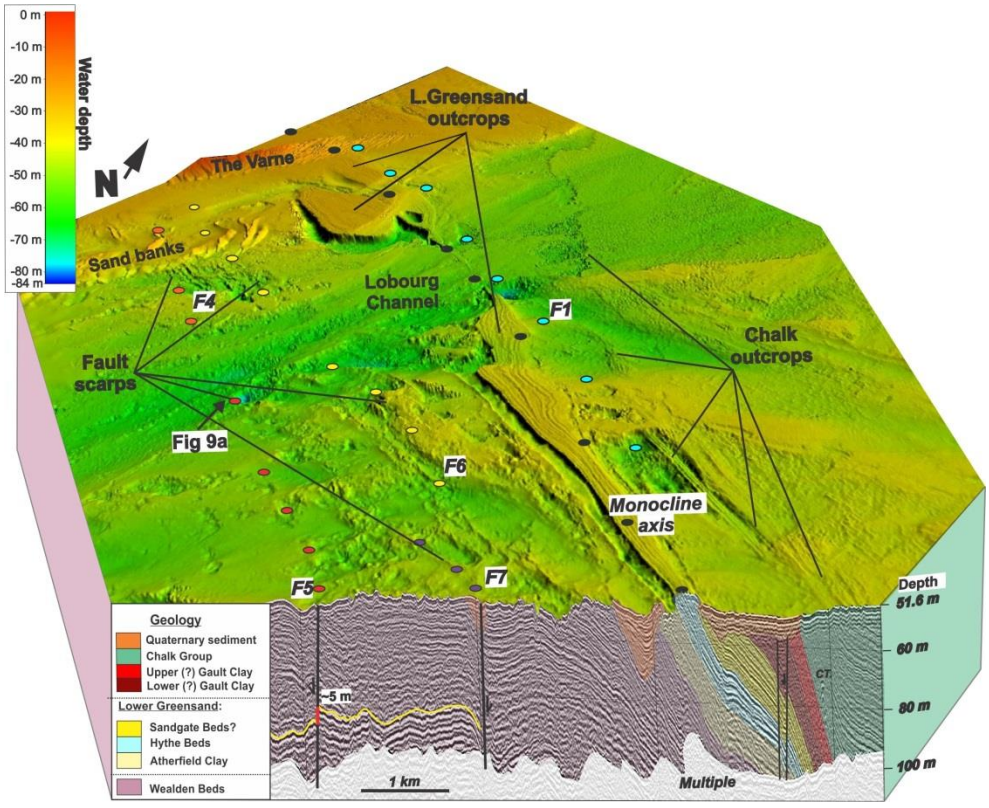

Mensen voor Aarde en Ruimte, Aarde en Ruimte voor Mensen

Des hommes et des femmes pour la Terre et l'Espace, La Terre et l'Espace pour l'Homme

Cover illustration: *3D block showing the central and south-eastern merged bathymetry in the Strait of Dover in relationship with the interpretation of one of the single-channel seismic-reflection profiles. Coloured circles in the bathymetry represent the fault traces and monocline axis inferred from the seismic investigation. (ROB)*

De activiteiten beschreven in dit verslag werden ondersteund door
Les activités décrites dans ce rapport ont été soutenues par
The activities described in this report were supported by

De POD Wetenschapsbeleid
Le SPP Politique Scientifique

De Nationale Loterij
La Loterie Nationale

Het Europees Ruimtevaartagentschap
L'Agence Spatiale Européenne

De Europese Gemeenschap
La Communauté Européenne

Het Fonds voor Wetenschappelijk Onderzoek – Vlaanderen

Le Fonds de la Recherche Scientifique

Table of contents

Preface

This report describes the highlights of scientific activities and public services at the Royal Observatory of Belgium in 2013.

A list of publications and the list of personnel is included at the end.

Due to lack of means and personnel the report is only in English. A description of the most striking highlights is available in Dutch and French.

If you need more or other information on the Royal Observatory of the Belgium and/or its activities please contact rob_info@oma.be or visit our website http://www.astro.oma.be.

Kind regards
Ronald Van der Linden
Director General

Reference Systems and Planetology

GPS and more generally Global Navigation Satellite System (GNSS) used at ROB for positioning, for space weather, for meteorology and for characterizing plate motions and deformations

EUREF

ROB has continued to host the Central Bureau (http://www.epncb.oma.be, over 2 million hits in 2013) managing the EPN GNSS tracking network distributed over 30+ European countries. This network provided access to the European Terrestrial Reference System (ETRS89), used a standard for georeferencing all over Europe. In addition, the EPN data are also used for a wide range of scientific applications such as the monitoring of ground deformations, sea level, space weather and numerical weather prediction.

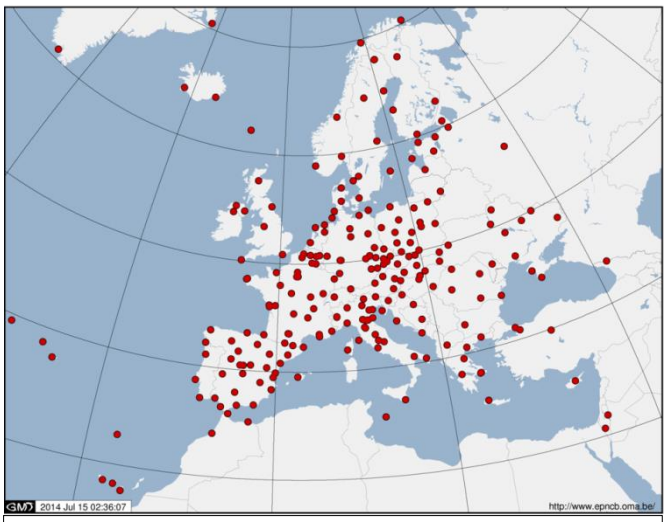

Figure 1: EPN GNSS tracking network managed by ROB.

In 2013, eight new permanent GNSS tracking stations joined the network bringing the total number of stations to 247 (see right figure**Error! Reference source not found.**). In ddition, the station operation guidelines have been updated in order to reflect the changing GNSS landscape focusing on real-time and multi-GNSS operations. As one of the EPN analysis centers, ROB upgraded the GNSS data analysis and improved the modelling of the troposphere, ionosphere and atmospheric loading.

DEFORMATIONS

IceCon is a project funded by the Federal Science Policy Office (BELSPO) and aims at constraining past and current mass changes of the Antarctic ice sheet in the coastal area of Dronning Maud Land, Antarctica. Within IceCon, the ROB is in charge of monitoring ground motions using GNSS. In 2013, the ROB already installed network of permanent GNSS stations was extended with a third station. This GNSS station was installed on Yet Nunten nunatak in the Roysane Mountains (~ 46 km for Princess Elisabeth Basis). In order to ensure year-round operation, like the other IceCon GNSS stations, the new station is equipped with wind turbines and solar panels.

GNSS station installed on the Yet Nunten nunatak

A preliminary analysis of the GNSS data of the first two stations already demonstrates a subsidence of more than one meter a year for the GNSS station installed on the Derwael ice rise.

In the frame of the International Association of Geodesy Working Group "Integration of dense velocity fields in the ITRF", which is chaired by the ROB, we are creating a dense velocity field based on permanently observing GNSS stations installed throughout the globe. A preliminary dense velocity field (see figure on the right) containing about 1800 GNSS stations has been presented at the IAG Scientific Assembly in September 2013 in Potsdam, Germany.

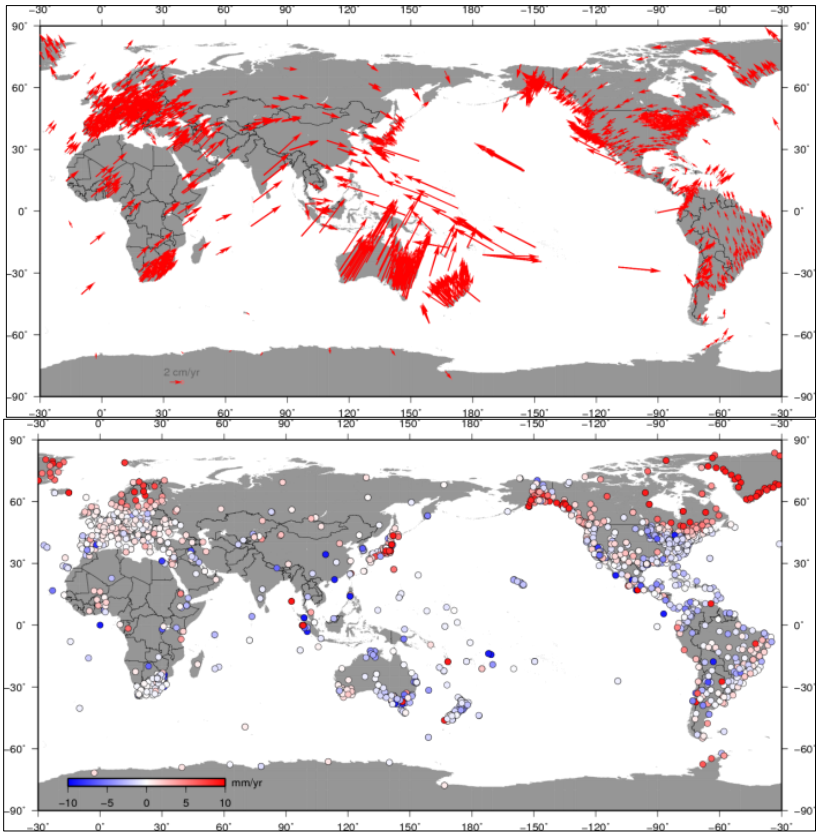

Preliminary horizontal (top) and vertical (bottom) velocity field

EPOS is the integrated solid Earth Sciences research infrastructure included in the European Strategy Forum on Research Infra-structures (ESFRI) Roadmap. EPOS aims at creating an e-infrastructure to better understand physical processes controlling earthquakes, volcanic eruptions, unrest episodes and tsunamis as well as those driving tectonics and Earth surface dynamics. The GNSS group has made efforts towards the integration of Belgium in EPOS (European Plate Observing System) involving discussions with the EPOS chair and participation to meetings/teleconferences. They are also heavily involved in EPOS Working Group 4 'GNSS data and other geodetic data' aiming at preparing the GNSS contribution to EPOS. Although Belgium is presently not one of the partners of EPOS, it is important that Belgium becomes a partner once EPOS is moving from its preparatory phase to its implementation phase (from 2014 on).

ANTENNA CALIBRATIONS

A study on the influence of antenna calibration models on GNSS-based position estimates has been finalized and a paper was published. The study demonstrated the complexity of GNSS antenna calibrations: 1) the calibrations themselves are not free from errors, 2) on site phase response can differ from the one from the calibration facility, 3) the effect of calibration errors on estimated site positions depends on the data analysis strategy.

TROPOSPHERE

The GNSS group has co-founded a new E.U. COST Action ES1206 "Advanced GNSS Tropospheric Products for monitoring Severe Weather Events and Climate" (GNSS4SWEC) that started in May 2013. A scientist of the group also co-chairs the second working group "Use of GNSS tropospheric products for high resolution NWP and severe weather forecasting".

Members of the GNSS group also received the contest award at the GfG² summer school 2013 for their recent developments in the framework of the project "Advanced Multi-GNSS Troposphere Modelling for Improved Monitoring and Forecasting of Severe Weather" funded by the STCE.

We also continued to develop and ensure the daily maintenance of the ROB near real-time "EUMETNET EIG GNSS water VApour Program" analysis center providing European meteorological institutes with

near real-time GPS-based tropospheric Zenith Path Delay estimates for assimilation in the Numerical Weather Prediction (NWP) models and for now casting applications (based in a network of a 840 GNSS stations).

The collaboration with the RMI and the BISA on the inter-comparison of different techniques of observing the atmospheric water vapour resulted in a paper submitted to Atmospheric Measurement Techniques.

IONOSPHERE

The ionosphere was monitored in near-real time and identified ionospheric disturbances were communicated to the public via the web-site www.gnss.be; 11 ionospheric events were reported in 2013. The software which routinely delivers these products was maintained and optimized. The comparison of ROB near-real time ionospheric products with other products from NOA and global ionospheric maps from CODE showed that the main parameters affecting the quality of the DIAS maps are the number of digisondes contributing with data to each specific map and their geographic distribution.

An empirical model in order to predict the total electron content over Europe every 15 minutes from the F10.7P index in entrance is under development. First results show differences lower or equal than 5 TECu for 92.3 % of the time between the modelled and observed values above Brussels.

Time – Time Transfer

The ROB scientists establish the Belgian time scale (UTC (ORB)) and participate in international timescales by incorporating Belgium in these timescales. We maintain presently 5 high-quality clocks for participation in two international timescales: the International Atomic Time (TAI) and the International GNSS Service Timescale (IGST). The present requirement for the clock precision and stability is at the level of the nanosecond over one day, which can only be achieved with high-quality clocks, when located

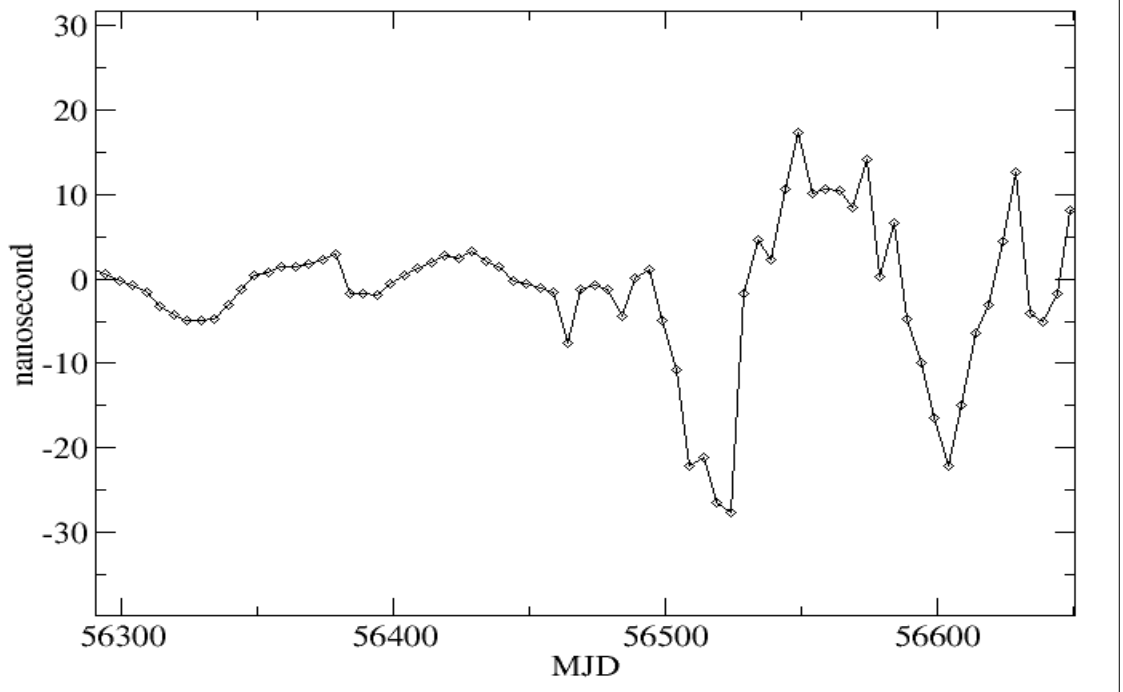

UTC-UTC(ORB) during 2013.

in temperature-controlled environment. Our 5 clocks are located in such an environment and their performances are continuously monitored by inter-comparison between themselves and also with atomic clocks of other laboratories participating to TAI or IGST. In order to perform these comparisons, as well as to transfer time at the centers where the computations for the international timescales are performed, we need methods which insure a time-transfer precision matching the required precision of the timescales. These comparisons are usually performed using code measurements of GPS satellites in common view. The scientists involved in the project work on the improvement of the time transfer by using both code and phase measurements of geodetic receivers, in order to enhance its precision and accuracy. This requires the establishment of new analysis strategies, new error modeling, and new computer codes. It also requires the installation of new equipment and the adaptation of the procedures to this new equipment. The scientists of this project also take care of the legal issues related to the legal time. An additional important part of the work is related to the quality control and maintenance of the clocks, as our involvement in the definition of international timescale impose us a quasi-perfect reliability.

Due to the failure of the H-maser clock used for the generation of the realization of UTC (ORB) in July, a Cesium clock was used for this task in the second half of the year. The stability of UTC(ORB) was therefore degraded, but the difference with respect to the true UTC remained however lower than 30 ns during that period, as illustrated in the figure above.

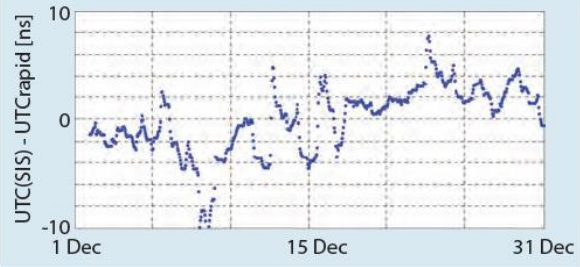

FIGURE 9 UTC dissemination accuracy

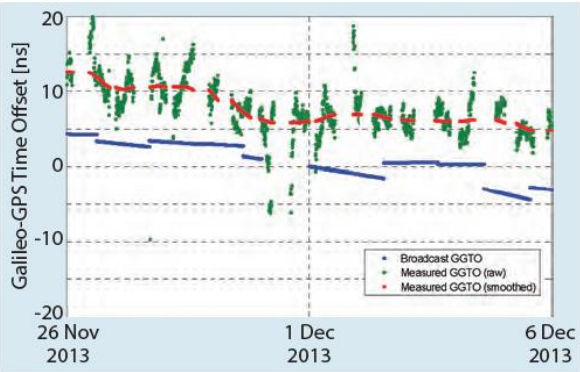

FIGURE 10 Measured and broadcast GGTO

Figures published by the ESA, based on the ROB results for the validation of UTC and GGTO as disseminated by Galileo.
(source: Inside GNSS, March 2014)

During the year 2013, the ROB started a contribution to the European Navigation Satellite system Galileo within the frame of the Time Validation Facility, in collaboration with five other European time-measurement institutions: the Physikalisch Technische Bundesanstalt in Germany, the National Physical Laboratory in the UK, the Système de References Temps Espace/Observatoire de Paris in France, the Real Instituto y Observatorio de la Armada in Spain, and the Istituto Nazionale di Ricerca Metrologica (INRIM). The ROB scientists were responsible for the monitoring and validation of the time informations disseminated by the Galileo satellites: the prediction of UTC and the Galileo to GPS Time Offset. This validation was performed using the measurements collected in our GNSS station BRUX, and using specific analysis procedures self-developed. The results of this validation were published by the European Space Agency (ESA) in early 2014 and are reproduced in the figure on the left.

In parallel, the use of Galileo signals for time transfer was instigated. One particular issue was the development of an original method to determine the hardware delays in the receiving GNSS stations, as nothing exist to date for Galileo signals. The method developed was based on the measure of the ionospheric delays of Galileo and GPS satellites appearing simultaneously in the same direction. As ionospheric delay is then the same for both satellites, it is possible to retrieve the station hardware delays for Galileo signals from the GPS hardware delays. This method was successfully applied to a set of stations and the use of Galileo for timing and time transfer is now hence possible.

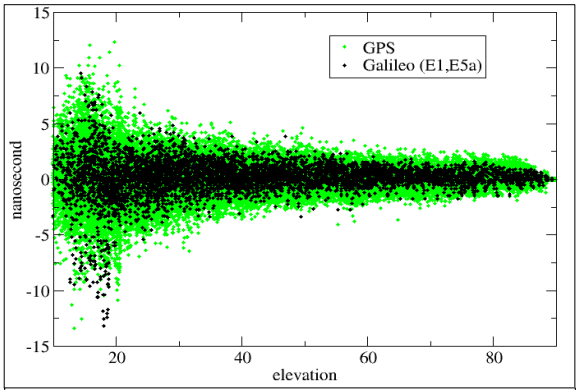

Noise of the time transfer results between Brussels and Turin, as a function of the satellite elevation.

The R2CGGTTS software tool developed at the ROB to generate the time transfer solutions in the international standard was then upgraded to provide solutions for Galileo as well as GPS. First results of time transfer were obtained for an atomic clock comparison between Brussels and Turin and showed that the Galileo solution is about 15% more precise than the GPS solution thanks to the Galileo frequencies giving a smaller noise increase in the dual-frequency ionosphere-free combination, as illustrated in the figure on the right which shows the noise of the Galileo results and GPS results as a function of the satellite elevation.

Plate tectonics on terrestrial exoplanets

OD1 scientists of Planet TOPERS have shown that the existence of plate tectonics on terrestrial exoplanets depends on the initial temperatures after accretion of the planet. Depending on the available initial heat in the interior of a super-Earth (a terrestrial planet with masses up to 10 times the mass of Earth), plate tectonics is either more, less or equally likely compared to Earth.

The scientists investigated the formation of continents on early Earth and exoplanets. For this they use (1) the 2D and 3D global mantle convection code GAIA developed at the DLR (German Aerospace Center) and (2) the convection code CHIC developed at the Royal Observatory of Belgium.

In the 2D/3D GAIA code, mantle convection is simulated together with subduction of crust via plate tectonics. Basaltic crust that is transported into the silicate mantle at the subduction zones is traced over time. This crust is treated differently than mantle silicates when re-molten, such that granitic (felsic) crust is produced (similar to the evolution of continental crust on early Earth).

The CHIC code is used to investigate these processes in more detail (e.g. subduction zone figure below). We included dehydration of subducted crust to simulate the formation of felsic crust in a more Earth-like approach, where crust forms under both hydrous and dehydrous conditions.

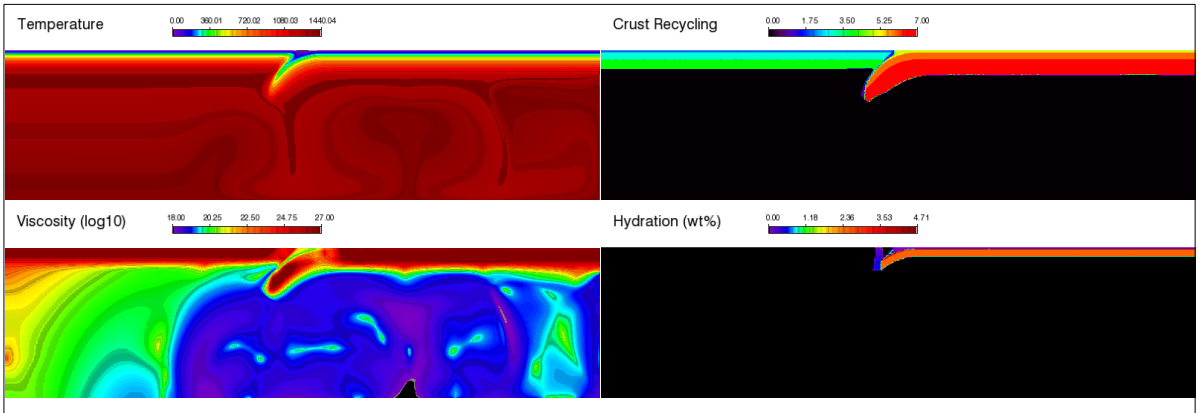

Example of a 2D box simulation of a subduction zone

The simulation of plate dynamics in a subduction zone (see figure above) was successfully benchmarked and was thus used to simulate subduction of hydrated basaltic crust including the release of water in the mantle wedge from destabilized materials. This additional water enhances continental production.

Compressibility of mantle rock was implemented and benchmarked for a more realistic treatment of the lower mantle of Earth as well as the simulation of super-Earths, where the high pressures in the silicate mantle lead to compression of the material and different thermal cooling behaviors than in the upper mantle.

Geodesy and Geophysics of Terrestrial Planets

ROB scientists investigate the rotation and orientation variations and the tides of the terrestrial planets and large natural satellites in order to gain insight into their interior structure, composition, evolution, dynamics, and atmosphere. Geodesy data on the gravity field and rotation of a planet can be obtained from spacecraft flying by, in orbit around, or landed on the planets. In this project, radio science data from spacecraft in orbit around Mars and Venus, such as MarsExpress (MEX), Mars Global Surveyor (MGS), Mars Odyssey, Mars Reconnaissance Orbiter (MRO), and VenusExpress (VEX) are the principal source of information. Radio science data from the upcoming BepiColombo mission to Mercury, the ExoMars mission to Mars, and the JUpiter Icy moon Explorer (JUICE) will be processed in the future. In addition, we use data from missions to the outer solar system like Voyager 1 and 2, Galileo, and Cassini.

The gravity field of planetary bodies is obtained by monitoring the trajectory of passing or orbiting spacecraft through performing Doppler and ranging measurements on radio links between the Earth and the spacecraft. For the analysis of these radio science data and for simulations of future experiments, a numerical code (GINS/DYNAMO) is used and further developed; this code is one of only a few codes in the world that can compute accurate orbits of spacecraft from radio science data. Because the gravity field of a planet is determined by the planet's mass distribution, spatial and temporal variations in the gravity field can be used to determine physical properties of the interior and atmosphere of the planet. Since the beginning of the space age, the large-scale structure of the gravity field of planets and moons has been successfully used to determine the moment of inertia, which is a measure of the radial density distribution and an important constraint on the interior structure. More recent efforts use tides, which can also be observed through their time-variable effect on the gravity field, to obtain more accurate information on the deep interior, in particular on global fluid layers such as a liquid iron core in terrestrial planets and an internal subsurface ocean in icy satellites.

Constraints on planetary interiors can also be obtained from rotation variations. Three broad classes of rotation variations are usually considered: rotation rate variations, orientation changes with respect to inertial space (precession and nutation), and orientation changes with respect to the rotation axis (polar motion and polar wander). They are due to both internal (angular momentum changes between solid and liquid layers) and external (gravitational torques) causes. By studying rotational variations of a terrestrial planet, more can be learn about the excitation processes. Moreover, as the rotational response depends on the planet's structure and composition, also insight into the planetary interior can be obtained. This is particularly so for the rotational variations due to well-known external gravitational causes, such as for example for the nutations of Mars and the librations of Mercury and natural satellites.

The OD1 scientists have a strong theoretical research component, which is oriented towards the investigation of the dependence of rotation variations, gravity field, and tidal variations on interior and atmosphere properties and orbital motion characteristics. These studies include the development of advanced models of rotation, the construction of detailed models for the structure and dynamics of solid and fluid layers of the planets, the investigation of the dynamical response of these models to both internal and external forcing, the modeling of the orbital motion of large bodies of our solar system, and the inclusion of general relativistic effects into the data analysis.

OD1 scientists are involved in several ESA solar system missions (Mars Express, Venus Express, BepiColombo, JUICE) and Cassini at Co-Investigator or Participating Scientist level, actively participate with ESA in preparations for new and upcoming missions, and lead the development of a coherent X-

band transponder and antenna for use in a future Mars lander mission. We also develop theories and strategies for the future exploitation of space data.

Highlights of results obtained in 2013 are listed below in order of increasing distance of the solar system body involved with respect to the Sun.

Mars: Methane and clathrates

OD1 scientists from the Interuniversity Attraction Pole "PLANET TOPERS" (Planets: Tracing the Transfer, Origin, Preservation, and Evolution of their ReservoirS) investigate the stability of methane and carbon dioxide clathrates in the crust of Mars. In recent years, several detections of methane in the atmosphere of Mars were reported from Earth-based observations and from Mars orbiter observations. This gas has a non-uniform distribution involving a lifetime of 200 days, smaller than the 300 years predicted by photochemical models. Moreover, its source is still unknown and could be either abiotic or biotic. Whatever the origin of methane, the latter may have been stored in reservoirs of clathrates placed in the crust of Mars. The dissociation of these chemical structures due to a change in temperature or pressure may cause the observed methane emissions on Mars.

Considering the effects of the variation of the heat flux and the soil composition, the zone where clathrates[1] are stable are shown to approach the surface with increasing latitudes. The thermal oscillations caused by the variation of the obliquity can induce destabilized clathrates on all latitudes while the thermal oscillations due to the succession of seasons destabilize clathrates at high latitude only.

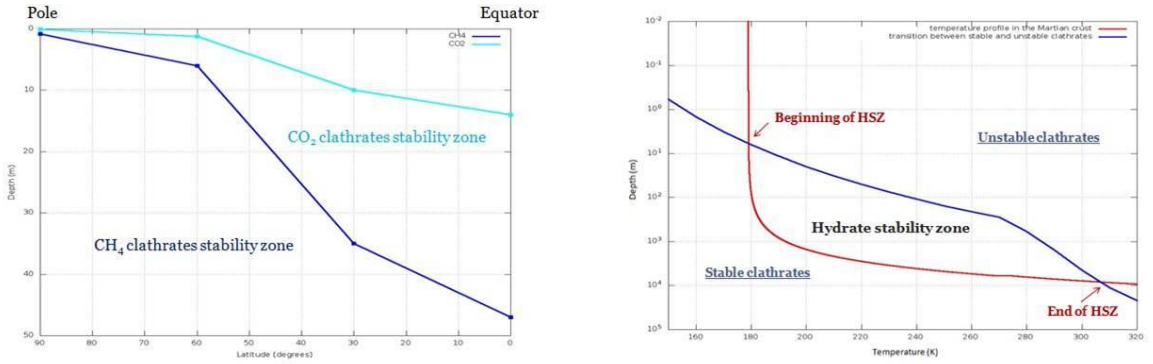

On left hand side, stability of clathrates (CH_4 and CO_2) in the Martian crust using clathrates phase diagrams and Calculation of temperature profiles in the crust for typical present-day conditions, and on the right hand side, destabilization of clathrates due to temperature oscillations; Seasonal variations (~ 4.4 m); Obliquity change (~ 1.5 km)

Reducing the heat flux has the effect of increasing the depth of the base of the clathrate stability zone. As regards the crust composition, the type of soil directly controls the geothermal conditions and therefore the depth of clathrate formation. Unconsolidated soil acts as a thermal insulator and prevents the clathrate formation in the crust except on a small part of a few tens of meters thick. For example, the stability zone of methane clathrates in unconsolidated soil can only exist at high latitudes and has a thickness of several tens to several hundreds of meters. In contrast, sandstone or ice-cemented soil allows the clathrate formation with a stability zone of several kilometers. This is explained by the fact that they evacuate heat more efficiently and thus maintain lower temperatures. Next page's right figure shows clathrate stability zone for different soil compositions.

[1] Clathrate, also called methane hydrate, is a solid compound similar to ice in which a large amount of methane is trapped within a crystal water structure.

ESA ExoMars 2016 EDM demonstrator and 2018 rover missions

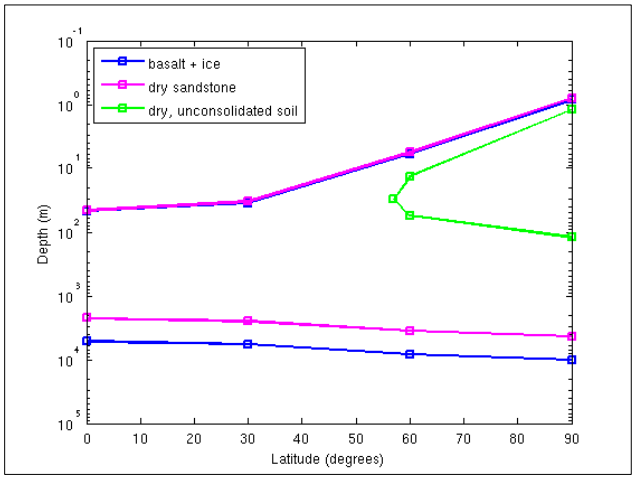

Stability zone of methane clathrates (between the lines of same color) in Martian subsurface for different soil compositions.

The stability zone of clathrates formed from a mixture of methane and hydrogen sulphide and the ones formed from a mixture of methane and nitrogen have been computed. Contrary to the addition of N_2, the addition of H_2S to CH_4 clathrates extends the stability zone and thus brings it closer to the surface. Therefore, mixed clathrates CH_4-H_2S will be more easily destabilized by changes in surface temperature than CH_4 clathrates.

Entry, Descent and Landing (EDL)

The ESA-Roscosmos 2016 ExoMars mission will attempt Europe's first successful landing on the surface of Mars. The 2016 demonstration mission is paving the way for a mobile rover in the subsequent 2018 ExoMars mission. Atmospheric entry consisting of Entry, Descent and Landing (EDL) presents an opportunity to observe the Martian atmosphere in-situ. The Royal Observatory of Belgium develops tools for the reconstruction of trajectories and atmospheric profiles during EDL in support of the 2016 ExoMars EDL Demonstrator Module (EDM) post-flight analysis. That is the science investigation using the flight data acquired during atmospheric entry.

EDM will enter the Martian atmosphere during dust season, the first such possibility to study dusty Mars atmosphere conditions in-situ. EDM is equipped with a novel instrumented heat shield: pressure sensors directly exposed to the atmospheric environment complement conventional measurements of vehicle acceleration and rotation rate. The additional flight instrumentation permits independent reconstruction of atmospheric conditions and can potentially observe atmospheric winds. Mars orbiters and landed platforms have so far provided practically no such wind observations.

OD1 scientist have performed trajectory and atmosphere reconstruction using self-developed tools to exploit both conventional and novel flight data. An entry flight simulator to generate synthetic flight data completes the tool set. These tools have been applied to the 2016 ExoMars EDM scenario to quantify the performance of post-flight atmospheric reconstruction. A parachute flight simulation model has further been developed for extending the study's scope. Normal and global dust storm scenarios have been considered, the latter based on quite extreme dust opacity estimates.

The figure compare density and temperature profiles between both weather scenarios. Density variations reach 300% but do not affect the trajectory much at high altitudes due to the very low absolute density there. The largest temperature variations between the two scenarios occur between 20 and 80 km. the figure below compares wind profiles. Very fast retrograde winds are predicted, exceeding 200 m/s above 80 km in the dust scenario. These are caused by migrating thermal tides due to solar heating forcing, which drag the atmosphere toward the sub-solar point. Predicted wind speeds in the normal weather scenario are smaller by about a factor two but still significant.

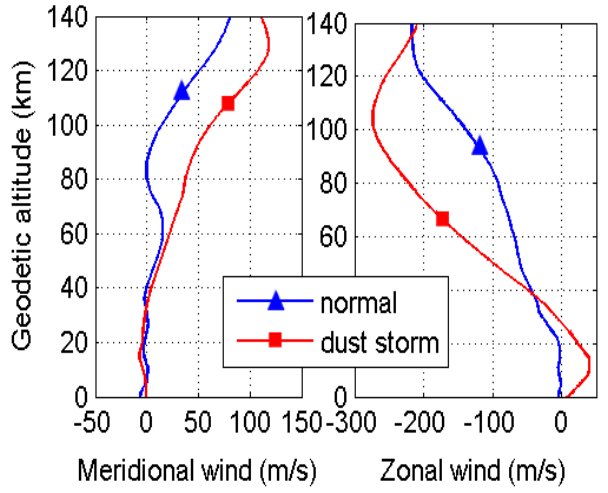

MCD normal and dust storm wind profiles

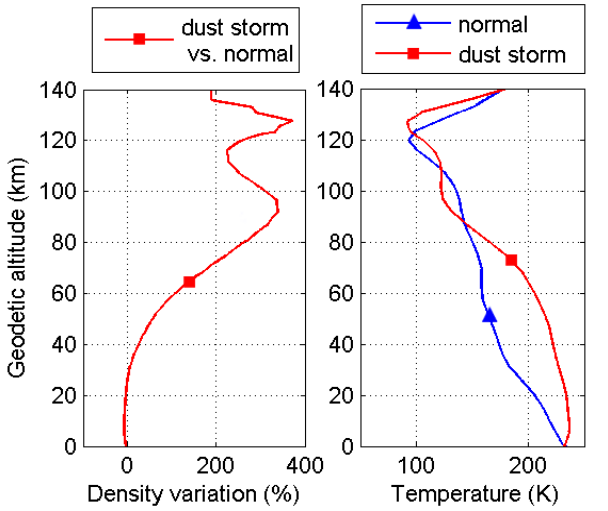

MCD normal and dust storm profiles

Phobos

The two Martian moons Phobos and Deimos might be asteroids captured by Mars' gravitational attraction or have formed in situ from accretion in a debris disk in Mars' orbit. The composition of Phobos and Diemos is important for getting an idea of their origin. The current measurement of the low-degree of the gravity field of Phobos (namely C_{20}) is not precise enough (-0.11 +/- 0.1) to constrain the porosity vs water ice content inside Phobos or the density of the rocky compound. Numerical simulations of the retrieval of the C_{20} coefficient from close flybys have been performed and conclued that the main source of error on the C_{20} solution is the correlation with the mass (the GM solution) and especially the error on the ephemeris of Phobos, both yielding a bias on the C_{20} solution of up to 40%. OD1 scientists have thus proposed to use the Super Resolution Camera (SRC) onboard Mars Express in order to perform astrometric position measurements of Phobos before and after a flyby event dedicated to the determination of Phobos' gravity field. From these images it is indeed be possible to improve Phobos' ephemeris in a short data-arc around the flyby event. The ESA's Mars Express (MEX) project has performed a very close flyby of Phobos at the closest approach) on December 29th 2013, where the proposed strategy has been implemented.

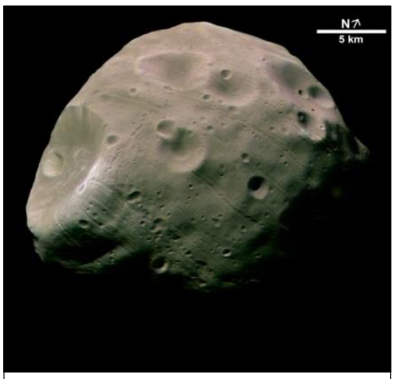

Image from Mars Express of Phobos, the closer to Mars of the two Martian moon (copyright ESA-DLR)

MarsExpress ESA spacecraft, presently around Mars (ESA)

Large natural satellites

Due to the presence of a subsurface ocean, the interior of icy satellites can perform translational oscillations with respect to the ice shell similarly to the translational oscillation of the inner core of the Earth (Slichter mode of the Earth).

The Slichter mode periods of Europa, Callisto and Titan range from a few hours to a few tens of hours, depending mainly on the ocean thickness (See figure on the right page). Observation of the Slichter mode period would then allow constraining the thickness of the ocean. This is especially true for thin oceans where a precision of one hour on the determination of the period result in an error on the ocean thickness of about 5 km (at a thickness of about 25 km) for Europa, an error of 15 km (at a thickness of about 50 km) for Callisto and an error of 25 km (at a thickness of about 50 km) for Titan. Due to the presence of two liquid layers in its interior, Ganymede can have two Slichter modes: one for the inner core within the outer core and the other for the mantle inside the ocean. Again, the Slichter mode periods of the mantle within the ocean range from a few hours to a few tens of hours, depending mainly on the ocean thickness.

As the shells of icy satellites are very thin in comparison with their interiors, the amplitude of motion of the shell is larger than for the Earth (for the same amplitude of motion of the interior). The Slichter modes of icy satellites would therefore be more easily detected than for the Earth. Alexis Coyette has calculated that an impact of a meteoroid with a radius of the order of a few kilometers or a few tens of kilometers would excite the Slichter mode of icy satellites to an observable level for a lander on the surface of these satellites. Such impacts occurred on average once in >50 My for Europa, Ganymede and Callisto and once in >0.4 Gy for Titan. Due to the dissipation timescale of the Slichter modes, the detection of the Slichter modes of icy satellites will require a fortunate recent impact on the surface of icy satellites.

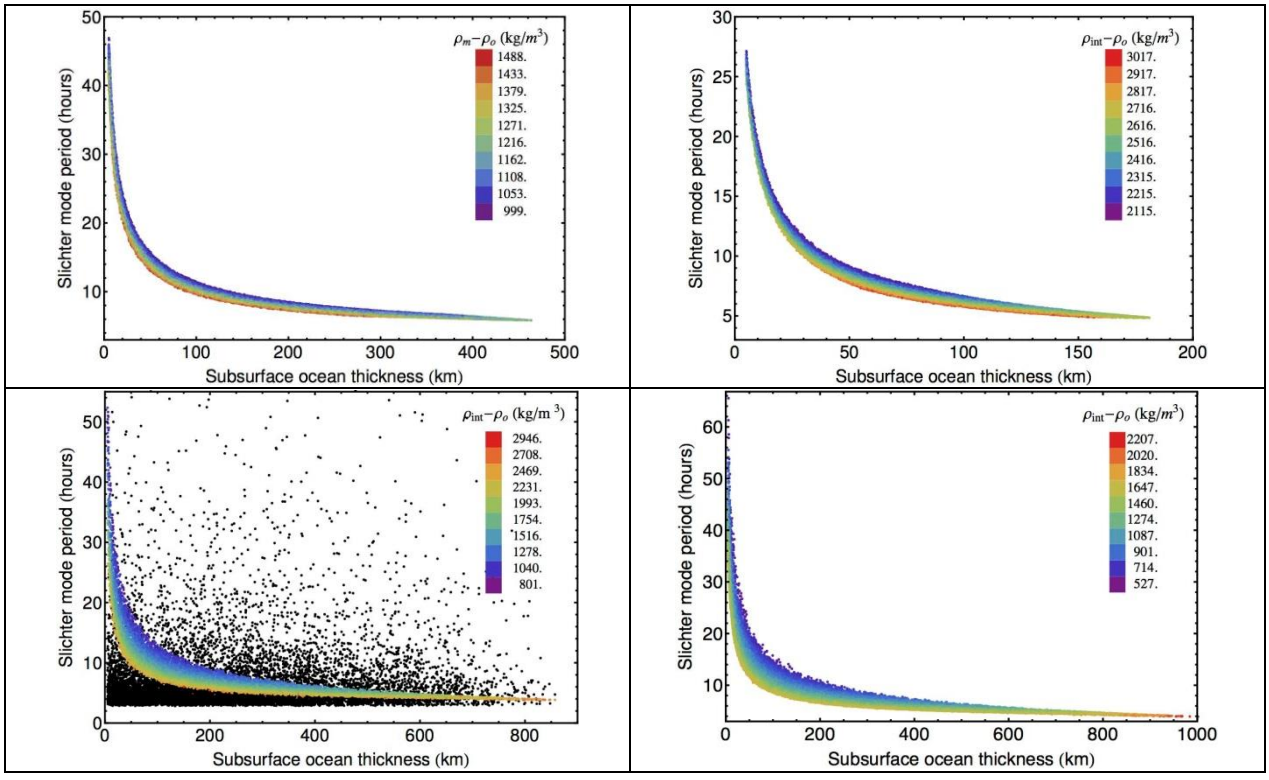

Slichter mode period as a function of subsurface ocean thickness for a set of models of Callisto (top-left), Europa (top-right), Ganymede (bottom-left) and Titan (bottom-right). The color scale represents the density jump between the interior and the subsurface ocean. For Ganymede, two translational mode periods are obtained due to the presence of two liquid layers in its interior (the outer core and the subsurface ocean).

Venus atmosphere from drag campaigns

The ten VExADE drag campaigns have been analysed. The density of the neutral polar atmosphere at altitudes between 165 and 185 km is lower than the predicted VTS3-model density by a factor of 0.6 for all campaigns. These globally low densities show that the modeled density, obtained by extrapolating the density at the equatorial latitudes at the terminator to the polar areas, cannot account for the observed densities. In addition, high variability of density values from one pericenter to the other, especially in campaign#4, #5 and #7, has been observed while not accounted for by the models. OD1 scientists have proposed a polar vortex in the polar thermosphere to explain this low measured density. However, the last campaign (campaign#10) seems to infirm this hypothesis unless the vortex has spread out to lower latitudes with increasing Solar activity. However, the Venusian thermosphere is known to be weakly reactive to Solar activity so that it seems unlikely that the Polar vortex might extend in latitudes with increasing Solar activity. An alternative explanation is the existence of a steady-state wave structure in the density of the thermosphere at altitude range between 160 and 190 km. This hypothesis needs however to be confirmed by completing the altitude range probed by VExADE, in particular the 165 to 175 km altitude range. An opportunity will occur with the aerobracking manoeuvre due for June-July 2014.

Venus and its habitability

OD1 has studied, in the frame of the IUAP Planet Topers, the long term evolution of terrestrial planets, taking into account many different mechanisms that have a direct effect on surface conditions and habitability, with the objective to obtain a precise and complete view of the planet's history from its solid part to its atmosphere. Among these mechanisms we consider mantle convection, surface conditions and potential resurfacing events, volcanic degassing, atmospheric escape, and the interactions between these layers. Venus is similar to the Earth (bulk composition, formation…) except for its massive atmosphere, which will enhance the coupling mechanisms. Planet Topers members of OD1 have thus studied:

- Atmospheric escape (hydrodynamic): relevant during the early evolution (0-500 Ma), when Extreme UV flux leads to massive loss of hydrogen and oxygen. Noble gases are fractionated during that time.
- Atmospheric escape (Non-thermal): the main escape mean during the bulk of the evolution, using different mechanism. ASPERA data for present day are used, as well as modern numerical simulations.
- Atmospheric surface conditions: vertical profiles of pressure and temperatures are monitored. A radiative-convective model is used for determining the atmospheric conditions, based on the greenhouse effect of water and CO_2.
- Mantle dynamics and volcanism: they are calculated with an adapted version of the state of the art StagYY code developed initially by Paul Tackley.
- Effects of meteoritic and cometary impacts on the atmosphere and the mantle of the planet.

These mechanisms and their feedback are summarized in the next figure.

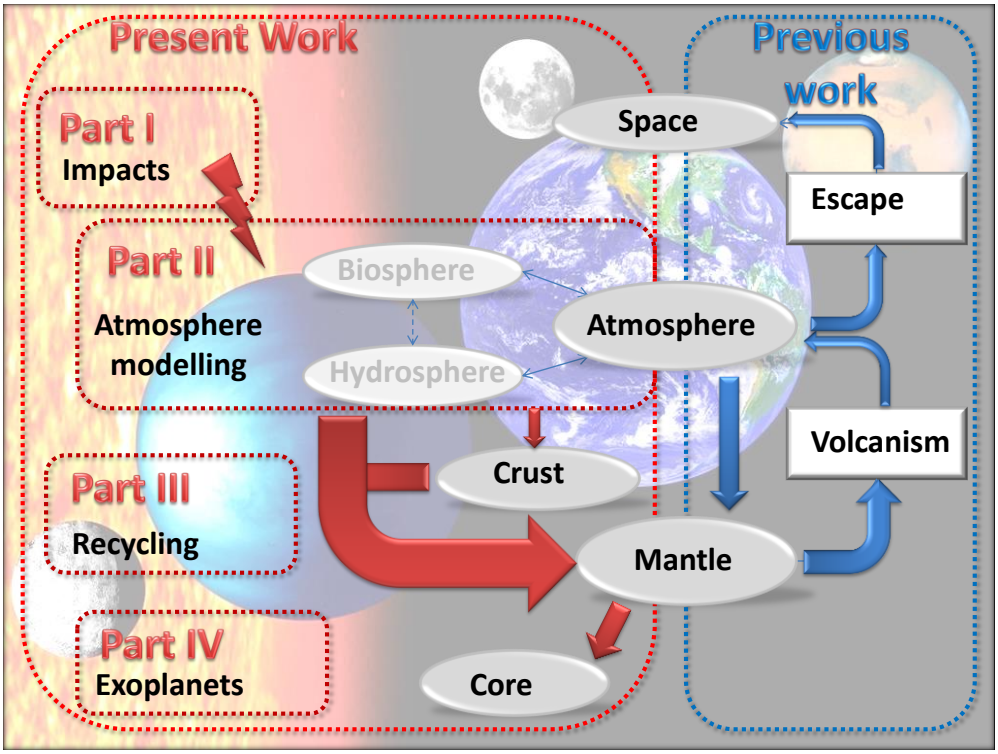

Mechanisms and feedbacks between layers in a terrestrial planet together with intended work. Stages of advancement of this project are in red while finished state is in blue.

During early atmospheric evolution hydrodynamic escape is dominant, while for later evolution we focus on non-thermal escape, as observed by the ASPERA instrument on the Venus Express Mission. The atmosphere is replenished by volcanic degassing from the mantle, using mantle convection simulations

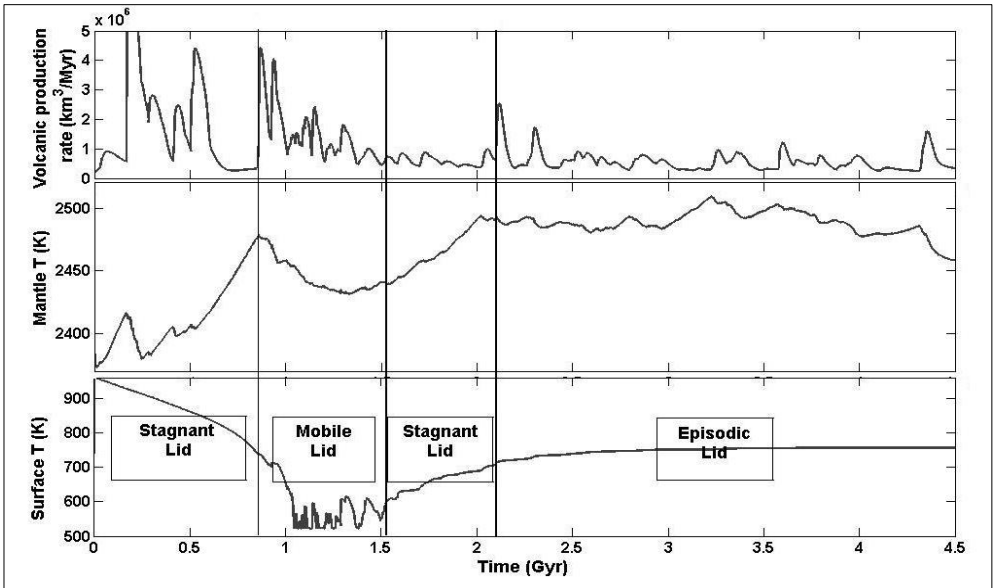

Comparative evolution of volcanic production rate, surface temperature and volume averaged mantle temperature with time for the reference case. Also indicated are the different convective regimes. The transition from mobile lid to stagnant lid is progressive. Early evolution (before 700Myr) follows an episodic, but mostly stagnant, lid pattern.

and including episodic lithospheric overturn. The evolving surface temperature is calculated from the amount of CO_2 and water in the atmosphere using a radiative-convective atmosphere model. This surface temperature in turn acts as a boundary condition for the mantle convection model. A Venus-like behavior (episodic lid) for the solid planet was obtained together with an atmospheric evolution leading to the present conditions. CO_2 pressure is unlikely to vary much over the history of the planet; with only a 0.25-20% post-magma-ocean build-up. In contrast, water pressure is strongly sensitive to volcanic activity, leading to variations in surface temperatures of up to 200 K, which have an effect on volcanic activity and mantle convection. Low surface temperatures trigger a mobile lid regime that stops once surface temperatures rise again, making way to stagnant lid convection that insulates the mantle.

This evolution model is also extended by incorporating erosion from meteorite impacts taking into account that meteorites and comets can bring volatiles as well. Due to large uncertainties in the simulation of the effects of large impacts, two different cases have been taken into account, as presented in next pages top figure. Mantle dynamics are modified since the impact itself can also bring a large amount of energy to the mantle. A 2D distribution of the thermal anomaly due to the impact is used and can lead to melting.

Short term and long term effects of the impacts on planetary evolution have been obtained. While small meteorites (less than kilometer scale) have a negligible effect, large ones (up to around 100 km) are able to bring volatiles to the planet and generate melt both at the impact and later on, due to volcanic events they triggered due to the changes they induce to mantle dynamics.

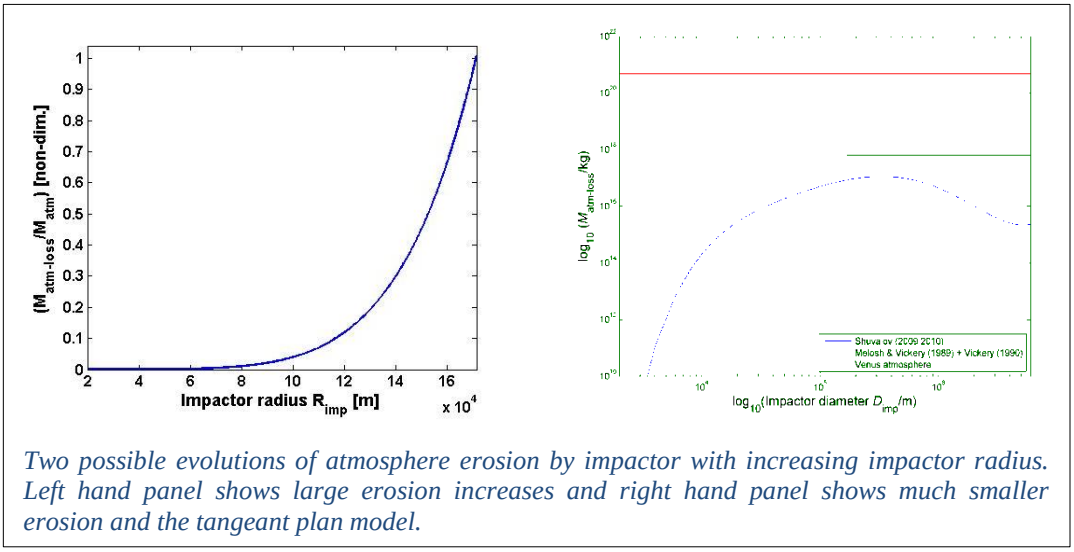

Two possible evolutions of atmosphere erosion by impactor with increasing impactor radius. Left hand panel shows large erosion increases and right hand panel shows much smaller erosion and the tangeant plan model.

A significant amount of volatiles can be released on a short timescale. Depending on the timing of the impact, this can have significant long term effects on the surface condition evolution. Atmospheric erosion caused by impacts, on the other hand, and according to recent studies seems to have a marginal effect on the simulations, although the effects of the largest impactors is still debatable.

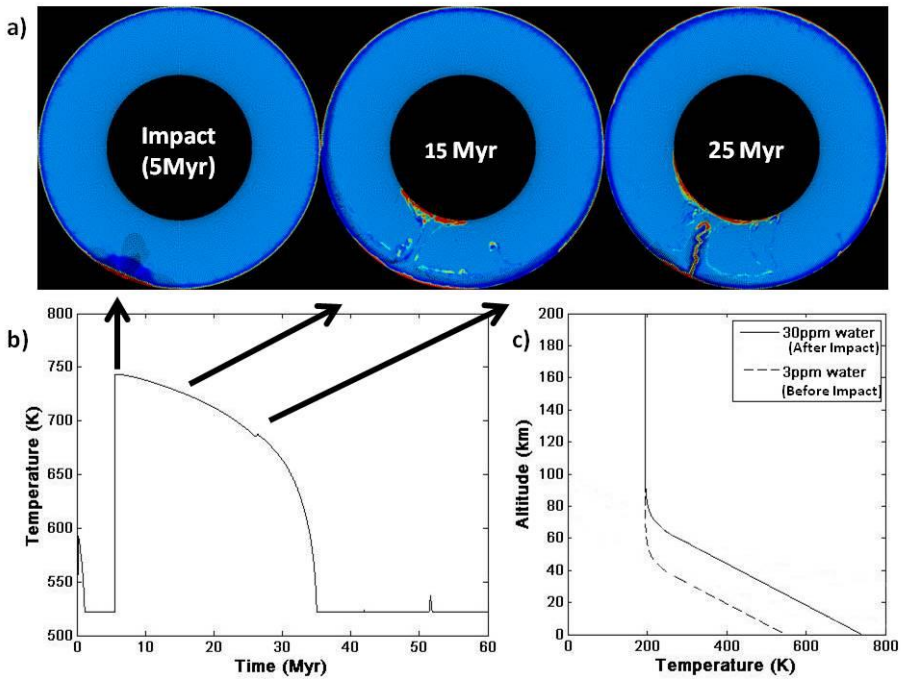

Coupled evolution of the atmosphere and mantle of Venus in the case of an early impact (5 Ma). (a) Composition of the mantle of Venus at three different times at and after the impact. Red colour represents basaltic rocks, while light blue is fertile and dark blue depleted mantle material. (b) Evolution of the Surface temperature of Venus. Thick black arrows indicate which part of the temperature profile corresponds to which stage of the simulation shown in (a). (c) Simple vertical temperature profile of the atmosphere before and just after the impact.

Seismology & Gravimetry

Activities of the operational direction seismology & gravimetry

The scientific activities of the operational direction seismology-gravimetry are partly related to the study of the seismic activity and their consequences in northwest continental Europe. Hence, during the last year, we finalized our different researches on the impact of past earthquakes in Belgium, we continued the study of historical earthquakes by searching original eyewitnesses in record-offices in Belgium and neighbouring regions and we synthetized our works on possible active faults in the Strait of Dover related to the large $5.5 < M < 6.0$ 1580 historical earthquake.

By managing the LISSA and GIANT projects at the Princess Elisabeth base in Antarctica, we investigate the lithospheric structure and its relationship to seismic activity. We also developed methodologies to monitor the volcanic activity in Indonesia [ANNEX 4]

In order to support its scientific research, its scientific expertise and to provide pertinent information to the public and the authorities, the section develops different operational projects with the purpose of:

- Monitoring the seismic activity in Belgium and surrounding regions by analysing the data from the Belgian seismic and accelerometric stations, developing and maintaining these networks;
- Developing the ways to provide fast and reliable information to the authorities and the public when an earthquake is felt or occurs in Belgium;
- Providing our measured seismic phases for worldwide seismic events and waveform data to the seismological international centres (EMSC, ORFEUS, IRIS and ISC);
- Providing the scientists in other institutions, the public, the administration and the private companies in Belgium with a scientific and technical expertise in earthquake seismology. In 2013, we strongly contributed to the seismic-hazard assessment for the Belgian nuclear sites.

Other scientific activities of the section are devoted to conduct and analyse gravity measurements at the Earth surface and also to analyse data from space experiments, mainly GRACE. Gravity measurements supply information on geographical structural heterogeneities in the underground and on geodynamical processes and their time evolution. An important part of this scientific work is devoted to evaluate crustal deformation using its imprint on the gravity signal. For this purpose, the section is in charge of the scientific and technical follow-up of the superconducting gravimeter installed in the Membach station, of an absolute gravimeter and one relative gravimeters. In 2013, we started contributing to a research program on the karst aquifer in the region of the Rochefort cave (Belgium).

The impact of earthquake activity in Belgium

The ROB seismology group studied the impact of the earthquake activity in the plate interior region extending from the Lower Rhine Embayment to southern England by developing methodologies combining the historical and architectural heritage records to better quantify moderate and extensive damage from past earthquakes. These methodologies have been applied to seven destructive earthquakes with magnitudes ranging from 4.5 to 6.0, characteristics of the seismic activity of this area [*The impact of the earthquake activity in Western Europe from the historical and architectural heritage records, In: P. Talwani (ed). Intraplate Earthquakes - Solid Earth Geophysic, Cambridge University Press (2014)]*.

The extremely high seismic vulnerability of this region is illustrated by the destructions resulting from small shallow earthquakes like the 1983 M=4.6 Liège (Belgium) and 1884 M=4 ¾ Colchester (England) earthquakes and the elevated financial losses produced by the 1992 M=5.3 Roermond (The Netherlands) earthquake, despite the low observed intensities. This vulnerability is directly related to the very high density of population and to the substantial part of poorly constructed masonry dwellings in the building inventory in most of the cities of Western Europe. Therefore, the consequences of a rare M~6.0 seismic event, like the Verviers (Belgium) 1692 earthquake, could certainly be catastrophic in terms of victims and destructions.

Comparing the damage caused by past earthquakes in large structures like churches or castles and classical dwellings provides information on their source and regional site effects. On the one hand, the earthquakes that caused moderate to heavy damage to large structures located far away from the epicentre had magnitudes greater than 5.0. On the other hand, the observation that churches were damaged in some localities of the Lower Rhine Embayment or the Brabant Massif while typical houses located in the same localities suffered less or had no damage is related to the presence of a low Q-factor sedimentary cover, and (or) a thickness corresponding to a soil fundamental period that enhances ground motion in the frequency range of the large building natural resonance frequency.

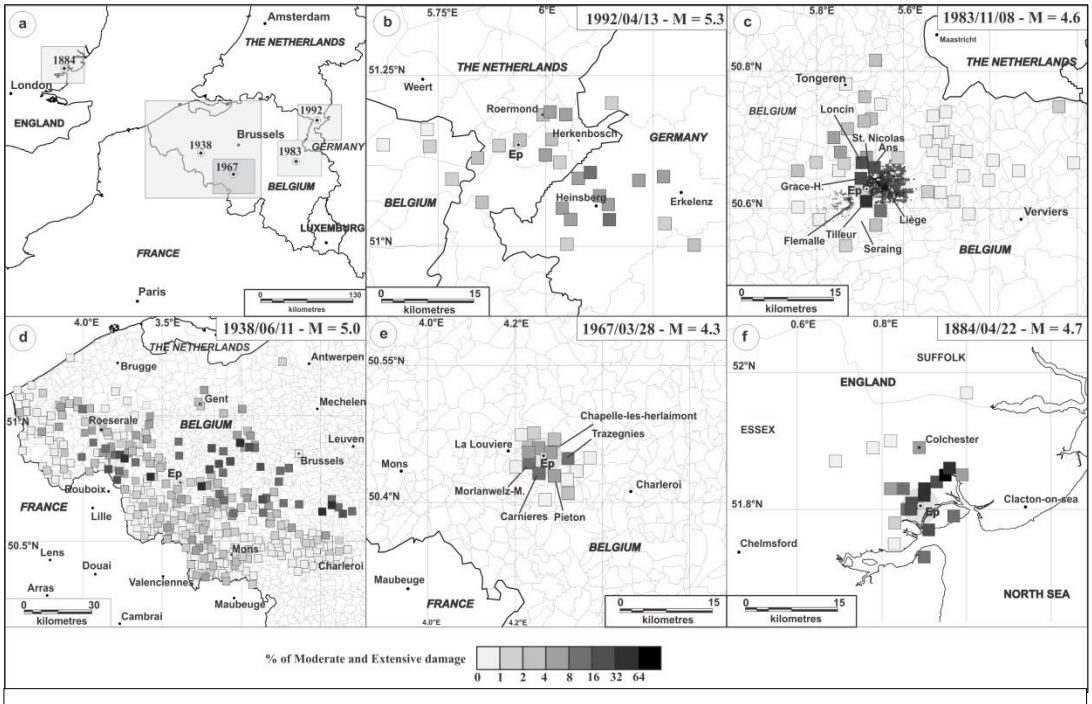

Statistics of the damage greater or equal than moderate for the 13 April 1992 Roermond (b), 8 November 1983 Liège (c), 11 June 1938 Nukerke (d), 28 March 1967 Carnières (e) and 22 April 1884 Colchester (f) earthquakes.

The 3 December 1828 earthquake at the border between Belgium and Germany

We conducted the first modern study of the 3 December 1828 moderate earthquake that occurred in the bordering region between Belgium and Germany. By conducting a systematic survey of contemporaneous historical sources, we added 40 eyewitnesses about the earthquake effects to the 21 that were previously known, improving our knowledge of the macroseismic field of the earthquake.

The strongest affected localities, where the fall of several chimneys and other slight damage were noticed, are Spa, Stavelot and Rocherath in the Hautes-Fagnes region [intensity VI-VII]. The earthquake also caused slight damage in Aachen [intensity V-VI]. Many people were frightened and ran outdoors, pieces of furniture were shifted and objects felt down from the tables and the walls in Burtscheid, Eupen, Henri-Chapelle, La Reid, Lontzen, Malmedy and Verviers [intensity V or V-VI]. At large distance, the earthquake was felt up to Düsseldorf to the north, Brussels to the west, Metz to the south and Wiesbaden to the east, corresponding to a radius of perceptibility of around 150 km.

From the intensity data points, we estimated the earthquake magnitude as M = 4.1 ± 0.5 and its focal depth as 10 ± 4 km. The earthquake location support the hypothesis that it occurred along the Hockay Fault zone which is the structure that is supposed to have generated the M = 6 ¼ 18 September 1692 Verviers earthquake, but more or less 20 km to the south-east.

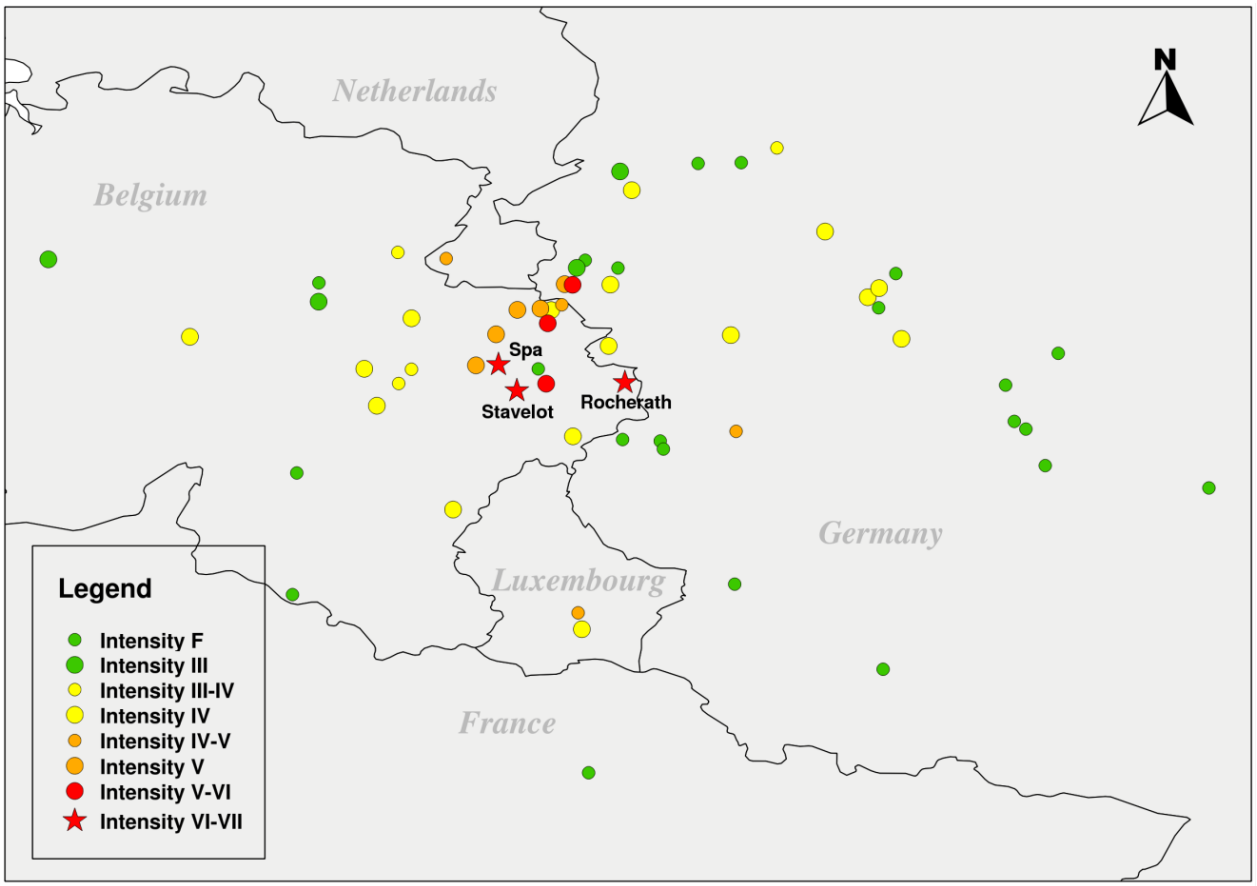

Macroseismic map of the 3 December 1828 earthquake

Fault activity in the epicentral area of the 1580 Strait of Dover earthquake

On April 6th, 1580 one of the strongest earthquakes of north-western Europe took place in the Dover Strait (*Pas de Calais*). The epicentre of this M = 6.0 seismic event has been located in the offshore continuation of the North Artois Shear zone, a major Variscan tectonic structure that traverses the Dover Strait. The location of this and two other historical moderate magnitude earthquakes in the Dover Strait suggests that this structure or some of its fault segments may be presently active.

In order to investigate the possible fault activity in the epicentral area of the AD 1580 earthquake, we have gathered a large set of bathymetric and seismic-reflection data covering the almost-entire width of the Dover Strait. The extent and quality of these data have resulted in very valuable information on the seabed morphology, fault geometry and geology of the Dover Strait. The data revealed a broad structural zone traversing the strait comprising several sub-parallel WNW–ESE trending faults and folds, some of them significantly offsetting the Cretaceous bedrock. The geophysical investigation has also shown some indication of possible Quaternary activity related to some of the identified faults. However, this activity only appears to have affected the lowest strata of Middle Pleistocene age, indicating very low slip rates during the Quaternary period. Hence, the AD 1580 earthquake appears to be a very infrequent event in the Dover Strait, representing a good example of the moderate magnitude earthquakes that sometimes occur in plate interiors on faults with unknown historical seismicity.

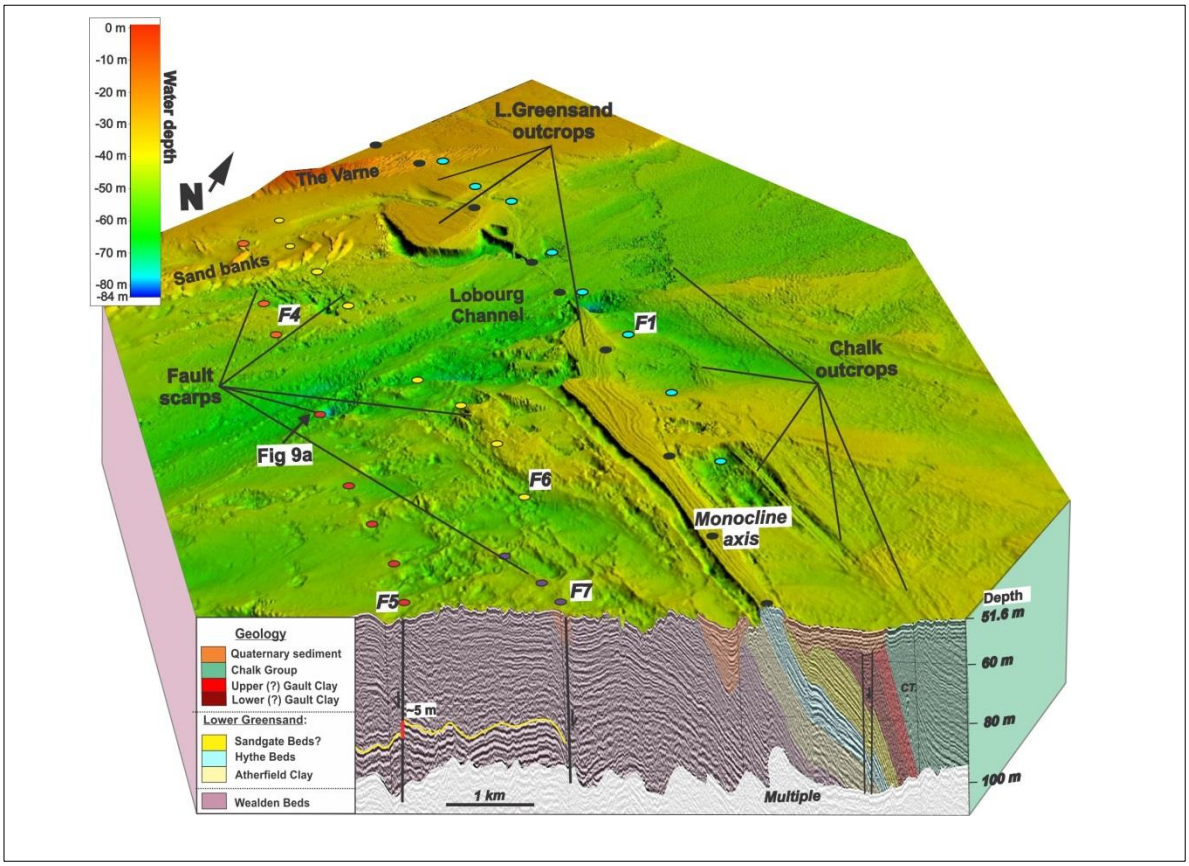

3D block showing the central and south-eastern merged bathymetry in the Strait of Dover in relationship with the interpretation of one of the single-channel seismic-reflection profiles. Coloured circles in the bathymetry represent the fault traces and monocline axis inferred from the seismic investigation.

Studying Indonesian volcanoes to better predict the behaviour of future eruptions

Since 2009 the ROB has been involved in research and monitoring on two Indonesian volcanoes situated on the island of Java. The Papandayan (West Java) and the Kawah Ijen (East Java) have been equipped with state of the art seismic stations in order to better study and understand their activity.
Our work on the Papandayan volcano shows that the states of the fluids within the volcano have changed during a crisis in 2011. These fluids, being a gas/water/steam mixture, are a good proxy for the state of unrest of the volcano. To obtain such information, seismic events called "long-period" (LP) have been analysed in depth. These events are characterized by a low frequency oscillation and represent fluid pressurisation associated with magmatic and/or hydrothermal fluids activities. The swarms of LP events have been split into two intervals. The first interval occurred between June and July 2011 (48 LP events), while the second interval extended from September to October 2011 (36 LP events). The frequencies of LP events observed during these intervals range between 1.1 and 6.2 Hz while the Q factors are widely scattered between 20 and 400. We estimate the compositions of fluids inside the crack during both intervals as either water foam (mixtures of water and H_2O gas/steam) or misty gas (mixtures of water droplets and H_2O gas/steam). We finally suggest that if an eruption were to have taken place following the 2011 unrest, it would have been in phreatic style rather than magmatic style. The results of our study therefore contribute to the effort in the prediction of the behaviour of future eruptions, and to volcanic hazards assessment, and therefore to volcanic risk mitigation [*Fluid dynamics inside a « wet » volcano inferred from the complex frequencies of long-period (LP) events: An example from Papandayan volcano, West Java, Indonesia, during the 2011 seismic unrest, Journal of Volcanology and Geothermal Research, doi:10.1016/j.jvolgeores.2014.05.005]*.

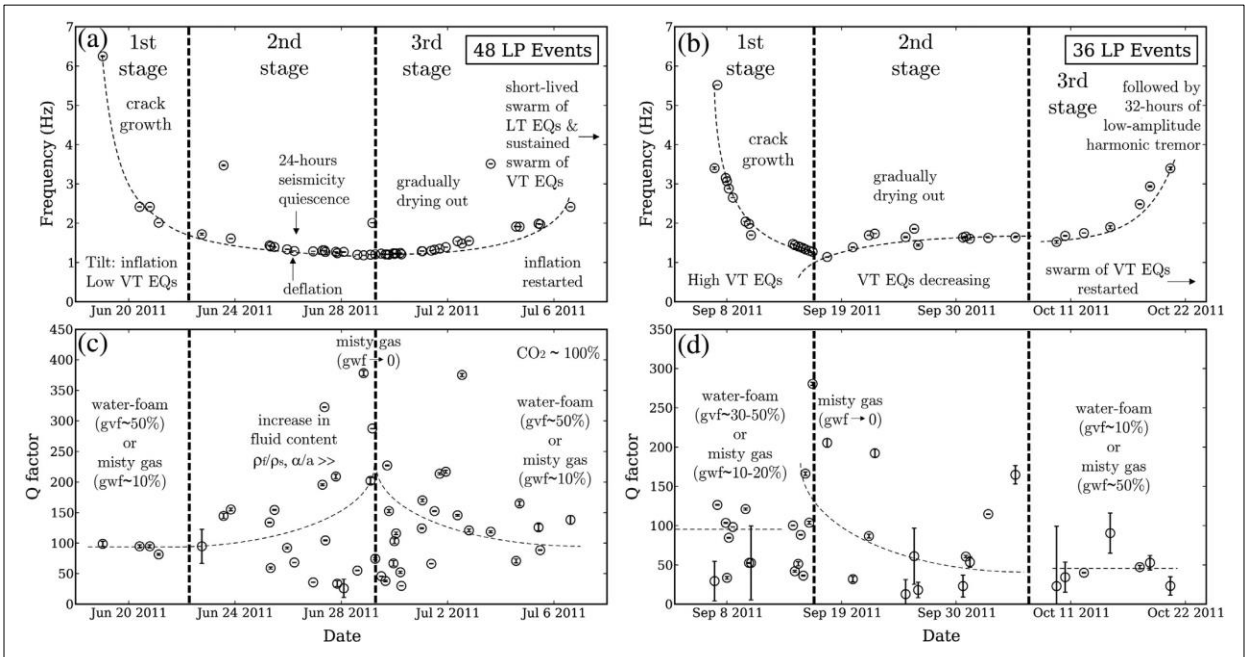

Temporal variations in the complex frequencies (f and Q factors) determined by spectral analysis for the dominant spectral peaks of LP events during two intervals: (a, c) between 19 June and 6 July 2011 (first interval) and (b, d) between 6 September and 20 October 2011 (second interval).

Karst aquifer research by geophysics

In cooperation with the universities of Namur, Mons and Luxembourg, The British Geological Survey and the Royal Meteorological Institute, our group started a project investigating aquifers in the Rochefort karst system in Belgium.

This F.R.S-FNRS project aims at leveraging our previous experience in karst, hydrogeology, gravimetry and geophysics to understand the water dynamics and storage in the Rochefort karst system. Of particular interest in Rochefort is the canalized Lomme River, which causes flash floods of the cave when the river spills off the dike. Hence, the continuous gravity measurements allow investigating the dynamics of karst system as a function of the degree of saturation at different time scales, from flash floods events to seasonal and interannual scales. A better knowledge of karst aquifers is paramount as they supply drinking water to 25% of the global population.

Combining the gravity measurements and other meteorologic, hydrologic and geophysics measurements will provide a better understanding of the water storage and transfer within the karst. As a preparatory phase, U. Luxembourg installed a gPhone spring relative gravimeter, while the ROB performed repeated absolute gravity measurements. The measurements have already evidenced the ability of the gPhone to measure the transient gravity changes caused by flash flooding's of the cave, as well as seasonal variations.

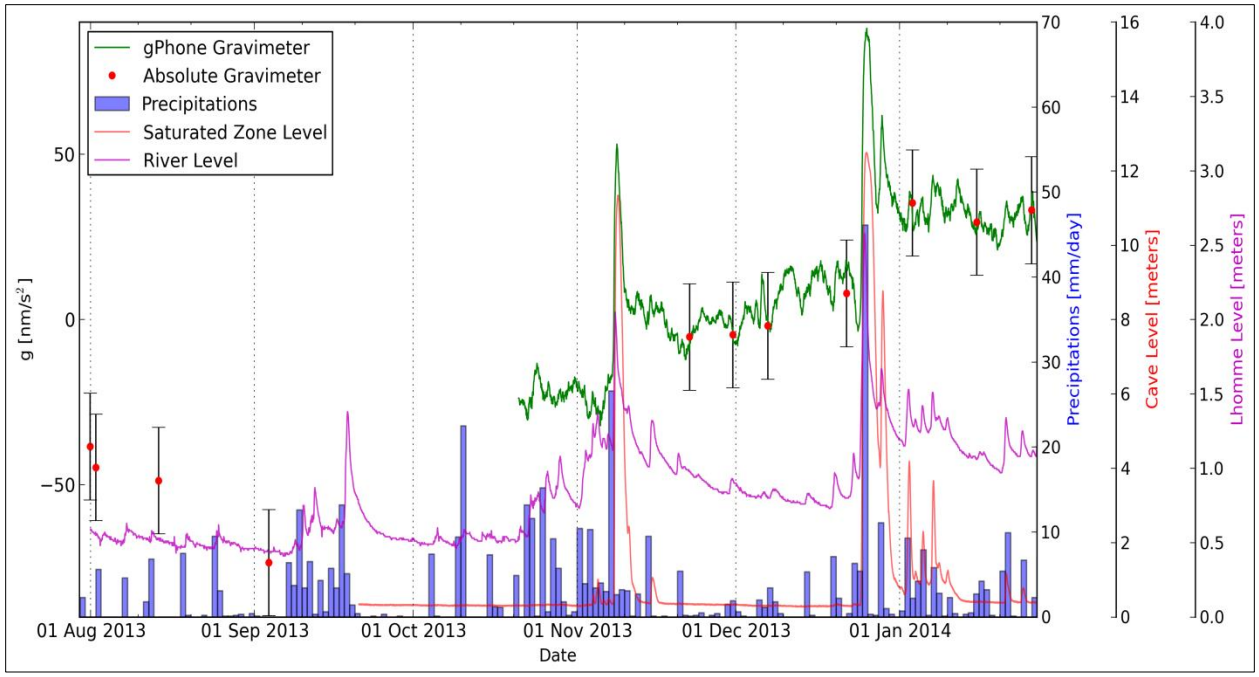

Gravity time series from the gPhone gravimeter (green), of which the instrumental drift was corrected using the absolute gravity measurements. Two steep increases in gravity of about 80 nm/s² are observed in November 2013 and December 2013, caused by flash floodings of the cave. Are also shown the precipitations (violet), the level of the Lomme river (purple) and of the aquifer (red). Concurrently to these transient events a slow increase in gravity is also observed, due to the recharge of the epikast and karst systems during the winter season. .

Astronomy and Astrophysics

Planetary Nebulae

The ESA satellite Herschel has provided several images of planetary nebulae. Planetary nebulae are the ejected outer layers of evolved stars. An international team led by ROB astronomers was able to deduce from these objects the properties of the central star and the dust in the nebulae. In 2013 the team published a paper discussing the Herschel PACS and SPIRE imaging of the evolved planetary nebula NGC 650 (the Little Dumbbell nebula). The images were used to construct a dust temperature map which showed that the hottest grains are in the low density regions in the hole of the torus. The colder grains on the other hand have a more or less spherical distribution. This is evidence for two radiation components heating the grains: direct stellar radiation which is readily absorbed in the torus and diffuse radiation (mainly Lyman α photons) which propagates everywhere and produces more or less circular isothermal contours. Based on modelling it was concluded that the grains in this nebula are large (0.15 μm), while excess emission around 25 μm could indicate the additional presence of very small grains (possibly PAHs, Polycyclic Aromatic Hydrocarbons) in the dense clumps in the torus. The model also indicated that the central star is hotter than hitherto assumed. The most plausible value is between 170000 and 190000 K.

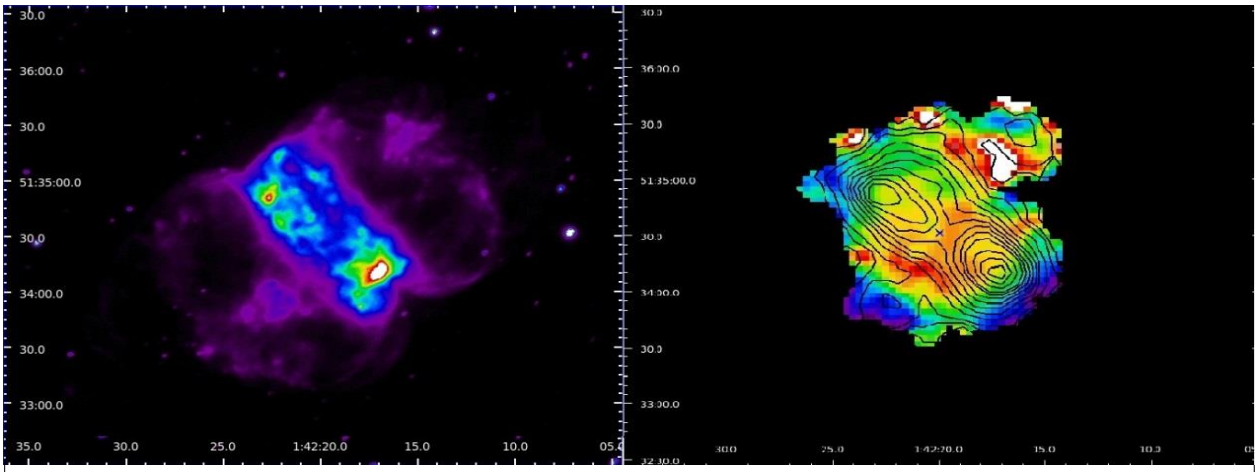

Optical image (Hα+[NII], Manchado et al., IAC catalogue, 1996) and a temperature map of the bipolar planetary nebula NGC 650, the Little Dumbbell. (van Hoof et al., A&A 2013)

Supernova SN 1987A observed with ALMA

The ROB participated in 2013 in the analysis of observations of supernova SN 1987A with ALMA, the Atacama Large Millimeter/submillimeter Array, located in Chile. The data showed the presence of cold molecular gas (CO and SiO) within the SN remnant, and demonstrated the power of using ALMA to gain insight into the physical conditions and chemical processes in the ejecta.

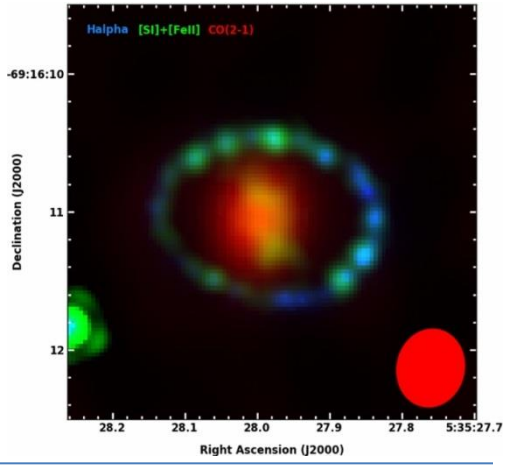

A color composite image of SN 1987A. The unresolved CO(2-1) line emission detected by ALMA is shown in red, and the red ellipse in the corner is the synthesized beam. Also shown are the Hα emission (blue) and [SiI]+[FeII] 1.644 μm emission (green in the ring, yellow in the ejecta) observed with the Hubble Space Telescope (From Kamenetzky et al., 2013)

Winds of massive stars

All massive stars have stellar winds, whereby they blow away their outer layers. When two such stars form a binary, their stellar winds collide, leading to increased X-ray and radio emission. ROB astronomers used archive data from the VLA (Very Large Array), covering a time range of 24 years, to study the radio emission of the hot massive O-type binary 9 Sgr. The light curve at a wavelength of 2 cm shows clear phase-locked variability with the 9.1 year orbit of this binary system. Fluxes are higher around periastron, as expected, because in this highly eccentric system the wind-wind collision is much stronger when the stars are closer to each other. To better study the periastron passage of 9 Sgr, additional radio observations were obtained in 2013.

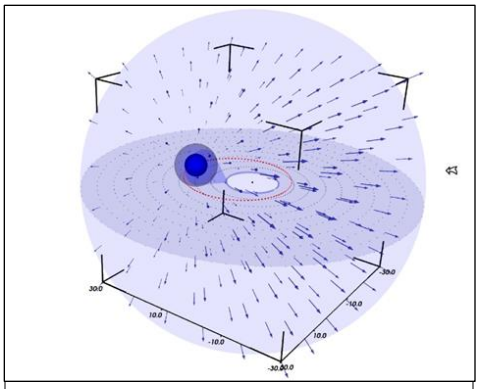

Model of the stellar wind in the binary system MWC314 (Alex Lobel, Astronomy & Astrophysics, 2013, © ESO)

A model of the stellar wind of the primary star of the binary system MWC314 was computed. This primary star is a luminous blue variable candidate with a mass of about 40 solar masses. Detailed radiative transfer fits show that the geometry of the wind density is asymmetric around the primary star. Wind accretion in the system produces a circumbinary disc. MWC 314 is in a crucial evolutionary phase of close binary systems, when the massive primary star has its H envelope being stripped and is losing mass to this circumbinary disc. The observations with the Hermes spectrograph from the Mercator telescope on La Palma were crucial in this study.

Interferometry and rotation

The sensitivity of interferometric observables on the position angle of the rotation axis of a rapidly rotating star was studied, using α Cep (Alderamin), a test star for the CHARA interferometer of Mount Wilson (Georgia, USA). It was concluded that the surface differential rotation can have a rather strong influence on the determination of the gravity darkening exponent. A new method of determining the inclination angle of the stellar rotational axis was suggested.

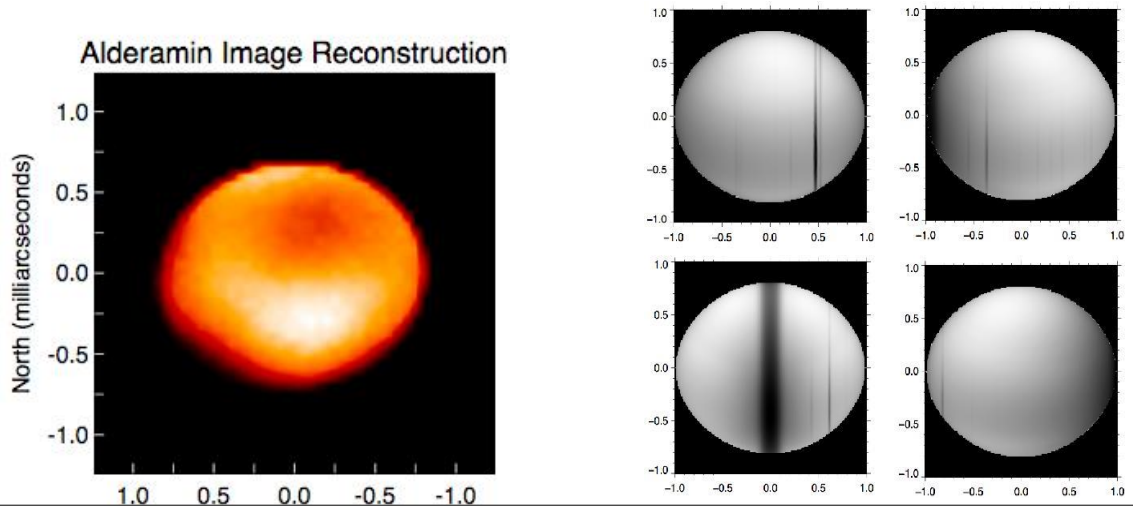

Left: Alderamin image reconstruction based on CHARA observations (Zhao et al, 2010)
Right: Surface brightness distribution in Alderamin at 4 different wavelengths: 6548.7 Å (top, left), 6557.7 Å (top, right), λ6562.8 Å (bottom, left), and 6568.5 Å, (bottom, right). Ordinates and abscissas are given in units of the equatorial radius of the star. The inclination angle used is i = 55°. (Delaa et al., 2013)

The ESA satellite GAIA launched

Soyuz VS06, with Gaia, lifted off from Europe's Spaceport, French Guiana, on 19 December 2013.

The ESA satellite Gaia was successfully launched on 19 December 2013. The launch was followed together with the press and guests directly in the Planetarium of the ROB. The ROB astronomers and co-workers contribute in different disciplines to the software development of the Gaia data reduction. This data reduction has been assigned to DPAC (Data Processing and Analysis Consortium). Inside DPAC several Coordination Units (CUs) were created. In CU4 (Object Processing) the ROB is involved in the Astrometric Reduction of Solar System Objects. For CU6 (Spectroscopic Processing) ROB has the responsibility to develop different techniques that will allow measuring the radial velocities of the stars. The characterization of variable objects, with emphasis on period search of variable stars is the main contribution of ROB to CU7 (Variability Processing). Within CU8 (Astrophysical Parameters) ROB develops algorithms and codes for the classification of extreme stars (mainly hot and emission lines stars).

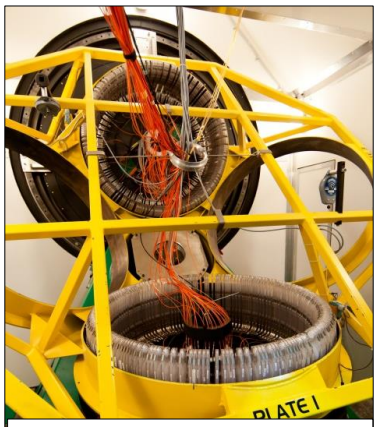

The two plates holding over 130 fibers each, for the multi-object spectrograph FLAMES on the VLT (ESO)

To realize the full potential of the Gaia space mission, a large consortium of astronomers, including staff members of the ROB, proposed the "Gaia-ESO Survey". This proposal was awarded 300 nights of observations (over 5 years) on the FLAMES instrument on the Very Large Telescope (VLT-UT2). The Gaia-ESO Survey is a public spectroscopic survey, targeting about 100,000 stars, systematically covering all major components of the Milky Way, from halo to star forming regions, providing the first homogeneous overview of the distributions of kinematics and elemental abundances. Specifically interesting for the ROB astronomers are the observations of massive stars in clusters. During 2013 spectra of 1210 stars were analysed at the ROB.

Solar Physics and Space Weather

Space Weather in 2013

The official annual sunspot number (SSN) for 2013, as determined by the WDC-SILSO (World Data Centre - Sunspot Index and Long-term Solar Observations), was 64.9. This is a 12% increase compared to the previous year.
The first nine months, long stretches of solar inactivity alternated with brief spurts of high flaring activity levels. Indeed, despite a brief outburst of active groups in April and May, the overall evolution was steady to a gradual decline, with rock-bottom in September when there was almost a spotless day on 10 September and an unusual long period of 10 days without a single solar flare (C-class or stronger). Then, driven by the southern solar hemisphere, sunspot activity quickly picked up with monthly sunspot numbers reaching the highest levels in two years. It is clear that solar cycle 24 (SC24) is heading for a new maximum, stronger than the one late 2011, and that most probably will be reached early 2014.

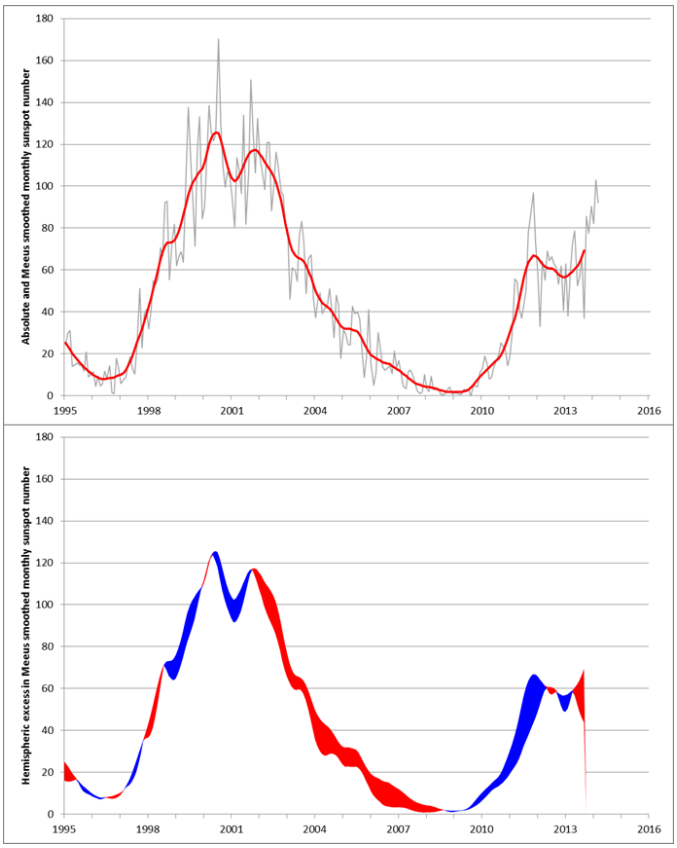

Right: The top chart displays the evolution of the monthly and monthly smoothed SSN (1995-2013), while the bottom chart shows the hemispheric excess with respect to the smoothed SSN, with blue an excess in northern SSN, and red an excess in southern SSN. Starting in the second half of 2013, a clear rise to a new and stronger maximum for SC24 can be seen, driven essentially by increased activity on the southern hemisphere.

Below: These pictures were taken using the white light telescope from the Uccle Solar Equatorial Table (USET), on 14 March (left) and 29 October (right) respectively. Over this time-interval, solar activity clearly switched hemispheres

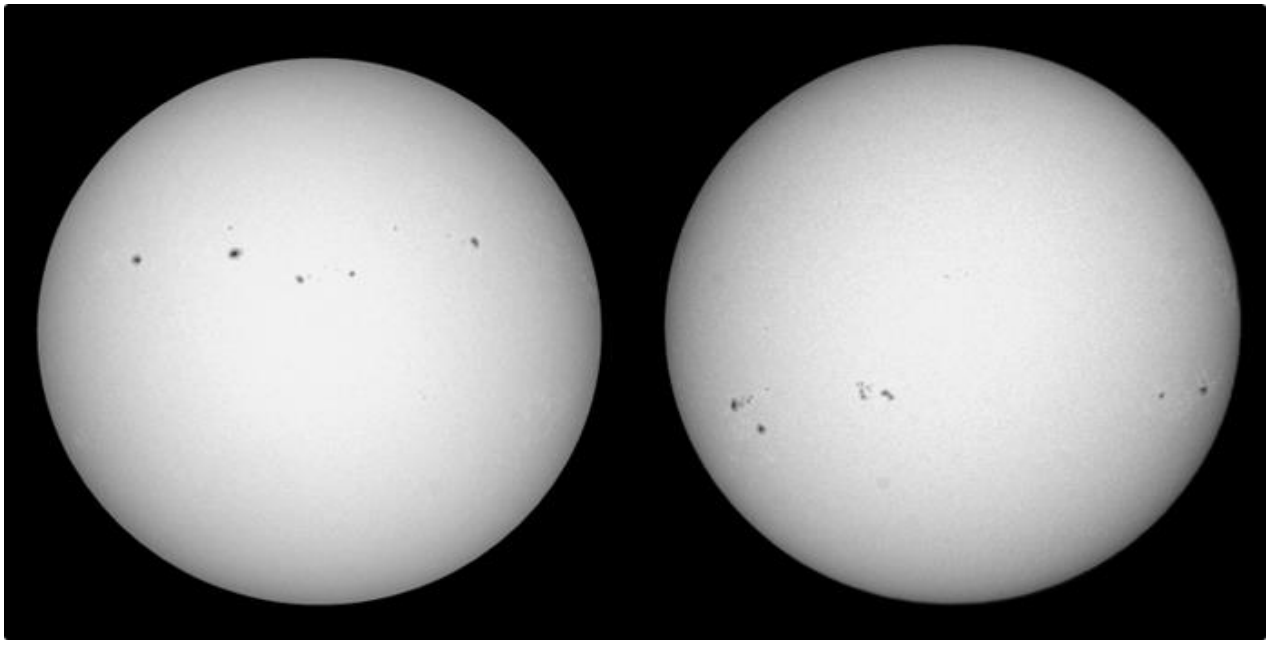

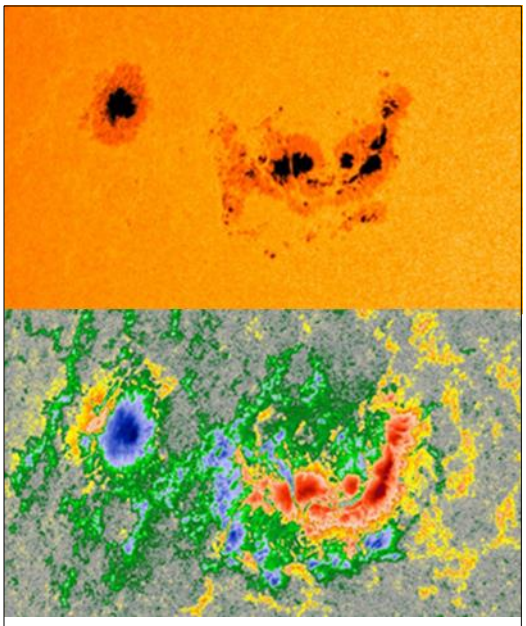

Above: NOAA 1654 was the largest sunspot group of 2013. Despite the complex outlook in white light, the opposite magnetic polarities were nicely separated, with the big sunspots in the main portion of the group all of the same magnetic polarity (red color).

The year opened immediately with the largest sunspot group that would be visible in 2013, NOAA 1654. According to the NOAA data, it reached its maximum sunspot area on 11 January, when it was more than 6 times as large as the surface of the Earth. Despite its size and its complex outlook, this sunspot group produced only 2 medium flares during its solar transit (on 11 January). The reason for this relatively meager flaring activity was that the opposite magnetic fields were nicely separated from each other, thus preventing the reconnections necessary to produce strong flares.

Most months of 2013 featured several filament and prominence eruptions, and *on the average* nearly half a dozen of coronal mass ejections (CMEs) every day. In particular the eruptions near the solar limb were truly spectacular. On several occasions they were featured in the STCE Newsletter (e.g. on 7 March, 31 July and 3 October). A few of the highlights are displayed in Figure xx. Note that due to their position close to the solar limb, Earth was hardly or not impacted at all.

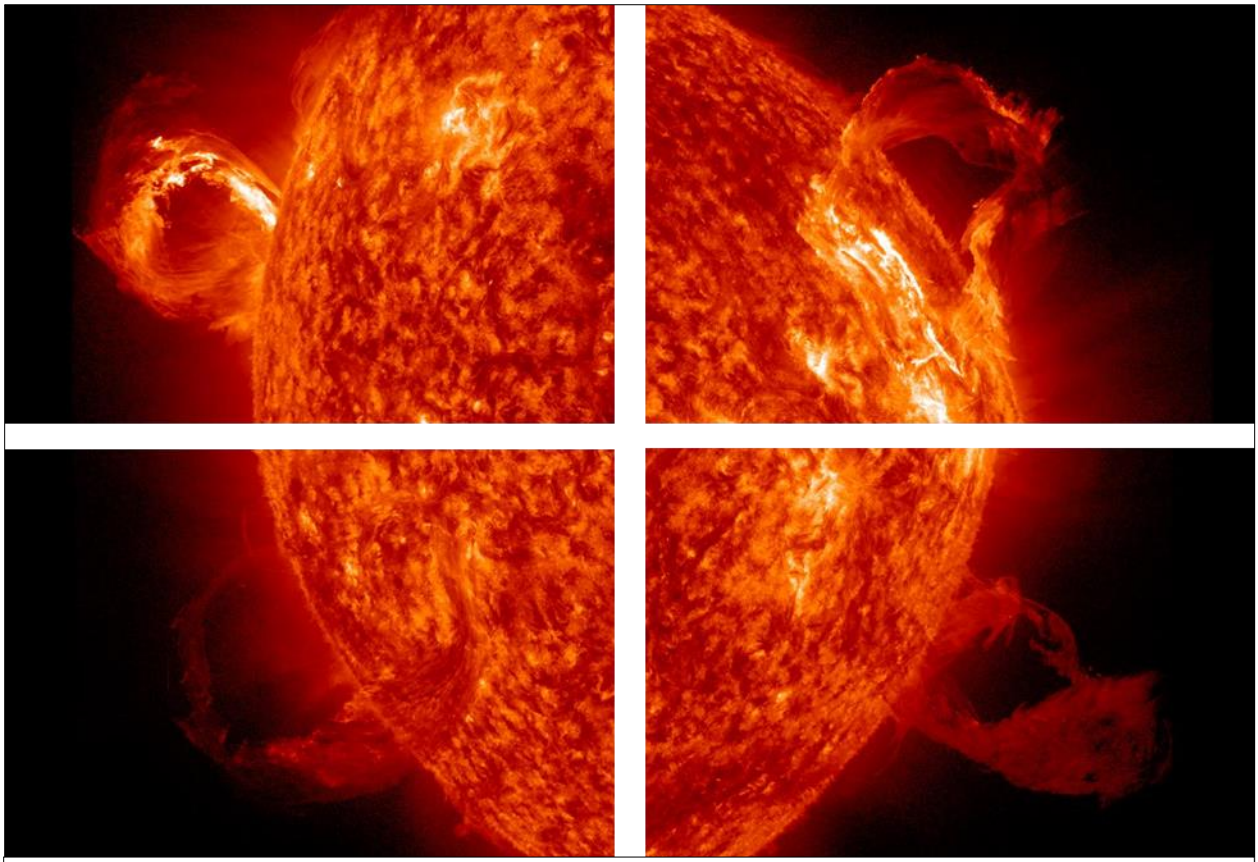

Above: Some of the finest filament and prominence eruptions in 2013. Top left: 1 May, top right: 16 March, bottom left: 31 January, and bottom right: 27 February.

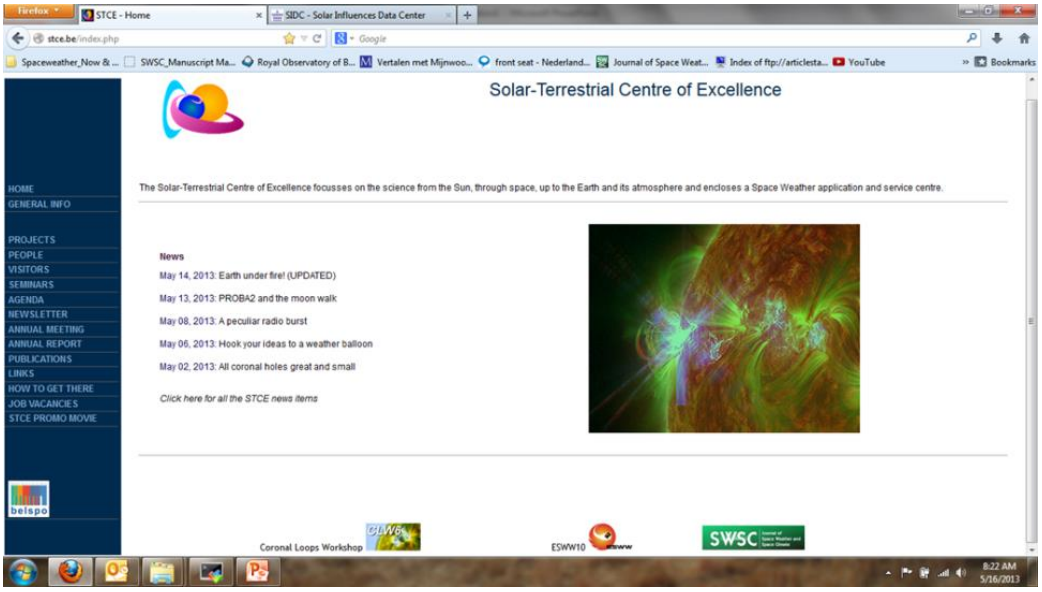

The X-class flares from NOAA 1748 were prominently featured and updated in near real-time on the STCE website (14-15 May 2013 and 21 May 2013, as well as in the STCE Newsletter).

The first spurt of high flaring activity occurred near mid-May, when in a time-span of only 48 hours NOAA 1748 managed to produce 4 X-class solar flares. This sunspot region was relatively small (4-5 times smaller than the aforementioned NOAA 1654), but was magnetically very complex. The first X-flare occurred when NOAA 1748 was still behind the east limb, and the 2 subsequent X-class events were actually white light flares (WLF) as seen by SDO's telescopes in visible light. During the last flare early on 15 May, NOAA 1748 had already rotated far enough onto the solar disk such that the associated CME became geo-effective on 18 May, sparking a minor geomagnetic storm.
One week later, on 22 May, an M5 flare took place in NOAA 1745 which was associated to the strongest proton event in 2013 (see STCE Newsitem of 29 May 2013). These protons can be seen as numerous white dots and stripes on the imagery from SOHO's coronagraphs. The event was 4 times less intense than the strongest proton event so far this solar cycle (March 2012).

The national sun observing day (7 July) in Belgium enjoyed sunny weather and the presence of a fine sunspot group (NOAA 1785). No wonder that the public observatories and local solar observing posts got a lot of visitors and media attention!

2013 saw the transit of various, large and persistent coronal holes over the solar disk.
One of the more impressive ones was visible in mid-July. This CH had an area equivalent to more than 300 times the surface area of the Earth (see STCE Newsitem of 25 July 2013). It managed to survive 8 solar rotations, with the first central meridian passage around 23 May, and the last one on 30 November (8 transits). It sparked geomagnetically active to minor storm conditions during the first 5 transits. The high-speed stream (700 km/s) also brought a whole bunch of high-energy electrons with it, and satellite operators noted a significant increase in anomalies during these periods, thought to be due to repeated electrostatic discharges. Fortunately, none of the spacecraft was permanently damaged. During its October and November transits, the CH had become too small to have a significant space weather impact (see STCE Newsitem of 23 October 2013).

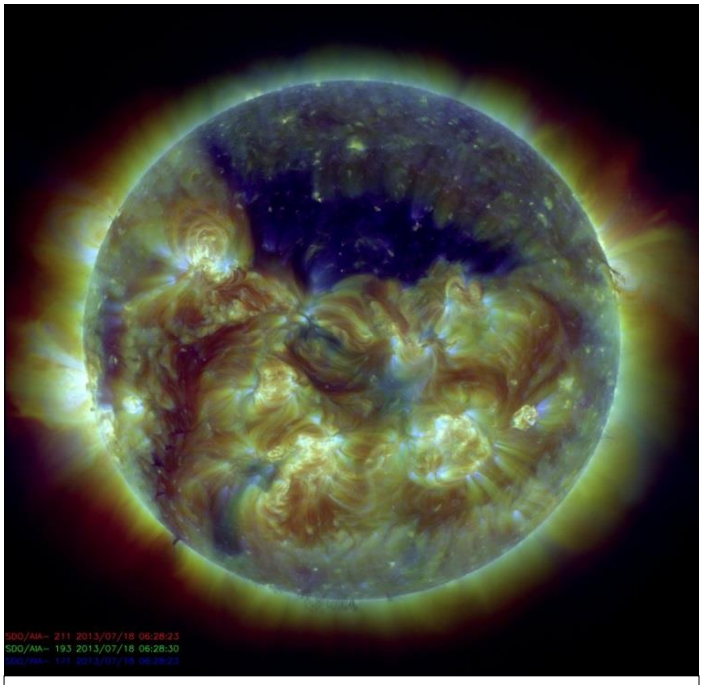

A large coronal hole was visible during the summer months. Its area was equivalent to more than 300 times the surface area of the Earth and resulted in geomagnetically active to minor storm conditions.

Late on 29 September, a long and solid filament in the Sun's northwest quadrant erupted in a spectacular way. The modest C1-flare (a so-called "Hyder" or "spotless" flare) lasted for more than 3 hours, and was also a moderate proton event. This long duration event (LDE) was accompanied by a CME shaped like a whip, and it definitely stirred the geomagnetic field. Indeed, this CME delivered a glancing blow to the Earth on 2 October, resulting in a strong geomagnetic storm (locally attaining even severe levels). Together with the storms of 17 March and 1 June, it belonged to the strongest geomagnetic disturbances of 2013 (see STCE Newsitem of 3 October 2013).

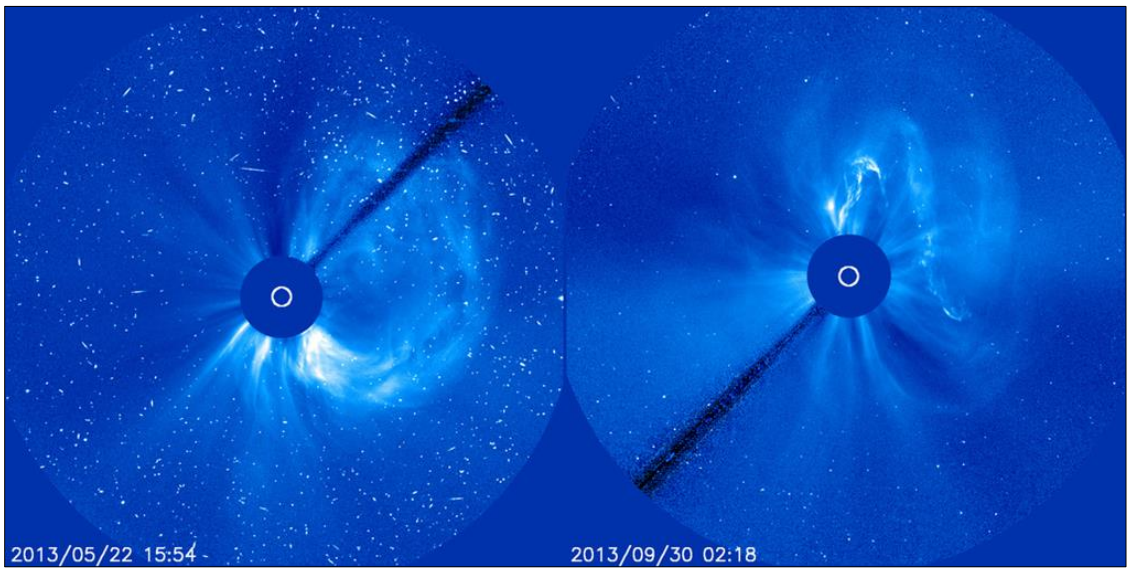

On the left the CME associated to the proton event on 22 May, and on the right the whip-like shaped CME associated to the filament eruption of 29 September.

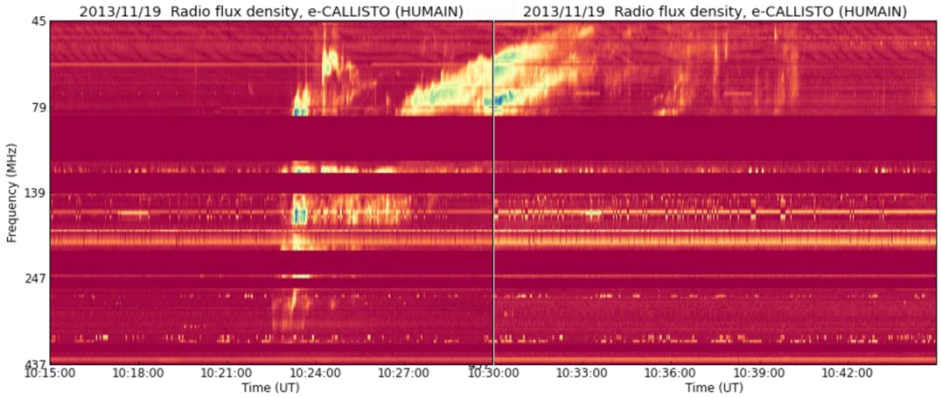

Geert Verbanck of the Belgian Solar Section captured this image of NOAA 1890 on 9 November, only hours before this sunspot group would unleash its third and final X-class solar flare.

A trio of complex sunspot groups significantly beefed up the flaring activity during the last week of October. From 22 till 29 October, no less than 26 M- and 4 X-class flares took place over the solar surface, making it one of the most flare intense periods so far this solar cycle. Responsible active regions NOAA 1875, 1877 and 1882 also destroyed a million km long solar filament in the process, and NOAA 1875 would stay very active during its subsequent backside transit of the Sun, as nicely recorded by the two STEREO-spacecraft.

On 5 November, NOAA 1890 produced an X3.3 flare, the strongest of the year and the number 3 -so far- in solar cycle 24. NOAA 1890 was a big sunspot group with a magnetically complex trailing part, and would produce another 2 X-class solar flares during its passage over the solar disk. All three were impulsive flares lasting 10 minutes or less, but they were each associated to a non-Earth directed CME. In total, there were 12 X-class flares in 2013, almost as many as 2011 and 2012 combined, and bringing the total for SC24 on 27. Yet, only 5 sunspot regions were responsible for these extreme explosions on the Sun. Meanwhile, the magnetic field near the solar north pole (finally) completed its reversal, whereas this magnetic flip is still ongoing at the south pole. These reversals testify we're close to the maximum of SC24. It remains to be seen how many ups and down this moderate solar cycle will show.

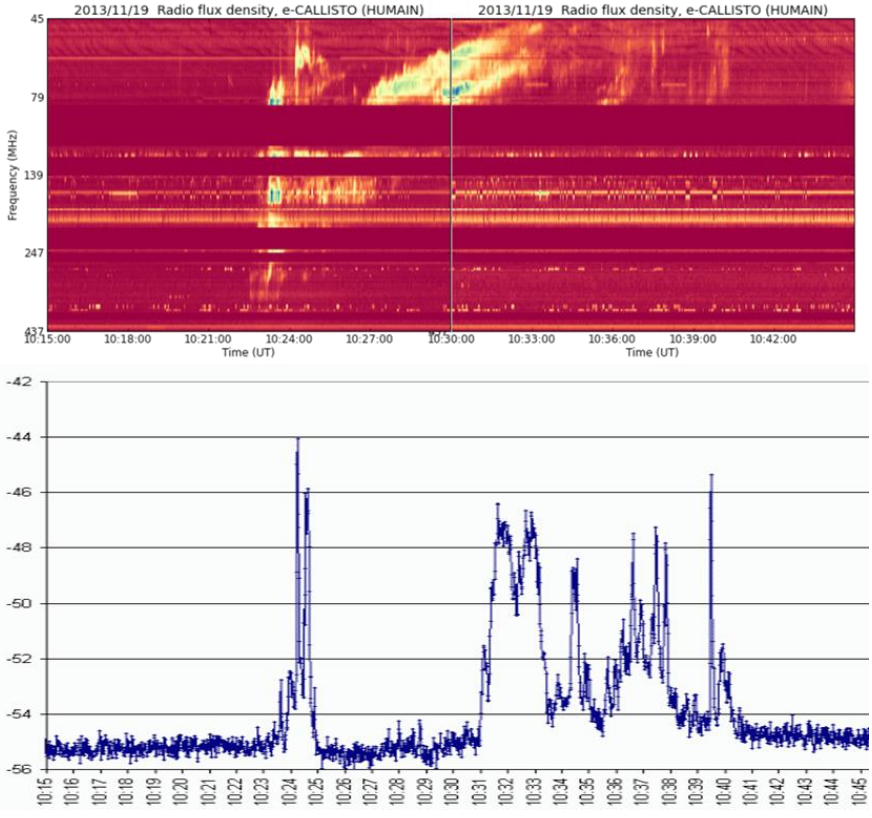

Radio observers from the BRAMS-network observed the X-class flare from NOAA 1893 at their frequency of 49.99 MHz on 19 November 2013 (bottom, and green dashed line on radio-spectrogram on top). The radio-spectrogram made by the Humain Solar Radio Observatory shows the full extent of the strong radio

COMESEP: forecasting the space weather impact

The COMESEP (COronal Mass Ejections and Solar Energetic Particles) Alert System was built under a three-year EU FP7 project (European Union Seventh Framework program) that concluded in January 2014. Tools for forecasting geomagnetic storms and solar energetic particle (SEP) radiation storms were developed validated and implemented into an operational space weather alert system that runs at present without human intervention. The COMESEP Alert System is triggered by solar phenomena such as CMEs (Coronal Mass Ejections) and solar flares. After the automatic detection in solar data of any of these transients, the different modules of the system communicate in order to exchange information. The system produces a series of coherent alerts that are then displayed online and sent via email to the subscribed users. In this way, COMESEP provides automatic notifications for the space weather community.

Arrival of CME / Likelihood of occurrence						
Ongoing (100%)	L	M	H	H	E	E
Very likely (90-100%)	L	M	H	H	E	E
Likely (70-90%)	L	M	M	H	H	E
Possible (40-70%)	L	L	M	M	H	E
Unlikely (10-40%)	L	L	M	M	H	H
Very Unlikely (0-10%)	L	L	L	M	M	H
Storm Level	None	Minor	Moderate	Strong	Severe	Extreme
Geomagnetic |Dst| in nT	<50	50-100	100-200	200-300	300-400	>400
SEP peak flux > 10 MeV in $s^{-1}sr^{-1}cm^{-2}$	$<10^1$	10^1-10^2	10^2-10^3	10^3-10^4	10^4-10^5	$>10^5$
SEP peak flux > 60 MeV in $s^{-1}sr^{-1}cm^{-2}$	$<7.9\times10^{-2}$	7.9×10^{-2} - 1.4	1.4 - 2.5×10^1	2.5×10^1 - 4.5×10^2	4.5×10^2 - 7.9×10^3	$>7.9\times10^3$
Kp	<5	5	6	7	8	9

The COMESEP risk matrix. The rows represent the probabilities of arrival of a CME or of an SEP event. The columns indicate the impact calculated for the corresponding geomagnetic storm or radiation storm (in two energy ranges).

The Alert system can be found online at http://comesep.eu/alert/. A general description of the system is available at http://comesep.eu/. The alerts are based on the COMESEP definition of risk that combines the likelihood of occurrence of the predicted event with its estimated impact at the Earth. This information, derived internally by the system, is then used to access the COMESEP risk matrix (right figure) and obtain the corresponding risk level for a particular event.

As an example, opposite page top figure shows the status of the alert system for the time period 24-27 February 2014. During that time, several flares and a CME occurred and were detected by the system (stars in the first two rows of the figure). The corresponding geo-magnetic storm and radiation storm predictions are shown in the last rows. The SEP storm with moderate risk predicted for February 25 actually arrived to the Earth and was measured by the GOES13 satellite (see opposite page). This occurred as a consequence of an X4.9 flare occurring at 00:49 UT, the COMESEP alert system dispatched the following e-mail alert correspondingly:

:Issued: 2014 Feb 25 0145 UTC
:Product: documentation at http://www.comesep.eu
#---#
COMESEP SEP Forecast message from BIRA-IASB (Brussels, Belgium),
forwarded by the SIDC (RWC-Belgium)
#---#
Forecast for a SEP radiation storm following a X4.9 flare with peak at
2014-02-25 00:49UT. The expected risk level is MEDIUM for a SEP storm of
protons > 10 MeV (occurance probability: POSSIBLE; storm level: MODERATE).
The expected risk level is MEDIUM for a SEP storm of protons > 60 MeV (occurance
probability: POSSIBLE; storm level: MODERATE).

#---#
Solar Influences Data analysis Center - RWC Belgium
Royal Observatory of Belgium
Fax : 32 (0) 2 373 0 224
Tel.: 32 (0) 2 373 0 491
# #
For more information, see http://www.sidc.be. Please do not reply
directly to this message, but send comments and suggestions to
'sidctech@oma.be'. If you are unable to use that address, use
'rvdlinden@spd.aas.org' instead.
To unsubscribe,
visit http://sidc.be/registration/unsub.php #
#---#

This example shows how an automated system can provide helpful aid to human forecasters in real time. The system is running continually 24/7.

Bottom Status of the COMESEP alert system for the period 24-27 February 2014. The first row shows the occurrence of solar flares (stars). The second row marks the eruption of CMEs. The third row shows the prediction for SEP storms. The last row displays the expected geomagnetic storms. The length of the bars in the last two rows is an indication of the expected duration of the corresponding radiation or geomagnetic storm, the color represents the risk level (see Figure 1).
Figure 3.right GOES 13 proton flux showing the SEP storm on February 25.

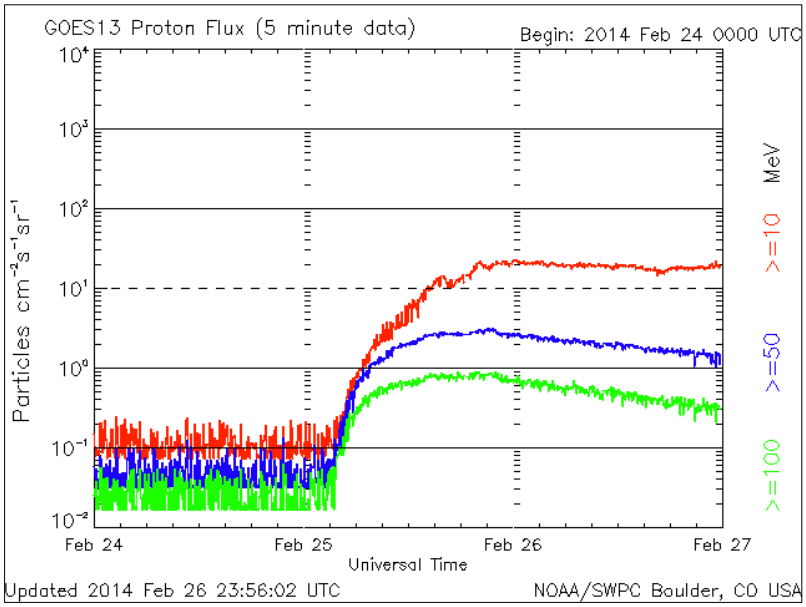

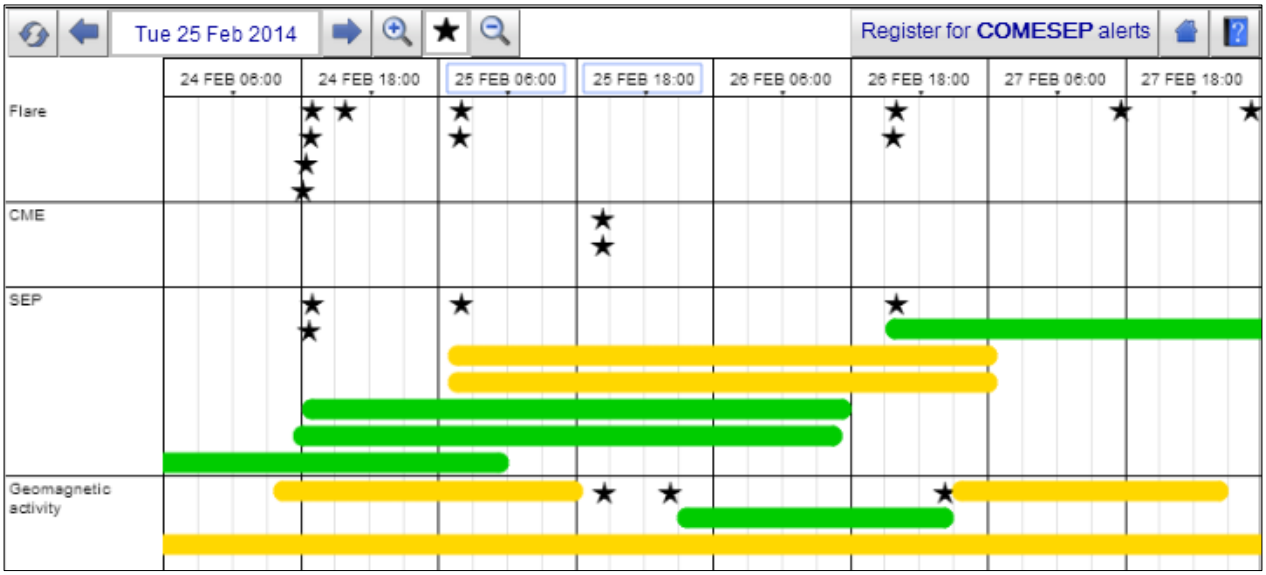

STCE workshops dedicated to the degradation and inter-calibration of solar instruments

Investigating and analyzing the degradation of space instruments are crucial to achieve their scientific goals. Remote–sensing instrumentation exposed to the space environment usually degrades due to the harsh environment in which the instruments operate. Solar instruments – telescopes, spectrographs and radiometers - are particularly vulnerable because their optical elements are exposed to unshielded solar radiation.
For example, the Large Yield Radiometer (LYRA) onboard PROBA2 has strongly suffered substantial degradation due to a combination of ultraviolet (UV) solar irradiation and instrumental contamination that can cause polymerization of organic material and, subsequently, irreversible deposition of this material on the instruments' optical surfaces (see right figure).

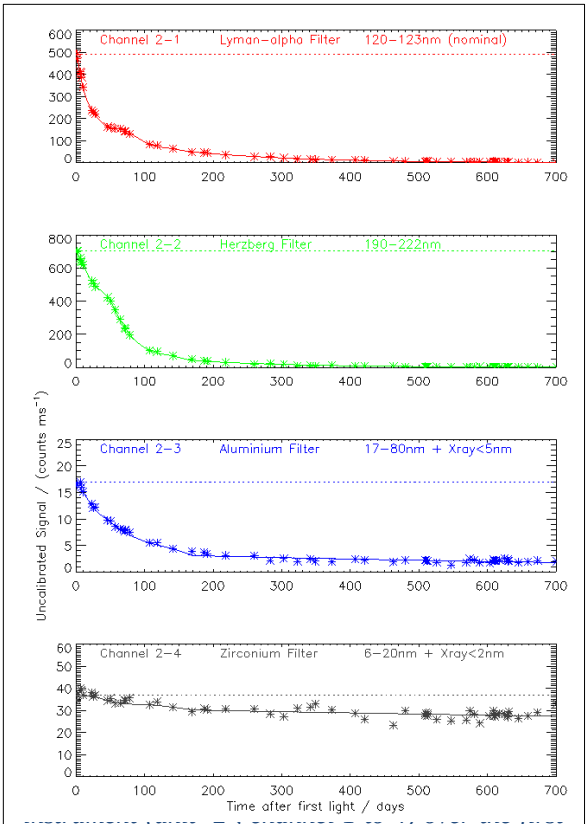

1500 hours of operation.

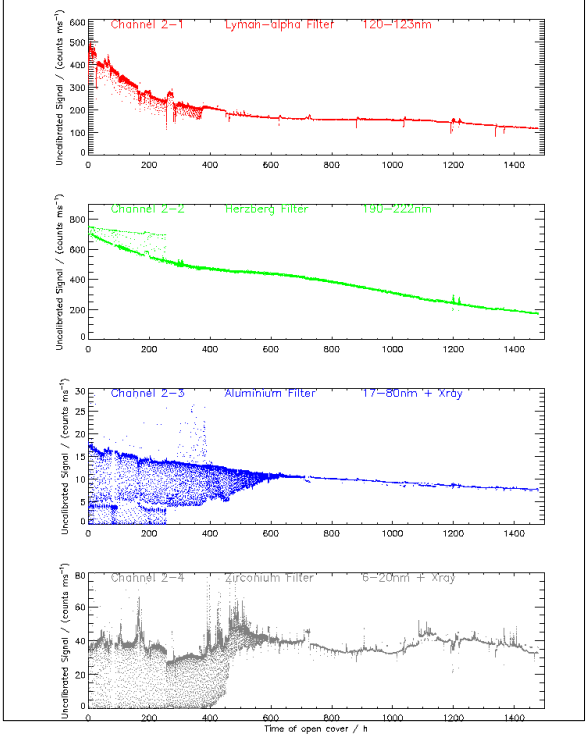

Different methods and approaches have been used to assess and monitor the evolution of these instruments' degradation (see photos on the opposite page). To reach a better understanding of how to both monitor and study this degradation, the Solar Terrestrial Centre of Excellence (STCE) at the Royal Observatory of Belgium organized a workshop on this subject on 3 May 2012 in Brussels, Belgium. Representatives from several active space-based solar instruments contributed to this workshop.

As an outcome of this meeting, the aim of this workshop was to bring up open discussions related to the degradation observed in Sun-observing instruments exposed to the effects of the space environment. The outcomes of this meeting and discussions, together with the written contributions of the different mission teams, have sparked in 2013 to an article focusing on the major lessons learned about in-orbit degradation of solar instruments. This article also provides a summary of the recommendations for best practices with the hope that this information will help scientists and engineers to prevent – or cope with – degradation of active and future space-based solar instruments. a global overview of the lessons learned from the current solar missions was published. The paper was a collaborative work of the main international instrument teams, under the lead of A. Ben Moussa.

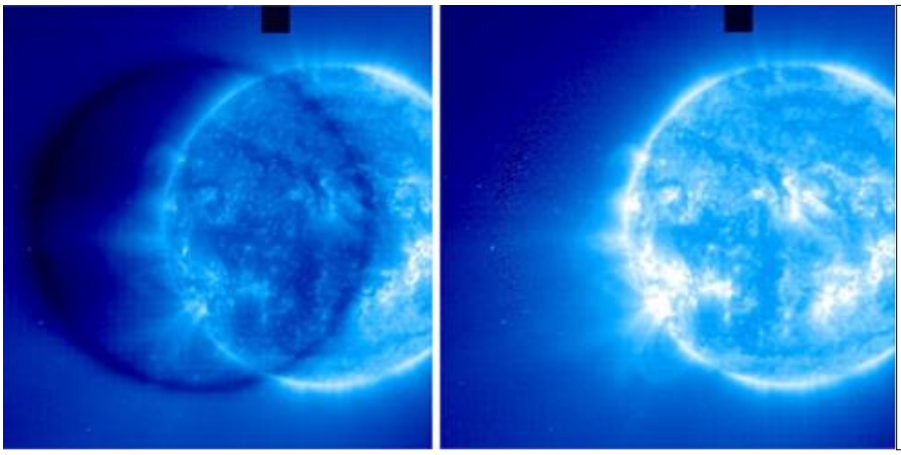

Left: EIT (Extreme Ultraviolet Imager) on-board SOHO 17.1 nm images taken during an off-point manoeuvre before and after correction. Right: Comparison between SDO/ESP channel 2 and its reconstruction based on SDO/EVE-MEGS A spectra before and after the release of EVE level 4 data.

It should be mentioned that the degradation of space instruments can be complex; their causes and mechanisms are, in many instances, difficult to understand, since they are often the result of the combination of several independent degradation processes. Once a spacecraft is in orbit, the stability of calibration can be monitored by carefully planned observations. Alternatively, it is possible to track instrumental calibration by inter-calibration using observations from occasional rocket underflights using similar instruments that can be carefully calibrated on the ground both before and after the flight. Another option for establishing absolute calibration using in-flight observations is the use of invariant sources – assuming they are accessible by the instrument – such as observations of celestial standard sources, or of Sun-center during quiet periods, or by inter-calibration of identical variable sources using different instruments with similar, corresponding wavelength sensitivities. Furthermore, qualified personnel and external expertise are often useful in the interpretation of data obtained, both on the ground and in-flight, in order to accurately assess the evolution of the degradation of a space-based solar instrument.

In this context and after the first degradation workshop in 2012, two workshops meeting in 2013 and 2014 were organized by the STCE gathering a small group of experts specifically interested in the degradation and inter-instrument comparison of radiometers and spectrometers observing the Sun in the X-rays and the extreme UV (EUV) ranges. These events resulted in a much deeper understanding of the differences between the instruments and were even at the origin of a review of the calibration procedure for some of them.

In conclusion, there are several approaches to assess and monitor the degradation of spaced-based solar instruments that give good results. A prime conclusion is that there is no single best method, but rather that a combination of methods must be critically selected, taking into account the applicability of the methods given both the mission targets and instrumental design itself. It is therefore important to continue to share regular and open information about what is working and what is not, in order to learn from the community's shared experiences. Prevention is far better and much cheaper than cure.

PROBA2 – 4 years in orbit

The PROBA2 special edition, containing several articles based around the PROBA2 mission, its observations and several research

PROBA2 is the second satellite in the European Space Agency's series of PRoject for OnBoard Autonomy (PROBA) missions. In 2013 PROBA2 reached the milestone of 4 years in orbit, which oversaw the period of solar maximum. It also produced its 750,000th image of the Sun and over 1500 GB of data. 2013 also saw the release of the PROBA2 topical issue.

The PROBA2 topical issue covers four broad sections, containing a collection of previously published articles in book form. These cover several aspects of the engineering and calibration involved in the satellite platform and the instruments on board. The book also covers several research highlights in different areas of research, some of the highlights include:

Jets and Outflows

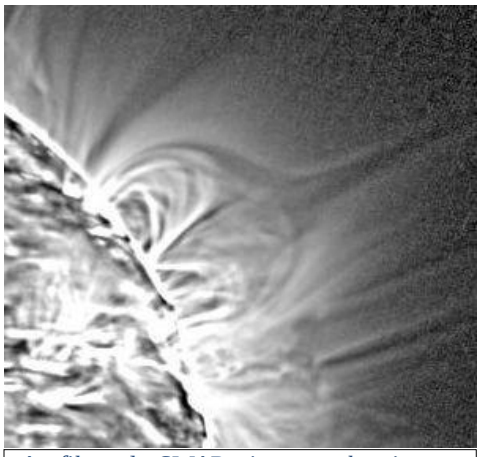

A filtered SWAP image showing a hyperbolic cavity forming to a large distance from the solar limb. The extended white-light jet is the long outward extension of the 'Eiffel-tower' structure.

Jets and outflows on the Sun come in various forms, they often originate lower down in the Suns atmosphere (the corona) before flowing out into the interplanetary medium.

Chandrashekhar et al. used PROBA2/SWAP data together with Solar Dynamics Observatory (SDO) observations to show that "bright points" observed on the Sun in the Extreme UltraViolet (EUV) wavelength range (observations around 500,000K) are associated with the emergence of new magnetic flux from below. This suggests that the emerging flux interacts with existing magnetic fields in the Suns atmosphere, whereby energy is released in a process known as "magnetic reconnection". This release of energy creates the bright points seen on the Sun. *Filippov et al.* also used SWAP and SDO data to look at magnetic configurations on the Sun. However, they used SWAPs extremely large field of view to look for the connectivity of coronal structures with outer coronal (the outer solar atmosphere) features that were imaged with the Large Angle Spectrometric Coronagraph (LASCO) on the Solar and Heliospheric Observatory (SOHO), where we note that a coronagraph is a type of telescope that blocks the bright solar disk in order to see the comparatively less bright surrounding solar atmosphere. The data-sets revealed an Eiffel-tower shaped jet configuration extending into a narrow jet in the outer corona. An example image of the structure can be seen in the above photo. The configuration provides a possibility for the plasma to escape along the open field lines into the outer corona, forming the white-light jet.

Flares and Eruptions

A flare is a sudden brightening observed over the Suns surface. The brightening is a signature of large energy release on the Sun, and is often associated with an ejection of hot plasma. Eruptions on the Sun don't necessarily have to be associated with a flare, but they often occur together. In the PROBA2 special edition *Bonte et al.* discuss new techniques to automatically detect solar flares with the PROBA2/SWAP imager, where they introduce the 'Solar Flare Automated Search Tool' (SoFAST), which will also be implemented on future solar missions. *Kretzschmar et al.* made use of the unique capabilities of the PROBA2/LYRA instrument to observe flares in a wavelength known as 'Lyman alpha', which is the strongest line of the solar spectrum. *Kretzschmar et al*., observed several flares, and studied one in detail, which was a powerful 'M2' flare that occurred on 8 February 2010. For this flare, the flux in the LYRA

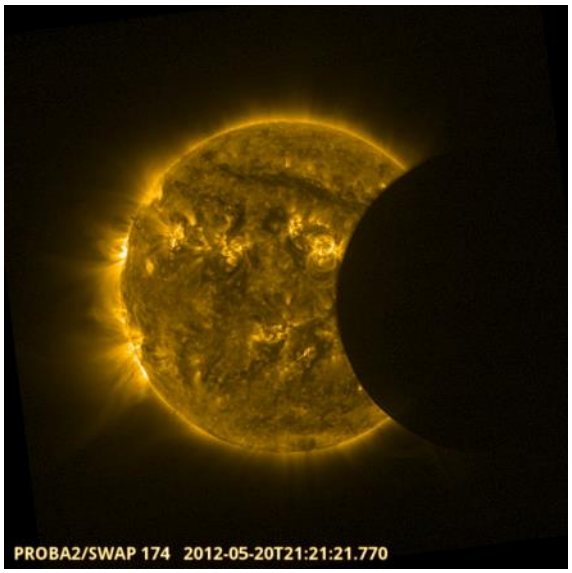

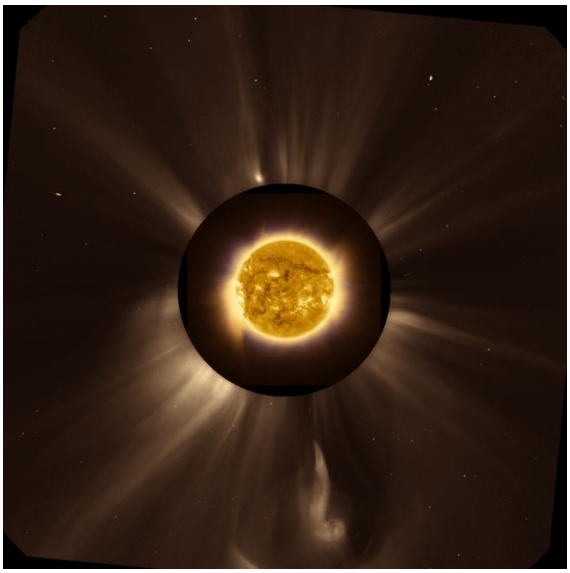

Left: a SWAP image of a solar eclipse.
Right: NASA picture of the day. An Active Sun During a Total Eclipse. Image Credit & Copyright: D. Seaton (ROB), A. Davis & J. M. Pasachoff (Williams College Eclipse Expedition), NRL, ESA, NASA, NatGeo

Lyman-alpha channel increased by 0.6 %, which represents about twice the energy radiated and observed in X-ray channels. However, it was found that the Lyman-alpha emission represents only a minor part of the total radiated energy of this flare.

A phenomenon often associated with Solar flares are EUV waves, these are huge waves that flow through the solar atmosphere, having an appearance like a ripple on the surface of water when a stone is dropped in it. *Kienreich et al.* used PROBA2/SWAP images together with observations from the Solar TErrestrial Relations Observatory-A (STEREO-A) satellite which orbits the Sun to observe EUV waves on the Sun from different angles. *Kienreich et al*. observed three such waves in total and observed them reflecting off different structures in the solar atmosphere.

Solar prominences are large loop like structures observed on the Sun, extending thousands of kilometers outwards into the solar corona. Prominences can become unstable and erupt in an event known as a "prominence eruption". *Mierla et al.*, made 3D reconstructions of such an event using PROBA2/SWAP and STEREO data showing its acceleration increased smoothly with height and concluded that the prominence is not accelerated immediately by local magnetic reconnection (energy releases) but rather is swept away as part of a large-scale relaxation of the coronal magnetic field.

Irradiance and Spectral analysis

The last section of the PROBA2 special edition focused on irradiance and spectral analyses. Such studies focus on power per unit area produced by the Sun in the form of electromagnetic radiation and are important in understanding the total energy output of the Sun and how this might impact upon the Earth. *Shapiro et al.*, used solar eclipse observations using PROBA2/LYRA to measure Solar center to solar limb variations in solar brightness, an image of Solar eclipse seen by PROBA2/SWAP can be seen in the figure above. In a separate paper *Shapiro et al.*, used PROBA2/LYRA to analyze the variability of the spectral solar irradiance over a period from 7 January, 2010 until 20 January, 2010 and developed an algorithm to extract solar variability from the LYRA data. Finally, *Bazin et al.* also used eclipse data to study prominence cavity regions observed using PROBA2/SWAP and simultaneous ground based eclipse flash spectra observations from the 11-July-2010 eclipse.

In a separate article, SWAP/PROBA2 data was once again used with ground based eclipse observations, but this time it made the NASA Astronomy Picture of the Day (http://apod.nasa.gov/apod/ap131111.html). In this composite image we see the Sun in several wavelengths, using several different observatories. The central image of the Sun is imaged using SWAP, showing the Sun in the EUV wavelength range. This is surrounded by a ground-based eclipse image, reproduced in blue, taken from

Gabon. Outside this we see the outer solar atmosphere, taken by the LASCO instrument aboard the Sun-orbiting SOHO spacecraft.

SILSO - Sunspots surveillance

A key service activity of the SIDC is the production of the sunspot number, which is the unique reference for the long-term solar activity over multiple centuries. As such, it is used worldwide in a wide range of scientific applications, from solar cycle modeling and predictions to climate change studies. Recent advances in those fields as well as the anomalous and unexpected evolution from cycle 23 to the current cycle 24 have brought a strong motivation to revisit and improve this unique time series that is maintained at the ROB since 1981, when the World Data Center for the International Sunspot Number was transferred from Zürich to Brussels. In this context, since 2011, the software and databases of the World Data Center (SILSO) have been intensively revised, expanded and improved.

This process involved a stringent control of the consistency of the new calculation with the official sunspot number still produced by the heritage FORTRAN programs. 2013 marked a new step in this process: the production of the official sunspot index was moved to a new server running the new validated software.

This transition also opened entirely new possibilities, in particular for the implementation of a global quality control of the base data collected by the worldwide SILSO network (currently 80 active stations). Indeed, all individual raw observations collected since 1981 (i.e. 34 years) are fully preserved and now accessible through a MySQL database, which now contains more than 540000 observations from 269 stations in 39 different countries. The top figure retraces the evolution of the yearly contributions from the network. Based on such an extensive data set, it is possible to build global statistics in order to check the stability of reported sunspot numbers from each station over the last 3 solar cycles. In particular, we first investigated the stability of the pilot station of the network, namely the Specola Solare Ticinese Observatory (Locarno, Switzerland). This station (on the left)

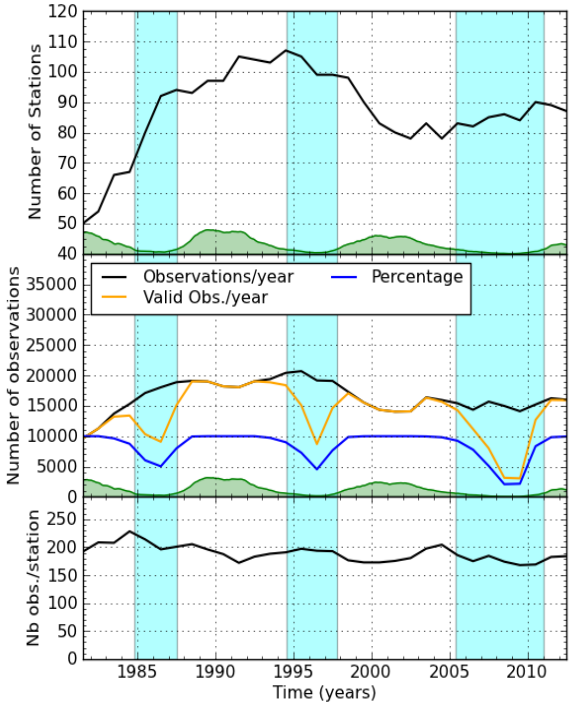

Evolution of the worldwide sunspot network: number of contributing stations (top panel), annual number of collected observations (middle panel) and average number of observations per station per year (lower panel). The solar cycles (shaded green) and minima intervals (shaded blue) are overlaid as time reference. In the middle panels, valid observations are days when both a given station and the reference pilot station give a non-null Wolf number (i.e. when a personal k coefficient can be established).

View of the Specola Solare Ticinese Observatory overlooking the Lake Major in Locarno. (Image courtesy Specola Solare Ticinese, Locarno)

played a key role to ensure the continuity with the past series built by the Zürich Observatory for all years before 1981, back to the 17th century.

Our study actually revealed a rather large and variable drift in the scale of the Locarno numbers that caused a corresponding bias in the scale of the sunspot number published over the past decades. This drift was established by computing the scale ratio k, also called the "personal coefficient", of each station of the network relative to the pilot station. By averaging over many stations and comparing between different network subsets, we derived an accurate mean ratio as a function of time as shown in the figure on the right. The diagnosed variations reached up to 20% with steady trends reversing around 1987 and 2008. This first result illustrates the potential of the new software and its associated huge data collection. The network-wide mean ratio determined in 2013 can now be used as a correction to restore a uniform absolute scale for the past sunspot number, bringing the first major recalibration of this reference time series since its creation. Moreover, the corrected series already addresses recent solar issues, like the unprecedented deviation between various parallel indices of solar activity since 2000. The figure below just shows the relation between the sunspot number and the F10.7cm radio flux, before and after applying the above correction. While the corrected sunspot number definitely provides a better overall match with the F10.7 proxy before 2000, a significant deviation still persists after 2003. This disagreement is confirmed by other index comparisons and thus points at an actual change in the source of solar magnetic activity. Therefore, new investigations will be required in coming months and years and our improved sunspot number series will definitely help researchers to get a cleaner picture of actual changes now happening on the Sun, in what seems to be the weakest solar cycle of the last 100 years. Our work continues and additional improvements spanning the full 400-years of the sunspot record will follow in 2014.

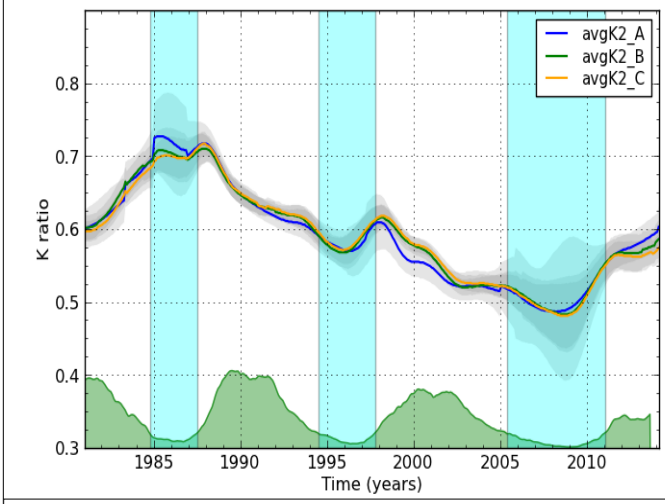

Plot of three different multi-station average k ratios. Three subsets of stations have been chosen, starting with the most reliable and long-duration stations (set A; 9 stations, in blue) and then adding more stations of shorter duration and lower stability (set B, 37 stations, in green; set C: 79 stations in orange). The gray shading gives the standard error of the average k ratio, which increases at cycle minima (blue shading). Although all three sets are very different, all curves display the same drifts and reversals,

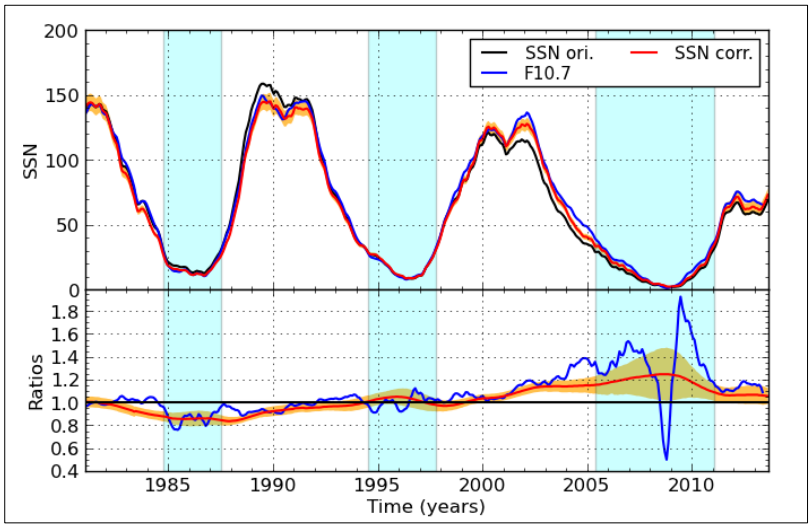

Comparison of the original sunspot number series (SSN_{ori}, black, upper panel) with the new corrected series (SSN_{corr} ,red) and the $F_{10.7}$-based proxy (blue) over the last 3 solar cycles. Lower panel: the ratios SN_{corr}/SN_{ori} (red) and $F_{10.7}/SSN_{ori}$ (blue), with the standard error in the corrected SN (orange shading). They show a better agreement between $F_{10.7}$ and the SN after the correction, but still with a significant though reduced divergence after 2002.

Solar Orbiter Science Working Team meeting and EUI engineering model

Solar Orbiter is the next ESA flagship for studying our closest star, the Sun. It is currently scheduled for launch in 2017. By approaching as close as 0.28 AU (astronomical unit; 1 AU is nearly 150 million km), Solar Orbiter will view the Sun with high spatial resolution and combine this with in-situ measurements of the surrounding heliosphere. Thanks to its unique orbit, Solar Orbiter will deliver images and data of the unexplored Sun's Polar Regions and the side of the Sun not visible from Earth. Scientists expect that this satellite will provide important new insights into our Sun and its influence on the inner Solar System.

The EUI engineering model displayed at the laboratory at the Centre Spatial de Liège, surrounded by the EUI team. This team consists of scientists and engineers from Belgium (ROB), France, Germany, the UK, and Switzerland.

Solar physicists at STCE/ROB have a leading role in the EUI instrument onboard Solar Orbiter. The instrument concept was conceived at the Solar Physics group of STCE/ROB including the use of some of its key technologies (APS detectors, compression …). EUI is now being built by an international consortium under the leadership of Pierre Rochus from the Centre Spatial de Liège (CSL). A group of about 10 researchers at STCE/ROB is actively supporting this development. In the operational phase of the mission (>2017), the EUI instrument will be operated from the EUI Data Center at STCE/ROB.At the end of November 2013, the engineering model of EUI was completed at the Centre Spatial de Liège. This is an exact copy of EUI without all optical and electrical components (which are state-of-the-art and still being developed). The engineering model will be tested thoroughly for its mechanical, thermal, and thermo-elastic stability to make sure that the instrument can handle the harsh conditions close to the Sun.

This photograph was taken during the Solar Orbiter Cleanliness Meeting at ROB on September 23, 2013 This satellite meeting immediately preceded the Solar Orbiter Science Working Team meeting.

In order to prepare the science of Solar Orbiter, the STCE/ROB organized the Solar Orbiter Science Working Team meeting from September 24 to 26, 2013. Fifty-four scientists gathered there to discuss how science can best profit from the unique opportunities offered by Solar Orbiter, which is a partnership between ESA and NASA. The scientific synergy of Solar Orbiter with Solar Probe Plus and other missions was also highlighted. Progress was made on data analysis and the collaboration between the various instruments in joint science campaigns. To ensure a successful mission, the status and work ahead for the Solar Orbiter spacecraft and the different instruments onboard were followed up.

Many STCE/ROB scientists participated actively in the talks and discussions. The meeting was chaired by Daniel Mueller (Project Scientist of Solar Orbiter, @ESA) and local organization was taken care of by the well-trained STCE team including Anne Vandersyppe, Jan Janssens, David Berghmans, Sarah Willems, Petra Vanlommel, Bram Bourgoignie, and Olivier Boulvin.

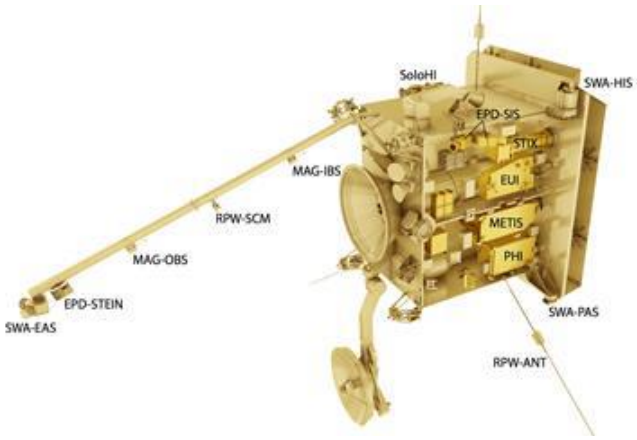

Solar Orbiter and its suite of remote sensing and in-situ instruments. Note in particular the heat shield in the back, the deployable high gain antenna at the bottom and the in-situ boom on the left. Belgium is a leading partner in the international consortium that is building the EUI instrument (EUI = Extreme Ultraviolet Imagers; Principal Investigator (PI): Pierre Rochus, CSL).

Space Weather Centre is providing support to ESA during spacecraft launch

ESA has set up a Space Situational Awareness (SSA) program dedicated to space weather, with the purpose to establish and provide access to a network of European space weather products for end users. The products include ESA owned applications, as well as, space weather products provided by different European expert groups.
In the context of the SSA program, the SSCC (SSA Space Weather Coordination Centre) is the focal point for space weather user support of. The SSCC was inaugurated on 3 April 2013 during a dedicated event, attended by key personnel of ESA, the SSA program and the collaborating partners of the project. The program included Philippe Mettens, Chairman of the Belgian Science Policy Office, ESA Director Thomas Reiter, SSA Program Manager Nicolas Bobrinsky, SSA Space Weather Segment Manager Juha-Pekka Luntama, and Michel Kruglanski, project manager leading the consortium responsible for implementing the SSCC.
The SSCC is monitoring the space weather services ensuring their availability to the users and their nominal performance. It also provides the first level user support for all those services. Located at the Space Pole premises in Brussels, its activities are gradually expanding as more services become online and users increasingly interact with the SSCC. The SSCC functions as a relay between the users and the European space weather products.

Picture of the inauguration event

GAIA is an ESA satellite constructed to produce the largest three-dimensional map of our galaxy. To that end, the spacecraft is observing one percent of all 100 billion stars of our galaxy. The satellite was launched on 19 December 2013 with a Soyuz-rocket from the launch basis of Kourou, French Guyana. In the period from 6 to 14 January 2014, the spacecraft did manoeuvre to its final destination.

The SSCC and the forecasters' team of the Regional Warning Center (RWC) in Belgium provided support on the days before, during and after the launch of the GAIA spacecraft.

During the launch window seven space weather bulletins were delivered, while six ones were sent during the spacecraft maneuvers. The bulletins provided a description of the current space weather activity and predictions for any activity that could result in increased risks for the spacecraft.

Specific attention was spent to the risks for increased amount of energetic particles, during which protons are accelerated to very high energies by a solar flare or by the interplanetary shock wave associated with a coronal mass ejection (CME). Monitoring the solar activity (by observing and classifying the sunspot groups) allows to forecast the flaring activity of the Sun. The solar flares are categorized in classes based on their peak burst X-ray emission. A CME could occur during a long duration flare or during the eruption of a solar filament. Major solar proton events could result from the acceleration of solar wind particles by an interplanetary shock wave of an Earth-directed CME.

An increased flux from energetic particles might for example result in damage of the spacecraft's instruments. A special bulletin was provided to the GAIA team during the rising phase of an energetic particle event on 6 January 2014 to inform them on the increased risks for radiation exposure to the spacecraft.

Launch of Gaia (ESA)

The STCE annual meeting 2013

Since 2008, the STCE organizes an annual meeting for its members. This event consists of a morning session with easy-going lectures and discussions on solar-terrestrial topics, followed by a lunch that lasts well into the afternoon. The practicalities are taken care of by the same people who organize the space weather week and other conferences, spearheaded by their mastermind Petra Vanlommel.

The 6th STCE annual meeting took place on 7 June 2013 in the ROB's Meridian room. About 60 people were welcomed by Ronald Van der Linden, the STCE's general coordinator, and Martine De Mazière, the Director General of BISA. Michel Kruglanski then gave a short talk on the SSCC, the first European SSA Space weather coordination center. This center was officially inaugurated just 2 months before (3 April), and had gathered a lot of media attention.

The summary reports from the workshops constitute the main body of the annual meeting. These workshops are organized by scientists in their respective field of research prior to the annual meeting. They sometimes last longer than 1 day, and usually have attendees and speakers from universities and institutions outside the Space Pole and Belgium. Hence, these meetings are valuable gatherings for the interested to get the latest in their area of expertise. As these are technical meetings, a non-specialist is assigned to assist to each of these workshops, in order to get a short and easy-to-understand summary at the annual meeting.

In advance of the 2013 annual meeting, 6 workshops were organized:

- Solar EUV Irradiance Working Group: Inter-calibration and degradation of EUV instruments (15-18 April 2013), organized by Marie Dominique, and presented by Steven De Witte
- Automatic detection of events in radio data (31 May 2013), organized by Hervé Lamy and Christophe Marqué, and presented by David Berghmans
- Water Vapor, Meteorology and Climate (26 November 2012), organized by Eric Pottiaux, and presented by Roeland Van Malderen
- Alfven Waves and Turbulence in Solar and Space Plasmas (30 May 2013), organized by Yuriy Voitenko and Andrei Zhukov, and presented by Jesse Andries
- EPN Local Analysis Centres Workshop (15-16 May 2013), organized and presented by Carine Bruyninx
- Ionosphere: monitoring, research, services (14 May 2013), organized by Stan Stankov and Nicolas Bergeot, and presented by Carine Bruyninx.

The program scheduled a short coffee break after the first two workshop reports. During this pause, participants could watch the space weather briefing live on the big screen. This was a last minute idea that was quickly and efficiently organized by Marc De Knijf and David Berghmans, and presented from the SSCC-room by the space weather forecaster on duty Jasmina Magdalenic. This intermezzo was very well appreciated by the audience.

During lunch, the participants had the opportunity to visit the recently finished Planeterrella. This is an aurora simulator which main purposes are both educational (public outreach) and scientific (e.g. study of polarization of auroral light). Eddy Equeter and Johan De Keyser provided the enthusiastic crowd with a word of explanation near BISA's Green room. By the end of the year, actions were already taken to start up the series of workshops for next year's annual meeting.

The Space Pole opened its doors!

In the context of the 100th anniversary of the Royal Meteorological Institute (RMI), an Open Door was organized on the premises of the Space Pole. This open door took place during the weekend of 25-26 May 2013, and attracted over 7000 visitors. The spotlight was certainly on the RMI which got the centroid of activities. The STCE participation was intense with various events in the solar-terrestrial domain.

Photos of the open door: left, visits of the solar dome; right: the Kids' tent

The Solar Dome

One of the highlights was certainly a visit to the Solar Dome. A small introductory presentation was first given in the corridor of the SIDC. Skilled observers and space weather forecasters explained in laymen terminology what sunspots are, how they are observed, why these observations are so important, and how solar eruptions affect us and our technology. Then, the small groups of 10-15 people were guided via more than 40 stairs towards the top of the solar dome. There, the various solar telescopes were shown and their specific applications discussed. Weather permitting it, the visitors could also make solar observations using a projected solar image from the white light solar telescope. During and after the visit, there was plenty of opportunity to ask questions to the guides.

The STCE-tent

A much appreciated activity was the series of presentations that were given in the STCE-tent. The presentations were short (15-20 minutes), and followed by 5-10 minutes for questions from the audience. Then there were 5 minutes to get the tent ready for the next group. The topics were various and included, aside the presentations on solar activity and space weather, also earthquakes, gravitational constant, astrophotography, the planet Mercury, atomic clocks, living on Mars, and research from Antarctica. A total of 26 (!) presentations were given, and they became the best-rated activity of the Open Door.

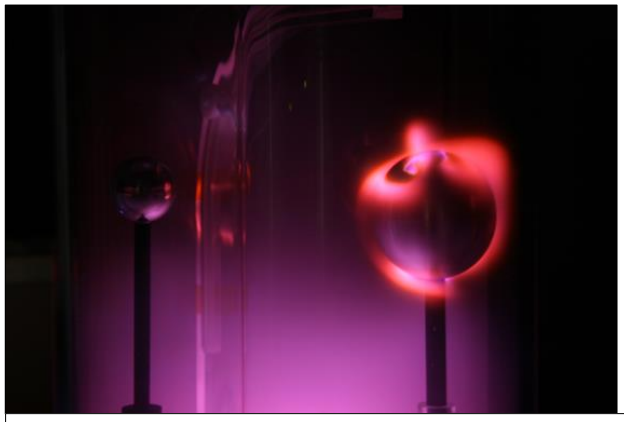

Left: the Planeterrella in the BISA's cellar; Right STCE-tent; Bottom installation for kids

The Kids-tent

In this tent, the STCE teamed up with the Planetarium to present activities which were most suited for families with children. Aside a series of fun and didactic activities, also a small introduction on space weather and polar light was given, tailored to children's level of course, and there was also a color corner having as main theme "The Sun". The teenagers could test their knowledge on space weather at the quiz table. This quiz, consisting of about 20 multiple choice questions, could also be accessed online with a QR-code.

The SSCC-room

In the SSCC-room, the newly inaugurated European space weather coordination centre (SSCC) was co-located with the Proba2 Science Centre (P2SC). Visitors got an overview of the tasks of the SSCC and how these were realized (see xxx). People from the P2SC explained how they operate the PROBA2 satellite, which was in part constructed by scientists from the STCE. It was the place-to-be for gadgets and posters on this fine solar satellite, and the full-scale model of PROBA2 impressed many visitors.

The Planeterrella

The STCE Planeterrella, based on a concept by Jean Lilensten (IPAG/CNRS), got completed just in time for the Open Door. This is an experiment which helps in understanding the mechanism of the polar lights. It consists of an electron gun and a conductive sphere placed in a vacuum chamber. The main advantage of the STCE Planeterrella is that it can be used for both scientific and educational purposes. The Planeterrella was built by technicians from BISA with financial support from the STCE and was on display during the Open Door, the STCE Annual meeting and other visits. As it required a dark room to fully appreciate the subtle plasma hues, the Planeterrella was placed in the cellar of the BISA.

The Open Door would not have been possible without the enthusiastic support of the entire Space Pole community. Scientists, IT-personnel, logisticians, general support, etc… all contributed significantly to the successful organization of this major event. An "encore" performance will be required, as in the framework of the 50th anniversary of the BISA, another open door will be organized in October 2014.

Information services

In 2013 the scientific information service of the ROB had to answer 1280 questions from the public sent to the ROB by email (510, including 60 requests for visits), telephone (700) or by letter or fax (70). As usual most were about sunset and sunrise, about astronomical phenomena (including all kind of sky objects) or calendar and time related matters.

Information to the media (TV, radio and written press) was given by the service on numerous occasions. The re-entry of the Soyouz rocket stage (14/02/2013), the impact of the meteorites in Chelyabinsk (Russia, 15/02/2013) and a life broadcast by RTBf (15/02/2013) from the dome of the Schmidt telescope about the close passage to earth of asteroid 2012DA14 were amongst the highlights. Other members of the ROB appeared in news items on other topics (Solar activity, space weather, seismic activity, …).

During the weekend May, 25-26 the three institutes (ROB, RMI, BISA) organised open doors days. Over 6000 persons visited our premises. Because of the centennial anniversary of the RMI, this institute made a larger than usual effort for this event. The activities of the Solar physics group and the STCE members are described in detail elsewhere, but all services of the ROB were heavily involved and participated enthusiastically. A leaflet describing the 3 institutes of the Space Pole and their activities, including BUSOC, STCE and Planetarium, was prepared. It was printed in 10000 copies, more than 3000 were distributed during the Open doors days.

A media event was organized at the Planetarium of the ROB on December 19, 2013, the day of the Gaia launch. The presentation of the mission was followed by a live transmission of the launch and the first hours of the flight. ROB members assisted in the preparation of this event, contributed to the press release documents, prepared and showed posters of their involvement and gave interviews to the media.

The Planetarium

Number of visitors

In 2013 the Planetarium welcomed 45.581 visitors, a great number but slightly decreasing since 2012: -6.8% entries, that is -3342 visitors. This decrease can be explained by the suppression of the combined ticket with the Atomium which was replaced by a less attractive offer: Atomium / Museums of the Far East / Planetarium. It generated a major drop of the number of visitors coming from the Atomium (-10.205) compared to 2012; but hopefully it was partly compensated by an increase of visitors (+1848 visitors) coming from the "Mini-Europe" (with another combined ticket offer) as well as the increase visitors who came only to the planetarium (+5015 visitors)

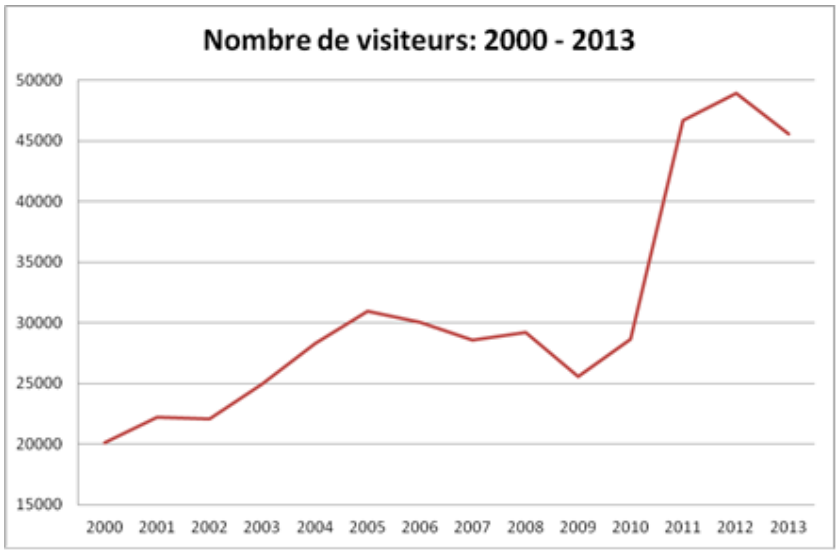

The new Show: "Secret Lives of Stars"

The preview of the new show "secret life of stars" took place on the 18th December; it explains the main aspects of the stellar evolution thanks to impressive full dome animations. The movie was produced by Evans & Surtherland and the Voice-over of the English version is played by Patrick Stewart (Star trek, X-Men).

The ASGARD project

Image extract form the show "secret lives of stars": a star attracting matter from its twin companion in a binary system

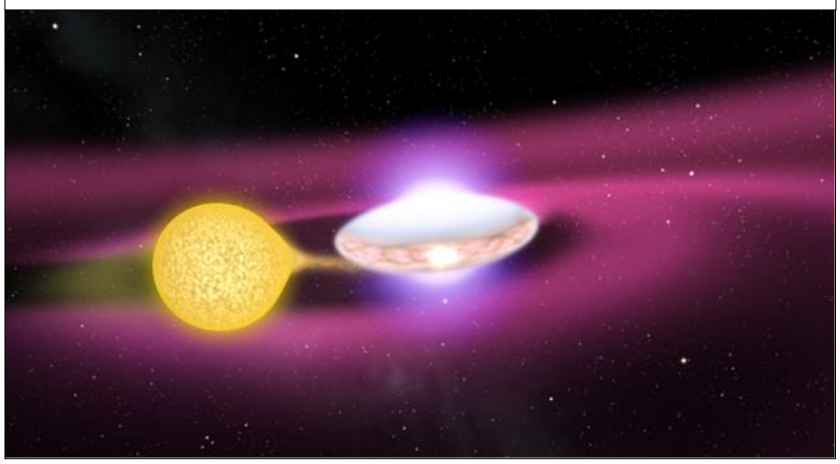

On the 25th April ESRO's office (an ESA's education project managed by the Planetarium in Belgium) organized the launching of probe-balloons with the Royal Meteorological Institute and the Royal Observatory of Belgium. The balloons were used to carry out the experiments of primary and secondary schools of the ASGARD project. The pupils were able to attend to a conference given by Dirk Frimout, to take part in the Planetarium's workshops and to visit the Observatory premises at Uccle. ESERO and the Planetarium were also involved in the CanSat competition from the Brussels' area. The ceremony took place at the Planetarium on May the 7th and the "école sciences" labels were given on May the 15th at Han-sur-Lesse.

World Space Week

The first edition of the World Space Week organized in Belgium took place on the 4th October at the Planetarium. Its theme was "Exploring Mars" and an interested audience came to ask questions to Frank De Winne (ESA astronaut) and to scientists of the Space Pole. ESA and Belspo also gave a press conference on the 21st October about the National Trainee Program.

Left: Probe-balloon launching for the ASGARD project.

Below: full dome show at the Planetarium for the world week of space: simulation of the sun rising above Mars

Researchers' Night 2013:

On the occasion of Researchers' Night 2013 on the 27th September, the planetarium organized a special evening on the theme "live better and longer". The full dome show "Water, a cosmic adventure" was projected in preview; it was a coproduction of the ESO and the APLF (French speaking association of planetariums) and presented the upcoming E-ELT telescope of the European Southern Observatory built in the Atacama Desert, Chili. An interactive workshop on the theme "will we live until … we're 120 years old?" was also organized by the Scientific Youth of Belgium.

The Night of darkness

Visitors looking through the planetarium's telescopes

On the 12th October, the fifth edition of night of Darkness was held at the Planetarium, on the Rouge-Cloître premises. Despite the cloudy sky, visitors came to attend to a conference, an outdoor concert or guided tour and to glance at the sky through one of the many telescopes.

Dag van de wetenschap

On the 24 November, the planetarium took part in the "Dag van de wetenschaps" and offered its 663 visitors an occasion to participate in several scientific activities organized by the Planetarium's and the JCW association's animators.

Top: Poster of the Night of the museums.

Right: inauguration of the exposition for the 100th anniversary of the Royal Meteorological Institute

Night of the Museums

The Planetarium participated to the night of the museums during two evenings and eight show sessions; 316 visitors came on the 31st October and 368 on the 28th November.

Exposition at the Royal Meteorological Institute (RMI)

For the 100th anniversary of the RMI, an exposition called "100 years of meteorology in Belgium" was inaugurated on the 19th September at the Planetarium in the presence of the state secretary M. P. Courard. This exposition gives the main highlights of the history and development of meteorology in Belgium through a display of meteorological instruments and documents from different periods of time.

Means implemented

On the December 31st 2013, the Planetarium's personnel was composed of 15 members who take care of: animation and teaching, projection, reception, public relationships, maintenance, technical service, ICT and graphics service.

The Planetarium is a member of different touristic associations: Toeristische Attracties, Attractions & Tourisme, Brusselse Museumraad, Office de Promotion du Tourisme Wallonie-Bruxelles.

The planetarium is also member of several association of planetariums: « International Planetarium Society (IPS) », « Vereniging van Nederlandstalige Planetaria (PLANed) », « Association des Planétariums de langue Française (APLF) », « Arbeitsgemeinschaft deutschsprachiger Planetarien (ADP) » and is represented at all the annual meetings.

Annex 1: Publications 2013

1. Bailer-Jones, C. A. L.; Andrae, R.; Arcay, B.; Astraatmadja, T.; Bellas-Velidis, I.; Berihuete, A.; Bijaoui, A.; Carrión, C.; Dafonte, C.; Damerdji, Y.; Dapergolas, A.; de Laverny, P.; Delchambre, L.; Drazinos, P.; Drimmel, R.; **Frémat, Y.;** Fustes, D.; García-Torres, M.; Guédé, C.; Heiter, U.; Janotto, A.-M.; Karampelas, A.; Kim, D.-W.; Knude, J.; Kolka, I.; Kontizas, E.; Kontizas, M.; Korn, A. J.; Lanzafame, A. C.; Lebreton, Y.; Lindstrøm, H.; Liu, C.; Livanou, E.; **Lobel, A**.; Manteiga, M.; Martayan, C.; Ordenovic, Ch.; Pichon, B.; Recio-Blanco, A.; Rocca-Volmerange, B.; Sarro, L. M.; Smith, K.; Sordo, R.; Soubiran, C.; Surdej, J.; Thévenin, F.; Tsalmantza, P.; Vallenari, A.; Zorec, J.
The Gaia astrophysical parameters inference system (Apsis).
Pre-launch description 2013, A&A 559, A74, 20 pages

2. Baire Q., Bruyninx C., Legrand J., Pottiaux E., Aerts W., Defraigne P., Bergeot N., Chevalier J.M.
Influence of different GPS receiver antenna calibration models on geodetic positioning
GPS Solutions (November 2013), online version, doi: 10.1007/s10291-013-0349-1

3. Balona, L. A.; Catanzaro, G.; Crause, L.; Cunha, M. S.; Gandolfi, D.; Hatzes, A.; Kabath, P.; Uytterhoeven, K.; **De Cat, P**.
The unusual roAp star KIC 8677585
2013, MNRAS 432, p.2808-2817

4. A. BenMoussa, B. Giordanengo, S. Gissot, Guy Menants, X Wang, B. Wolfs, J. Bogaerts, U. Schuehle, G. Berger, A. Gottwald, C. Laubis, U. Kroth, F. Scholze
Characterization of backside-illuminated CMOS APS prototypes for the Extreme Ultraviolet Imager on-board Solar Orbiter
IEEE Transactions on Electron Devices, 60, pp.1701-1708

5. A. BenMoussa, S. Gissot, B. Giordanengo, Guy Menants, X Wang, B. Wolfs, J. Bogaerts, U. Schuehle, G. Berger, A. Gottwald, C. Laubis, U. Kroth, F. Scholze, A. Soltani, T. Saito
Irradiation Damage Tests on Backside-Illuminated CMOS APS Prototypes for the Extreme Ultraviolet Imager On-Board Solar Orbiter
IEEE Trans. on Nuclear Science, 60, Iss. 5, pp.3907-3914

6. A. BenMoussa, S. Gissot, U. Schuehle, F. Auchere, D.B. Seaton, I.E. Dammasch, D. Berghmans, M. Dominique, B. Giordanengo, M. Kretzschmar, B. Nicula, + 39 coauthors
On-Orbit Degradation of Solar Instruments
Solar Physics, 288, Iss. 1, pp.389-434

7. A. BenMoussa, A. Soltani, J-C Gerbedoen, T. Saito, Stanislav Averin, S. Gissot, B. Giordanengo, G. Berger, U. Kroth, J-C. De Jaeger, A. Gottwald
Developments, characterization and proton irradiation damage tests of AlN detectors for VUV Solar Observations
Nucl. Instruments & Methods in Physics Research section B: Beam interactions with Materials and Atoms, 312, pp.48-53

8. Bergeot N., Tsagouri I., Bruyninx C., Legrand J., Chevalier J.M., Defraigne P., Baire Q., Pottiaux E.,
The Influence of Space Weather on Ionospheric Total Electron Content during the 23rd Solar Cycle
Journal of Space Weather and Space Climate, 3 (2013) A25, DOI: 10.1051/swsc/2013047.

9. D. Berghmans, A. De Groof, M. Dominique, J.-F. Hochedez, J.W. Leibacher
Preface
Solar Physics, 286, pp.1-3

10. Beuthe M.
Spatial patterns of tidal heating
Icarus, 223, 308-329 (2013),
doi:10.1016/j.icarus.2012.11.020

11. Blomme, R., Nazé, Y., Volpi, D., De Becker, M., Prinja, R. K., Pittard, J. M., Parkin, E. R., Absil, O.
The 2.35 year itch of Cygnus OB2 #9. II. Radio monitoring
2013, A&A 550, A90,

12. Blomme, R., Volpi, D.
Non-thermal radio emission from O-type stars. V. 9 Sagittarii.
2013, A&A 561, A18

13. K. Bonte, D. Berghmans, A. De Groof, K. Steed, S. Poedts
SoFAST: Automated Flare Detection with the PROBA2/SWAP EUV Imager
Solar Physics, 286, pp.185-199

14. Bruyninx C., Legrand J., Altamimi Z., Becker M., Craymer M., Combrinck L., Combrink A., Dawson J., Dietrich R., Fernandes R., Govind R., Griffiths J., Herring T., Kenyeres A., King R., Kreemer C., Lavallée D., Sánchez L., Santamaria-Gomez A., Sella G., Shen Z., Wöppelmann G.
IAG WG SC1.3 on Regional Dense Velocity Fields: First Results and Steps Ahead
Reference Frames for Applications in Geosciences, Altamimi Z. and Collilieux X. (Eds.): IAG Symposia 138:137-145, doi:10.1007/978-3-642-32998-2_22

15. Thierry Camelbeeck, Olivier de Viron, Michel Van Camp, Dimitri Kusters
Local stress sources in Western Europe lithosphere from geoid anomalies
Lithosphere 5, 235-246 (2013)

16. K. Chandrashekhar, S. K. Prasad, D. Banerjee, B. Ravindra, D.B. Seaton
Dynamics of Coronal Bright Points as seen by SWAP, AIA, and HMI
Solar Physics, 286, pp.125—142

17. Chatzikos M., Ferland G.J., Williams R.J.R., van Hoof P.A.M., Porter R.
Effects of External Radiation Fields on Line Emission—Application to Star-forming Regions
ApJ, 779, 122

18. Cioni M.-R.L., Kamath D., Rubele S., van Loon J.Th., Wood P.W., Emerson J.P., Gibson B.K., Groenewegen M.A.T., Ivanov V.D., Miszalski B., Ripepi V.
The VMC Survey VI. Quasars behind the Magellanic system
2013, A&A 549, A29, 16 pages

19. E.W. Cliver, F. Clette, L. Svalgaard
Recalibrating the Sunspot Number (SSN): the SSN Workshops
Central European Astrophysical Bulletin, 37 (2), pp.401-416

20. David, M., Blomme, R., Frémat, Y., Damerdji, Y., Delle Luche, C., Gosset, E., Katz, D., Viala, Y.
A multi-method approach to radial-velocity measurement for single-object spectra
2013, A&A 562, A97

21. De Cat, P. ,
Positions of asteroids,
2013, MPC 82023

22. J. Deceuster, Olivier Kaufmann, Michel Van Camp
Automated identification of changes in electrode contact properties for long-term permanent ERT monitoring experiments
Geophysics 78(2) (2013).

23. Delaa, O.; Zorec, J.; Domiciano de Souza, A.; Mourard, D.; Perraut, K.; Stee, Ph.; Frémat, Y.; Monnier, J.; Kraus, S.; Che, X.; Bério, Ph.; Bonneau, D.; Clausse, J. M.; Challouf, M.; Ligi, R.; Meilland, A.; Nardetto, N.; Spang, A.; McAlister, H.; ten Brummelaar, T.; Sturmann, J.; Sturmann, L.; Turner, N.; Farrington, C.; Goldfinger, P. J.
Spectrally resolved interferometric observations of α Cephei and physical modeling of fast rotating stars
2013, A&A 555, A100

24. M. Dominique, J.-F. Hochedez, W. Schmutz, I.E. Dammasch, A. I. Shapiro, M. Kretzschmar, A.N. Zhukov, D. Gillotay, Y. Stockman, A. BenMoussa
The LYRA instrument onboard PROBA2: description and in-flight performance
Solar Physics, 286, pp.21-42

25. Dumberry, M., Rivoldini, A., Van Hoolst, Yseboodt, M., 2013
The effect of a large solid inner core on the long-term libration of Mercury
Icarus 225, 62–74

26. E. Elst,
4 positions of asteroids,
2013, MPS 466950.

27. E. Elst, H. Debehogne,
5 positions of asteroids,
2013, MPS 453875.

28. L. Feng, B. Inhester, M. Mierla
Comparisons of CME Morphological Characteristics Derived from Five 3D Reconstruction Methods
Solar Physics, 282, pp.221—238

29. Ferland G.J., Kisielius R., Keenan F.P., van Hoof P.A.M., Jonauskas V., Lykins M.L., Porter R.L., Williams R.J.R.
Improved iron UTA spectra – probing the stability limits in AGN clouds
ApJ, 767, 123

30. Ferland G.J., Porter R.L., van Hoof P.A.M., Williams R.J.R., Abel N.P., Lykins M.L., Shaw G., Henney W.J., Stancil P.C
The 2013 Release of Cloudy
Rev. Mexicana Astron. Astrofis., 49, 137

31. T.G. Forbes, E.R. Priest, D.B. Seaton, Y.E. Litvinenko
Indeterminacy and instability in Petschek reconnection
Physics of Plasmas, 20, pp.052902

32. Olivier Francis, Henri Baumann, T. Volarik, C. Rothleitner, G. Klein, M. Seil, N. Dando, R. Tracey, C. Ullrich, Stefaan Castelein, et al.
The European Comparison of Absolute Gravimeters 2011 (ECAG-2011) in Walferdange, Luxembourg: results and recommendations
Metrologia 50, 257-268 (2013)

33. Frandsen, S.; Brogaard, K.; Beck, P. G.; Lampens, P.; Garcia, R. A.; Hekker, S.; Southworth, J.; Degroote, P.,
Detached Eclipsing Binaries and heartbeat stars in the Kepler field
EAS Publications Series, Volume 64, 2013, pp.393-394 (poster contribution)

34. Grasset, O., Dougherty, M.K., Coustenis, A., Bunce, E.J., Erd, C., Titov, D., Blanc, M., Coates, A., Drossart, P., Fletcher L.N., Hussmann, H., Jaumann, R., Krupp, N., Lebreton, J.-P., Prieto-Ballesteros, O., Tortora, P., Tosi, F., Van Hoolst, T., 2013
JUpiter ICy moons Explorer (JUICE): an ESA mission to orbit Ganymede and to characterise the Jupiter system
Planetary and Space Science 78, 1–21,

35. Groenewegen M.A.T.
Baade-Wesselink distances to Galactic and Magellanic Cloud Cepheids and the effect of metallicity
2013, A&A 550, A70, 25 pages

36. Grott, M., Baratoux, D., Hauber, E., Sautter, V., Mustard, J., Gasnault, O., Ruff, S., Karato, S.-I., Debaille, V., Knapmeyer, M., Sohl F.., Van Hoolst, T., Breuer, D., Morschhauser, A., Toplis, M.J., 2013
Long-term evolution of the crust-mantle system of Mars
Space Science Reviews 174, 49-111, doi: 10.1007/s11214-012-9948-3

37. C Guennou, F. Auchere, J.A. Klimchuk, K. Bocchialini, S. Parenti
Can the Di_fferential Emission Measure constrain the timescale of energy deposition in the corona?
ApJ, 774, pp.31
Hajduk M., van Hoof P.A.M., Zijlstra A.A.
CK Vul: evolving nebula and three curious background stars
MNRAS, 432, 167

38. Hajduk M., van Hoof P.A.M., Zijlstra A.A.
CK Vul:
evolving nebula and three curious background stars
MNRAS, 432, 167

39. J.P. Halain, D. Berghmans, D.B. Seaton, B. Nicula, M. Mierla, Alexandra Mazzoli, J.-M. Defise, P. Rochus
The SWAP EUV Imaging Telescope. Part II: In-flight Performance and Calibration
Sol. Phys., 286, pp.67—91

40. Hamilton, C.W., Beggan C.D., Still S., Beuthe M., Lopes R.M.C., Williams D.A., Radebaugh J., Wright W.
Spatial distribution of volcanoes on Io: implications for tidal heating and magma ascent
Earth and Planetary Science Letters, 361, 272-286 (2013), doi:10.1016/j.epsl.2012.10.032

41. Harmegnies A., Defraigne P., Petit G.,
Combining GPS and GLONASS in All in View for time transfer
Metrologia 50 (2013) 277–287.

42. Hensberge, H.; Bakış, V.; De Cat, P.; Bloemen, S.; Scaringi, S.; Sódor, Á.; Raskin, G.; Van Winckel, H.; Prins, S.; Pessemier, W.; Waelkens, C.; Frémat, Y.; Dumortier, L.; Jorissen, A.; Van Eck, S.; Lehmann, H.
The triple B-star system DV Cam
2013, EAS Publications Series, Volume 64, pp.397-398

43. Jurcsik, J.; Smitola, P.; Hajdu, G.; Pilachowski, C.; Kolenberg, K.; Sódor, Á.; Fűrész, G.; Moór, A.; Kun, E.; Saha, A.; Prakash, P.; Blum, P.; Tóth, I.
What is the Difference? Blazhko and Non-Blazhko RRab Stars and the Special Case of V123 in M3
2013, The Astrophysical Journal Letters, Volume 778, Issue 2, article id. L27, 5

44. Kamenetzky J., McCray R., Indebetouw R., Barlow M.J., Matsuura M., Baes M., Blommaert J., Bolatto A., Decin L., Dunne L., Fransson C., Glenn J., Gomez H., Groenewegen M.A.T., Hopwood, R. Kirshner R.P., Lakicevic M., Marcaide J, Marti-Vidal I., Meixner M., Royer P., Soderberg A., Sonneborn G, Staveley-Smith L., Swinyard B.M., Van de Steene G., van Hoof P.A.M., van Loon J.Th., Yates Y. Zanardo G.
Carbon Monoxide in the Cold Debris of Supernova 1987A
2013, ApJ 773, L34, 6 pages

45. I. W. Kienreich, N. Muhr, A. M. Veronig, D. Berghmans, A. De Groof, M. Temmer, B. Vrsnak, D.B. Seaton
Solar TErrestrial Relations Observatory-A (STEREO-A) and PRoject for On-Board Autonomy 2 (PROBA2) Quadrature Observations of Reflections of Three EUV Waves from a Coronal Hole
Solar Physics, 286, pp.125—142

46. E. Kilpua, A. Isavnin, A. Vourlidas, H. E. J. Koskinen, L. Rodriguez
On the relationship between interplanetary coronal mass ejections and magnetic clouds
Annales Geophysicae, 31, pp.1251-1265

47. M. Kretzschmar, M. Dominique, I.E. Dammasch
Sun-as-a-Star Observation of Flares in Lyman α by the PROBA2/LYRA Radiometer
Solar Physics, 286, pp.221-239

48. Kuchynka P., Folkner W.M., Konopliv A.S., Park R.S., Le Maistre S., and Dehant V.
New constraints on Mars rotation determined from radiometric tracking of the Opportunity Mars Exploration Rover.
Icarus, 222(1), pp. 243-253, DOI: 10.1016/j.icarus.2012.11.003.

49. Lammer H., Chassefière E., Karatekin Ö., Morschhauser A., Niles P.B., Mousis O., Odert P., Möstl U.V., Breuer D., Dehant V., Grott M., Gröller H., Hauber E., and Pham L.B.S.
Outgassing History and Escape of the Martian Atmosphere and Water Inventory.
Space Sci Rev, 174(1-4), pp. 113-154, DOI: 10.1007/s11214-012-9943-8.

50. Lampens, P.; Prieur, J.-L.; Argyle, R. W.; Cuypers, J.;
Relative astrometry and near-infrared differential photometry of nearby southern orbital binaries with adaptive optics,
2013, Astronomische Nachrichten, Vol.334, Issue 3, p.237-250

51. Lampens, P.; Tkachenko, A.; Lehmann, H.; Debosscher, J.; Aerts, C.; Beck, P. G.; Bloemen, S.; Kochiashvili, N.; Derekas, A.; Smith, J. C.; Tenenbaum, P.; Twicken, J. D.
Low-frequency variations of unknown origin in the Kepler delta Scuti star KIC 5988140 = HD 188774
2013, A&A 549, A104, 9 pages

52. Le Maistre S., Rosenblatt P., Rambaux N, Castillo-Rogez J.C., Dehant V, and Marty J.C.
Phobos interior from librations determination using Doppler and star tracker measurements.
Planetary and Space Science, 85, 106-122, DOI: 10.1016/j.pss.2013.06.015.

53. Lobel A.; Groh, J. H.; Martayan, C.; Frémat, Y.; Torres Dozinel, K.; Raskin, G.; Van Winckel, H.; Prins, S.; Pessemier, W.; Waelkens, C.; Hensberge, H.; Dumortier, L.; Jorissen, A.; Van Eck, S.; Lehmann, H..
Modelling the asymmetric wind of the luminous blue variable binary MWC 314
2013, A&A 559, A16, 28 pages

54. Lykins M.L., Ferland G.J., Porter R.L., van Hoof P.A.M., Williams R.J.R., Gnat O.
Radiative cooling in collisionally ionized and photoionized plasmas
MNRAS, 429, 3133

55. O. Malandraki, A. Devos, M. Dumbovic, L. Rodriguez, E. Robbrecht, B. Vrsnak, + 20 authors
Statistical analysis of geomagnetic storms, coronal mass ejections and solar energetic particle events in the framework of the COMESEP project
EGU General Assembly, EGU2013-10389

56. Martinez Belda M., Defraigne P., Bruyninx C.
On the Potential of Galileo E5 for Time Transfer
IEEE Transactions on Ultrasonics, Ferroelectrics and Frequency Control, 30(1), 121-131

57. Mayer A., Jorissen A., Kerschbaum F., Ottensamer R., Nowotny, W., Cox, N.L.J., Aringer, B., Blommaert J.A.D.L., Decin L., van Eck S., Gail H.-P., Groenewegen M.A.T., Kornfeld K., Mecina M., Posch Th., Vandenbussche B., Waelkens C.
The large-scale environments of binary AGB stars probed by Herschel: I. Morphology statistics and case studies of R Aqr and W Aql
2013, A&A 549, A69, 14 pages

58. M. Mierla, D.B. Seaton, D. Berghmans, I. Chifu, A. De Groof, B. Inhester, L. Rodriguez, G. Stenborg, A.N. Zhukov
Study of a Prominence Eruption using SWAP/PROBA2 and EUVI/STEREO Data
Solar Physics, 286, pp.241—253

59. J. Molenda-Żakowicz, S.G. Sousa, A. Frasca, K. Uytterhoeven, M. Briquet, H. Van Winckel, D.Drobek, E. Niemczura, P. Lampens, J. Lykke, S. Bloemen, J.F. Gameiro, C. Jean, D. Volpi, N. Gorlova, A. Mortier, M. Tsantaki, G. Raskin
Atmopheric parametersof 169 F, G, K and M-type stars in the Kepler field of view
2013, MNRAS, 434, 1422

60. David Garcia Moreno, Thierry Camelbeeck
Comparison of ground motions estimated from prediction equations and from observed damage during the M=4.6 1983 Liège earthquake (Belgium)
Natural Hazards and Earth System Sciences 13, 1983-1997 (2013).

61. Noack L. and Breuer D.
Interior and surface dynamics of terrestrial bodies and their implications for the habitability.
Book chapter in: Habitability on other planets and satellites: The quest for extraterrestrial life. Eds. J.-P. de Vera and F. Seckbach, Springer, ISBN: 978-94-007-6545-0, pp 203-233, 2013.

62. Noack L. and Breuer D.
First- and second-order Frank-Kamenetskii approximation applied to temperature-, pressure- and stress-dependent rheology.
GJI, 2013, 195, 27-46, doi: 10.1093/gji/ggt248, 2013.

63. Noack L. and Tosi N.
High-Performance Modelling in Geodynamics.
Book chapter in: Integrated Information and Computing Systems for Natural, Spatial, and Social Sciences. Ed. C.-P. Rückemann, IGI Global, 324-352, doi:10.4018/978-1-4666-2190-9, ISBN13: 9781466621909, 2013.

64. Paparó, M.; Bognár, Zs.; Benkő, J. M.; Gandolfi, D.; Moya, A.; Suárez, J. C.; Sódor, Á.; Hareter, M.; Poretti, E.; Guenther, E. W.; Auvergne, M.; Baglin, A.; Weiss, W. W.
CoRoT 102749568: mode identification in a δ Scuti star based on regular spacings
2013, A&A 557, A27, 13 pages

65. T. Pauwels,
12 positions of asteroids,
MPS 465566, 465567, 475308.

66. T. Pauwels, Z. Bognár,
6 positions of asteroids,
MPS 461735.

67. Rui Pinto, Roland Grappin, Marco Velli, Andrea Verdini
Coupling the solar surface and the corona: coronal rotation, Alfvén wave-driven polar plumes
SOLAR WIND 13: Proceedings of the Thirteenth International Solar Wind Conference. AIP Conference Proceedings, 1539, pp.74-77

68. L. A. Rachmeler, S.E. Gibson, J. Dove, C. R. DeVore, Y. Fan
Polarimetric Properties of Flux-Ropes and Sheared Arcades in Coronal Prominence Cavities
Sol. Phys., 288, pp.617-636

69. C.L. Raftery, D.S. Bloomfield, P.T. Gallagher, D.B. Seaton, D. Berghmans, A. De Groof
Temperature Response of EUV Imagers
Sol. Phys., 286, pp.111—124

70. Rivoldini, A., Van Hoolst, T., 2013
The interior structure of Mercury constrained by the low-degree gravity field and the rotation of Mercury
Earth and Planetary Science Letters 377–378, 62–72

71. Sarti P., Abbondanza C., Legrand J., Bruyninx C., Vittuari L., Ray J.
Intra-site motions and monument instabilities at Medicina ITRF co-location site
Geophysical Journal International (March, 2013) 192(3): 1042-1051 doi:10.1093/gji/ggs092
Solar Physics, 286, pp.271-287

72. D.B. Seaton, D. Berghmans, B. Nicula, J.P. Halain, A. De Groof, T. Thibert, D.S. Bloomfield, C.L. Raftery, P.T. Gallagher, F. Auchere, J.-M. Defise, E. D'Huys, J.H. Lecat, E. Mazy, P. Rochus, L. Rossi, U. Schuehle, V.A. Slemzin, M.S. Yalim, J. Zender
The SWAP EUV Imaging Telescope Part I: Instrument Overview and Pre-Flight Testing
Sol. Phys., 286, pp.43—65

73. D.B. Seaton, A. De Groof, Paul Shearer, D. Berghmans, B. Nicula
SWAP Observations of the Long-Term, Large-Scale Evolution of the EUV Solar Corona
ApJ, 777, pp.72

74. Semaan, T.; Hubert, A. M.; Zorec, J.; Martayan, C.; Frémat, Y.; Gutiérrez-Soto, J.; Fabregat, J.
Study of a sample of faint Be stars in the exofield of CoRoT. I. Spectroscopic characterization
2013, A&A 551, A130, 20 pages

75. A.V. Shapiro, A. I. Shapiro, M. Dominique, I.E. Dammasch, C. Wehrli, E. Rozanov, W. Schmutz
Detection of Solar Rotational Variability in the Large Yield RAdiometer (LYRA) 190 - 222 nm Spectral Band
Solar Physics, 286, pp.289-301

76. A. I. Shapiro, W. Schmutz, M. Dominique, A.V. Shapiro
Eclipses Observed by Large Yield RAdiometer (LYRA) - A Sensitive Tool to Test Models for the Solar Irradiance

77. V.A. Slemzin, L. K. Harra, Alexander Urnov, S.V. Kuzin, Farid Goryaev, D. Berghmans
Signatures of Slow Solar Wind Streams from Active Regions in the Inner Corona
Solar Physics, 286, pp.157-184

78. Tatton B.L., van Loon J.Th., Cioni M.-R., Clementini G., Emerson J.P., Girardi L., de Grijs R., Groenewegen M.A.T., Gullieuszik M., Ivanov V.D., Moretti M.I., Ripepi V., Rubele S.
The VMC Survey VII. Reddening map of the 30 Doradus field and the structure of the cold interstellar medium
2013, A&A 554, A33, 26 pages

79. Tkachenko, A.; Aerts, C.; Yakushechkin, A.; Debosscher, J.; Degroote, P.; Bloemen, S.; Pápics, P. I.; de Vries, B. L.; Lombaert, R.; Hrudkova, M.; Frémat, Y.; Raskin, G.; Van Winckel, H.
Detection of a large sample of γ Doradus stars from Kepler space photometry and high-resolution ground-based spectroscopy
2013, A&A 556, A52, 12 pages

80. Tsagouri I., Belehaki A., Bergeot N., Cid C., Delouille V., Egorova T., Jakowski N., Kutiev I., Mikhailov A., Nunez M., Pietrella M., Potapov A., Qahwaji R., Tulunay Y., Velinov P., Viljanen A. and Watermann J.
Progress in space weather modeling in an operational environment
J. Space Weather Space Clim., 3 A17, DOI: 10.1051/swsc/2013037, 2013

81. Pierre Valty, Olivier de Viron, Isabelle Panet, Michel Van Camp, Juliette Legrand
Assessing the precision in loading estimates by geodetic techniques in Southern Europe
Geophysical Journal International 194, 1441-1454 (2013).

82. Vamvatira-Nakou C., Hutsemékers D., Royer P., Nazé Y., Magain P., Exter K., Waelkens C., Groenewegen M.A.T.
Herschel imaging and spectroscopy of the nebula around the Luminous Blue Variable star WRAY 15-751
2013, A&A 557, A20, 17 pages

83. Michel Van Camp, Olivier de Viron, Richard Warburton
Improving the determination of the gravity rate of change by combining superconducting with absolute gravimeter data
Computers in Geosciences 51, 49-55 (2013).

84. van Hoof P.A.M., Van de Steene G.C., Exter K.M., Barlow M.J., Ueta T., Groenewegen M.A.T., Gear W.K., Gomez H.L., Hargrave P.C., Ivison R.J., Leeks S.J., Lim T.L., Olofsson G., Polehampton E.T., Swinyard B.M., Van Winckel H., Waelkens C., Wesson R.
A Herschel study of NGC 650
2013, A&A 560, A7, 18 pages

85. Van Hoolst, T., Baland, R.-M., Trinh, A., 2013
On the librations and tides of large icy satellites
Icarus 226, 299–315

86. Van Hove B., Karatekin O., Chazot O., Lacor C.
Post-flight reconstruction using conventional and novel instrumentation
Review of the VKI Doctoral Research 2012-2013, 4-6 March 2013, Rhode-Saint-Genese, Belgium, pp. 263-274 in print
ISBN 978-2-8716-060-7, edited by prof. T. Magin

87. Kris Vanneste, Thierry Camelbeeck, Koen Verbeeck
A Model of Composite Seismic Sources for the Lower Rhine Graben, Northwest Europe
Bulletin of the Seismological Society of America 103, 984-1007 (2013).

88. Andrea Verdini, Roland Grappin, Rui Pinto, Marco Velli
Building small scales in MHD turbulence
SOLAR WIND 13: Proceedings of the Thirteenth International Solar Wind Conference. AIP Conference Proceedings, 1539, pp.58-61

89. Vlemmings W.H.T., Maercker M., Lindqvist M., Mohamed S., Olofsson H., Ramstedt S., Brunner M., Groenewegen M.A.T., Kerschbaum F., Wittkowski M.,
ALMA observations of the variable $^{12}CO/^{13}CO$ ratio around the asymptotic giant branch star R Sculptoris
2013, A&A 556, L1, 6 pages

90. van Hoof P.A.M., Van de Steene G.C., Exter K.M., Barlow M.J., Ueta T., Groenewegen M.A.T., Gear W.K., Gomez H.L., Hargrave P.C., Ivison R.J., Leeks S.J., Lim T.L., Olofsson G., Polehampton E.T., Swinyard B.M., Van Winckel H., Waelkens C., Wesson R.
A Herschel study of NGC 650
2013, A&A 560, A7, 18 pages

91. Weidmann W.A., Gamen R., van Hoof P.A.M., Zijlstra A.A., Minniti D., Volpe M.G.
Near-Infrared Photometry of Galactic Planetary Nebulae with the VVV Survey
A&A, 552, A74

92. Wils, Patrick; Ayiomamitis, Anthony; Vanleenhove, Maarten; Hambsch, Franz-Josef; Panagiotopoulos, Kostas; Lampens, Patricia; Van Cauteren, Paul; Van Wassenhove, Jeroen; van de Stadt, Inge; Staels, Bart; Hautecler, Hubert; Robertson, C. W.; Baillien, Antoine; Pickard, Roger D.; Carreno Garceran, Alfonso; Nieuwenhout, Frans; Wollenhaupt, Guido
Photometry of High-Amplitude Delta Scuti Stars in 2012
2013, Information Bulletin on Variable Stars, 6049, 1

93. Yseboodt, M., Rivoldini, A., Van Hoolst, T., Dumberry, M., 2013
Influence of an inner core on the long period forced librations of Mercury
Icarus 226, 41–51

94. J. Zender, D. Berghmans, D.S. Bloomfield, C. Cabanas Parada, I.E. Dammasch, A. De Groof, E. D'Huys, M. Dominique, P.T. Gallagher, B. Giordanengo, P. Higgins, J.-F. Hochedez, M.S. Yalim, B. Nicula, Erik Pylyser, L. Sanchez-Duarte, G. Schwehm, D.B. Seaton, A. Stanger, K. Stegen, S. Willems
The Projects for Onboard Autonomy (PROBA2) Science Centre: Sun Watcher Using APS Detectors and Image Processing (SWAP) and Large-Yield Radiometer (LYRA) Science Operations and Data Products
Sol. Phys., 286, pp.93-110

95. J. Zender, D. Berghmans, D.S. Bloomfield, C. Cabanas Parada, I.E. Dammasch, A. De Groof, E. D'Huys, M. Dominique, P.T. Gallagher, B. Giordanengo, P. Higgins, J.-F. Hochedez, M.S. Yalim, B. Nicula, Erik Pylyser, L. Sanchez-Duarte, G. Schwehm, D.B. Seaton, A. Stanger, K. Stegen, S. Willems
The PROBA2 Science Center: SWAP & LYRA science operations and data products
Sol. Phys., 286, pp.93—110

96. F. Zuccarello, L. Balmaceda, G. Cessateur, H. Cremades, S. L. Guglielmino, J. Lilensten, T. Dudok de Wit, M. Kretzschmar, F. M. Lopez, M. Mierla, S. Parenti, J. Pomoell, P. Romano, L. Rodriguez, N. Srivastava, R. Vainio, M. West, F. P. Zuccarello
Solar activity and its evolution across the corona
Journal of Space Weather and Space Climate, 3, pp.A18

Annex 2: Human Resources 2013

Personeel / Personnel

Algemeen directeur: Van der Linden Ronald

Vastbenoemd personeel / Personnel statutaire

Wetenschappelijk personeel / Personnel scientifique :

Name/Nom	*Functie/Fonction*
Alexandre Pierre	Premier assistant 80 %
Alvarez Rodrigo	Premier assistant
Berghmans David	Werkleider
Blomme Ronny	Eerstaanwezend assistent
Bruyninx Carine	Eerstaanwezend assistent
Camelbeeck Thierry	Chef de travaux
Clette Frédéric	Premier assistant
Collin Fabienne	Premier assistant
Cuypers Jan	Eerstaanwezend assistent
De Cat Peter	Eerstaanwezend assistent
Defraigne Pascale	Premier assistant
Dehant Véronique	Chef de travaux – Chef de section
Frémat Yves	Assistant
Groenewegen Martin	Eerstaanwezend assistent
Hochedez Jean-François	Premier assistant
Lampens Patricia	Onderzoeksleider - Departementshoofd
Lecocq Thomas	Assistant
Legrand Juliette	Assistant
Pauwels Thierry	Werkleider - Afdelingshoofd
Robbrecht Eva	Assistent
Roosbeek Fabian	Premier Assistant
Van Camp Michel	Chef de travaux
Van De Steene Griet	Eerstaanwezend assistent
Van Hoolst Tim	Eerstaanwezend assistent
Vanneste Kris	Werkleider
Yseboodt Marie	Assistant

Technisch en administratief personeel / Personnel technique et administratif

Name/Nom	Functie/Fonction
Milis Andre	Attaché A2 Adviseur A3 (vanaf 01/03/2013)
De Knijf Marc	Attaché A2
Dufond Jean-Luc	Attaché A2
Rogge Vincent	Attaché A2
Jans Thimoty	Attaché A1
Kochuyt Anne-Lize	Attaché A1
Rapagnani Giovanni	Attaché A1
Rezabek Oleg	Attaché A1
Wellens Véronique	Attaché A1
Asselberghs	Technisch deskundige
Somnina	Expert technique
Boulvin Olivier	Expert technique
Bukasa Baudouin	Technisch deskundige
Castelein Stefaan	Expert technique
Coene Yves	Experttechnique
Driegelinck Eddy	Expert ICT
Dumortier Louis	Expert ICT
Duval David	Expert technique
Ergen Aydin	Expert technique
Frederick Bert	Expert technique
Danloy Jean-Marie	Assistant administratif
Depasse Béatrice	Assistant administratif
De Wachter Rudi	Technisch assistent
Feldberg Liesbeth	Administratief assistent
Jacques Jean-Claude	Assistant technique
Janssens Paul	Assistant technique

Name/Nom	Functie/Fonction
Hendrickx Marc	Expert technique80%
Herreman David	Expert ICT
Langenaken Hilde	Technisch deskundige
Martin Henri	Expert technique 80%
Mesmaker Dominique	Expert technique
Moyaert Ann	ICT deskundige 80%
Renders Francis	Technisch deskundige (pensioen : 01/07/2013)
Somerhausen André	Expert ICT
Strubbe Marc	Technisch deskundige
Van Camp Lydia	Technisch deskundige 80%
Van De Putte William	Technisch deskundige
Van Der Gucht Ignace	Technisch deskundige
Vandekerckhove Joan	Technisch deskundige
Vandercoilden Leslie	Expert technique
Vanraes Stéphane	deskundige
Vermeiren Katinka	ICT deskundige 80%
Van de Meersche Olivier	Expert Financier
Wintmolders Sabrina	Administratief deskundige
Bizerimana Philippe	Assistant technique
Brebant Christian	Assistant administratif
Bruyninckx Martine	Administratief assistent
Lemaitre Olivier	Assistant technique
Trocmet Cécile	Assistant administratif
Van Den Brande Theophilis	Technisch assistent
Vanden Elshout Ronny	Assistant technique
Verbeeren Anja	Administratief assistent
Consiglio Sylvia	Administratief assistent

Personeel met externe beurzen / Personnel sur bourses externes

Name/Nom	Functie/Fonction
Hees Aurélien	Boursier FRIA
Kusters Dimitri	Boursier FRIA

Name/Nom	Functie/Fonction
Koot Laurence	Boursier FNRS

Contractueel personeel beheerd door de POD Wetenschapsbeleid / Personnel contractual géré par le SPP Politique Scientifique

Name/Nom	Functie/Fonction
De Dobbeleer Rudy	Technisch assistant
Motte Philippe	Collaborateur technique
Mouling Ilse	Administratief assistent 80 %

Name/Nom	Functie/Fonction
Semeraro Vanessa	Administratief assistant
Vandersyppe Anne	Administratief expert
Verbeeck Koen	Assistent SW1 50%

Contractueel personeel / Personnel contractuel

Wetenschappelijk personeel / Personnel scientifique

Naam/Nom	Functie/Fonction	Contract
Aerts Wim	Assistent	STCE
Andries Jesse	Assistent (vanaf 01/04/2013)	PRODEX
Baire Quentin	Assistant	Chercheur supp
Benmoussa Ali	Chef de travaux	PRODEX
Berckmans Julie	Assistent-stagiaire	STCE
Bergeot Nicolas	Chef de travaux	STCE
Beuthe Mikael	Chef de travaux	PRODEX
Bourgoignie Bram	Assistent	STCE
Caudron Corentin	Assistant	Actie 2
Champagne Georges	Assistant	Service contract/ Cherch. Sppl.
Chevalier Jean-Marie	Assistant	STCE
Dammasch Ingolf	Assistant	PRODEX
De Cuyper Jean-Pierre	werkleider	DIGITALISATION
Delouille Véronique	Chef de travaux	PRODEX
De Visscher Ruben	Assistent-stagiair (tot 01/08/2014)	PRODEX
Devos Andy	Assistent (tot 01/04/2014)	PRODEX
D'Huys Elke	Assistent	STCE
Dolla Laurent	Assistant	STCE
Dominique Marie	Assistant	PRODEX
Garcia Moreno David	Assistant (tot 31/12/2013)	UE_SHARE
Gloesener Elodie	Assitant-stagiaire (tot 01/04/2013)	2PAI_PLANETTOP
Gillmann Cédric	Assistant (jusqu'au 15/11/2014)	2PAI_PLANETTOP
Giordanengo Boris	Chef de travaux	PRODEX
Gissot Samuel	Chef de travaux	PRODEX
Janssens Jan	Assistent	STCE
Joukov Andrei	Chef de travaux	STCE
Karatekin Ozgur	Chef de travaux	PRODEX
Knuts Elisabeth	Assistant	HAZARDS.
Kraaikamp Emil	Assistent stagiair (tot 28/02/2014)	PRODEX
Kudryashova Maria	Assistant	3UE_ESPACE
LeMaistre Sébastien	Assistant	PRODEX
Lefevre Laure	Assistant (jusqu'au 31/10/2013)	SOTERIA
Lobel Alex	werkleider	3 GAIA
Lombardini Denis	Assistant	Antartique
Magdalenic Jasmina	Chef de travaux	Action 1
Marqué Christophe	Chef de travaux	STCE
Mierla Marilena	Assistent (tot 31/07/2016)	ACTION 1
Mitrovic Michel	Assistant	PRODEX
Nicula Bogdan	Chef de travaux	STCE
Noack Léna	Assistant (tot 01/10/2014)	2PAI_PLANETTOP
Parenti Suzanna	chef de travaux	PRODEX
Pham Lê Binh San	Assistant (tot 01/10/2013)	2PAI_PLANETTOP
Podladchikova Olena	Chef de travaux	STCE
Pottiaux Eric	Assistant (jusqu'au 28/02/2013)	STCE
	Chef de travaux (à p du 01/03/2013)	STCE

Pylyser Eric	Assistant	PRODEX
Rachmeler Laurel	Assistent (vanaf 01/04/2013)	PRODEX
Rivoldini Attilio	Assistant	PRODEX
Rodriguez Luciano	Chef de travaux	PRODEX
Rosenblatt Pascal	Chef de travaux	PRODEX
Seaton Daniel	Chef de travaux	PRODEX
Sodor Adam	Assistent (tot 01/07/2014)	ACTION 1
Stegen Koen	Assistent	PRODEX
Trinh Anthony	Assistent (vanaf 01/12/2013)	UE_DESCARTES
Van Hoof Peter	Werkleider	PRODEX
Van Hove Bart	Assistent (tot 31/03/2014)	CHERSUPP
Vanlommel Petra (80%)	Eerstaanwezend assistent	STCE
Van Noten Koen	Assistent (tot 28/02/2014)	Actie 1
Vansintjan Robbe	Assistent (vanaf 01/02/2013)	PRODEX
Verbeeck Francis	Eerstaanwezend assistent	PRODEX
Verbeeck Koen (50%)	Assistant	HAZARDS
Verbruggen Wim	Assistent-stagiaire (tot 30/09/2013)	CHERSUPP
Verdini Andrea	Assistant	PRODEX
Verstringe Freek	Assistent (tot 01/04/2014)	STCE
Vleminckx Bart	Assistent-stagiaire (tot 31/03/2014)	CHERSUPP
Wauters Laurence (60%)	Premier assistant	STCE
West Matthew	Assistant (tot 15/07/2014)	PRODEX
Zhu Ping	Assistant (tot 31/12/2013)	Action 2

Technisch en administratief personeel / personnel technique et administratif

Naam/Nom	Functie/Fonction	Contract
Van Elder Sophie (50%)	Attaché A1	STCE
Cornet Denis	Attaché A1	ESERO
De Decker Georges	Attaché A2	Digitalisation
Hanjoul Michel	Attaché A2	1modernisation
Willems Sarah	Attaché A2	STCE
Mampaey Benjamin	Attaché A2	PRODEX
Van Hemelryck Eric	Attaché A2	PRODEX
Malisse Vincent	ICT-deskundige (vanaf 14/03/2012)	PRODEX
Vander Putten Wim	ICT-deskundige	Dotatie
Claerhout Alexandre	Expert ICT (à partir du 01/07/2013)	1Modernisation
Bastin Véronique	Expert technique	Dotation
Coeckelberghs Hans	Technisch deskundige	1Planetarium
Rigo Ghislain	Expert technique	STCE
Vandercoilden Myriam	Assistant administratif	Dotation Pole
Hernando Ana Maria	Assistant administratif	STCE
Schodts Ivan	Administratief assistent (vanaf 01/06/2013)	Dotation Pole
Smet Gert	Technisch assistent	Dotatie
Wijns Erik	Technisch medewerker	Dotatie
Vandeperre Arnold	Technisch assistent	Dotatie
Mertens Philippe	Administratief medewerker (tot 31/03/2013)	1Planetarium
El Amrani Malika	Collaborateur technique	Dotation
Herman Viviane (20%)	Collaborateur technique	Dotation
Ipuz Mendez Adriana (50%)	Collaborateur technique	Dotation

Reghif Harraz Mohammed (50%)	Collaboratuer technique	Dotation
Trindade Josefina	Collaborateur technique	Dotation
Vermeylen Jacqueline	Collaborateur technique	Dotation
Kurudere Hulya	Technisch medewerker	1Planetarium

Gedetacheerd personeel / Personnel détaché

Naam/Nom	Functie/Fonction	Contract
De Rijcke Hendrick	Leraar	Onderwijs Vlaamse Gemeenschap